ANALYSIS AND DESIGN OF FIR MULTIRATE FILTER BANKS

by

ADNAN M.S. AL-ADNANI

Doctor of Philosophy

1995

Signal Processing Division

Department of Electronic and Electrical Engineering

UNIVERSITY OF STRATHCLYDE

Glasgow G1 1XW

Scotland

United Kingdom

ANALYSIS AND DESIGN OF FIR MULTIRATE FILTER BANKS

A THESIS

SUBMITTED TO THE SIGNAL PROCESSING DIVISION,

DEPARTMENT OF ELECTRONIC AND ELECTRICAL ENGINEERING

AND THE COMMITTEE FOR POSTGRADUATE STUDIES

OF THE UNIVERSITY OF STRATHCLYDE

FOR THE DEGREE OF

DOCTOR OF PHILOSOPHY

By

Adnan M.S. Al-Adnani

June 1995

© Copyright 1995

The copyright of the Thesis belongs to the author under the terms of the United Kingdom Copyright Acts as qualified by University of Strathclyde Regulation 3.49. Due acknowledgement must be made of the use of any material contained in, or derived from, this Thesis.

To My Parents

Declaration

I declare that this Thesis embodies my own research work and that it is composed by myself. Where appropriate, I have made acknowledgment to the work of others.

Adnan Al-Adnani

Abstract

This thesis is concerned with the analysis and design of FIR multirate filter banks. Focusing on the time-frequency relation of the filter bank structures, various design methods have been developed. Standard digital filtering techniques are used such as windowing, and least squares in conjunction with the multirate structures of the filter banks to obtain efficient designs that will allow a great degree of flexibility in controlling the frequency characteristics of the filters. A spectral factorisation technique is introduced to design three-channel based systems in the z-domain. This method extends the well known two-channel based design, and requires no numerical optimization. Time-domain algorithms are introduced to design M-channel systems with arbitrary length filters and arbitrary system delays. Aliasing cancellation and perfect reconstruction conditions in the time domain are addressed. A recursive technique is proposed which uses the synthesis filters from one iteration to update the analysis filters for the next. Wavelets provide a new method for time-scale analysis of non-stationary signals. Filter banks are used to construct several classes of wavelet transforms; orthonormal, bi-orthogonal, and new low delay wavelets using the time-domain formulation.

Acknowledgments

I would like to thank my supervisor and friend Roy Chapman for his advice, encouragement, motivation , and for making research interesting and fun.

I would also like to thank Professor Tariq Durrani for giving me the opportunity to join his group, and also for his support and encouragement.

Special thanks to all present and past members of the Signal Processing Division, and colleagues Abdul Rahim Layman, Druti Shah, Cameron Speirs, Iain Hunter, Neal Harvey, Kate Woodham, Noaman Khan, and the rest of the SPD members for providing a friendly and stimulating environment.

Finally, I am indebted to my family for their constant support, without them my university career would not be possible.

List of Abbreviations

FIR	Finite Impulse Response
IIR	Infinite Impulse Response
QMF	Quadrature Mirror Filter
CQF	Conjugate Quadrature Filter
PR	Perfect Reconstruction
MFB	Multirate Filter Bank
FB	Filter Bank
STFT	Short-Time Fourier Transform
CWT	Continuous Wavelet Transform
DWT	Discrete Wavelet Transform
IDWT	Inverse Discrete Wavelet Transform
DCT	Discrete Cosine Transform
LOT	Lapped Orthogonal transform
AC	Alias Component
LS	Least Square

List of Symbols

$H_k(z)$	Analysis Filters
$F_k(z)$	Synthesis Filters
$G_k(z)$	Product Filters
$T(z)$	Overall Transfer Function
$x(n)$	Input Signal
$\hat{x}(n)$	Reconstructed Signal
$det[\mathbf{A}]$	Denotes Determinant of Matrix $\mathbf{A}$
$\mathbf{A}^T$	Denotes Transpose of Matrix $\mathbf{A}$
$\mathbf{I}$	Identity Matrix
$\mathbf{J}$	Exchange Matrix
Δ	System Delay
η_{kl}	Wavelet Basis
$\delta(k)$	Dirac Delta Function
$\psi(t)$	Wavelet Function
$\phi(t)$	Scaling Function

Contents

Declaration v

Abstract vi

Acknowledgments vii

List of Abbreviations viii

List of Symbols ix

1 Introduction and Motivation 1

1.1 Introduction 1

1.2 Overview of the Thesis 4

1.2.1 New Research Results 5

2 Review of Multirate Filter Banks 6

2.1 Introduction 6

2.2 Multirate Signal Processing 7

2.2.1 Downsampling 7

2.2.2 Upsampling 10

2.2.3 Decimation and Interpolation Filters 12

2.2.4 Fractional Sampling rate Alterations 12

2.2.5 Multirate identities 14

2.2.6 The Polyphase representation 15

2.3 The Two-Channel Filter Bank 15

2.3.1 The Classical QMF 18

2.3.2 Perfect Reconstruction QMF bank 19

2.3.3 Linear Phase Filter Bank 20

2.4 M-Channel Filter Bank 22

2.4.1 Lossless, paraunitary filter banks 23

2.4.2 Modulated filter banks 27

2.4.3 Time-domain techniques 28

2.5 Wavelets and Filter Banks 28

2.5.1 Regularity 32

2.6 Summary 33

3 A Spectral Factorisation Approach to 3-Channel Filter Banks 34

3.1 Introduction 34

3.2 Review of Spectral Factorization 35

3.2.1 The Two-Channel System 35

3.2.2 M-Channel Filter Bank 37

3.3 3-Channel System 38

3.4 Product Filter Design 39

3.5 Spectral Factorization 40

3.6 Minimum/Maximum Phase Design 42

3.6.1 Aliasing Error 43

3.7 Optimal Third-Band Filter Design 47

3.8 Design Examples 48

3.9 Tree Structures 55

3.10 Conclusion 57

4 Time-Domain Analysis and Design of FIR Multirate Filter Banks 58

4.1 Introduction 58

4.2 Time-Domain Analysis 60

4.2.1 The Two-Channel Filter Bank 60

4.2.2 The M-Channel System 66

4.3 Paraunitary Time-Domain Conditions 72

4.4 Least Square Minimization 74

4.5 Design Algorithm 76

4.6 Two Channel Filter Bank Design 79

4.6.1 PR Paraunitary Design 79

4.6.2 Linear Phase Design 90

4.7 M-channel Filter Bank Design 94

4.7.1 Modulated Filter Bank 97

4.8 Performance Analysis 101

4.9 Conclusions 102

5 Low Delay Multirate Filter Banks 103

5.1 Introduction 103

5.2 The Two Channel Low Delay System 104

5.2.1 Design Procedure 106

5.3 Time-Domain Formulation 113

5.4 Time-Domain Design 114

5.4.1 Design Examples 117

5.5 Conclusions 131

6 Wavelets and Filter Banks **132**

6.1 Introduction 132

6.2 Non-uniform Filter Banks and Wavelets 134

6.3 Orthonormal Wavelets 138

6.4 Bi-orthogonal Wavelets 143

6.5 Low Delay Wavelets 145

6.6 Conclusions 147

7 Conclusions and Future Work **148**

7.1 Conclusions 148

7.2 Future Work 149

A Eigenfilters **151**

B Publications **154**

Bibliography **155**

List of Figures

2.1 (a) Downsampling (b) Upsampling 7

2.2 Downsampling in the time domain; x(n) is the input sequence; y(n) is the downsampled sequence for M=2. 9

2.3 Downsampling in the frequency domain;(a) Input spectra; (b) Downsampled by 2, the spectral replicas stretch by a factor of 2 9

2.4 Upsampling in the time domain for $L = 2$. 11

2.5 Upsampling in the frequency domain; (a) Input spectra; (b) Upsampled by 2, spectral replicas compressed by a factor of 2. 11

2.6 Sampling rate alteration by a factor L/M 12

2.7 (a) The decimation operation; (b) Typical magnitude response of a decimation filter 13

2.8 (a) The interpolation operation; (b) Typical magnitude response of an interpolation filter 13

2.9 Multirate identities 14

2.10 The two Channel Filter Bank 16

2.11 Maximally Decimated M-Channel Filter Bank 21

2.12 The Polyphase structure of the filter bank 26

2.13 Transformed Polyphase structure of the filter bank 26

2.14 Filter bank implementation of the DWT; $H_l(z)$ and $H_h(z)$ are low-pass and high-pass analysis filters respectively. 31

2.15 Filter bank implementation of the IDWT; $F_l(z)$ and $F_h(z)$ are low-pass and high-pass synthesis filters respectively. 31

3.1 Maximally decimated 3-channel system 39

3.2 (a),(b),(c) Magnitude responses of the analysis filters (bold) and their aliasing versions. (d) Magnitude responses of the synthesis filters. 45

3.3 Residual alias terms with $l = 1$ 46

3.4 Residual alias terms with $l = 2$ 46

3.5 The product filters 50

3.6 Impulse responses of the product filters (Amplitude vs Time) . . . 50

3.7 Product filters zeros 51

3.8 Transformed zeros 51

3.9 Analysis filters 52

3.10 Aliasing error 52

3.11 The Least square product filters 53

3.12 Least square Analysis filters 54

3.13 Least square aliasing error 54

3.14 Two level tree-structure 55

3.15 Equivalent 9 channel filter bank 56

3.16 9 Channel System 56

4.1 Two-channel filter bank 60

4.2 M-channel filter bank 71

4.3 Design Flowgraph 78

4.4 (a) Linear phase filter (b)Linear phase zeros 81

4.5 (a) Minimum phase filter (b) Minimum phase zeros 81

4.6 Initial Eigenfilter $h_0^0(n)$ 82

4.7 Analysis Filters for Example 4.6.1.1 84

4.8 Synthesis filters for Example 4.6.1.1 84

4.9 Magnitude error for Example 4.6.1.1 85

4.10 Aliasing error for Example 4.6.1.1 85

4.11 Initial Minimax filter 86

4.12 Analysis filters for Example 4.6.1.2 87

4.13 Synthesis filters for Example 4.6.1.2 87

4.14 Magnitude error for Example 4.6.1.2 88

4.15 Aliasing error for Example 4.6.1.2 88

4.16 Convergence Characteristics 89

4.17 Initial linear phase filters 91

4.18 Analysis filters for Example 4.6.2.1 92

4.19 Synthesis filters for Example 4.6.2.1 92

4.20 Magnitude error for Example 4.6.2.1 93

4.21 Aliasing error for Example 4.6.2.1 93

4.22 Analysis filters for Example 4.7.1 95

4.23 Synthesis filters for Example 4.7.1 95

4.24 Magnitude error for Example 4.7.1 96

4.25 Aliasing error for Example 4.7.1 96

4.26 Prototype filter 98

4.27 Modulated filter bank 98

4.28 Analysis filters for Example 4.7.1.1 99

4.29 Synthesis filters for Example 4.7.1.1 99

4.30 Magnitude error for Example 4.7.1.1 100

4.31 Aliasing error for Example Example 4.7.1.1 100

5.1 Magnitude responses of the product filters for d=0 (solid line), d=2 (dashed line), d=4 (dotted line) 108

5.2 Zeros of the product filters for (a) d=0, (b) d=2, (c) d=4 108

5.3 Magnitude response of the product filter 110

5.4 zeros of the product filter 110

5.5 (a) Magnitude response of $H_0(z)$ (b) zeros of $H_0(z)$ for Example 5.2.2 111

5.6 (a) Magnitude response of $H_1(-z)$ (b) zeros of $H_1(-z)$ for Example 5.2.2 111

5.7 (a) Magnitude response of $H_0(z)$ (b) zeros of $H_0(z)$ for Example 5.2.3 112

5.8 (a) Magnitude response of $H_1(-z)$ (b) zeros of $H_1(-z)$ for Example 5.2.3 112

5.9 Low Delay Design Flowgraph 116

5.10 Analysis filters for $\Delta = 31$ in Example 5.4.1.1 118

5.11 Synthesis filters for $\Delta = 31$ in Example 5.4.1.1 118

5.12 Analysis filters for $\Delta = 28$ in Example 5.4.1.1 119

5.13 Synthesis filters for $\Delta = 28$ in Example 5.4.1.1 119

5.14 Analysis filters for $\Delta = 23$ in Example 5.4.1.1 120

5.15 Synthesis filters for $\Delta = 23$ in Example 5.4.1.1 120

5.16 Analysis filters for $\Delta = 25$ in Example 5.4.1.2 122

5.17 Synthesis filters for $\Delta = 25$ in Example 5.4.1.2 122

5.18 Analysis filters for $\Delta = 18$ in Example 5.4.1.2 123

5.19 Synthesis filters for $\Delta = 18$ in Example 5.4.1.2 123

5.20 Analysis filters for $\Delta = 15$ in Example 5.4.1.2 124

5.21 Synthesis filters for $\Delta = 15$ in Example 5.4.1.2 124

5.22 Analysis filters for $\Delta = 10$ in Example 5.4.1.2 125

5.23 Synthesis filters for $\Delta = 10$ in Example 5.4.1.2 125

5.24 Analysis filters for $\Delta = 54$ in Example 5.4.1.3 127

5.25 Synthesis filters for $\Delta = 54$ in Example 5.4.1.3 127

5.26 Analysis filters for $\Delta = 40$ in Example 5.4.1.3 128

5.27 Synthesis filters for $\Delta = 40$ in Example 5.4.1.3 128

5.28 Analysis filters for $\Delta = 33$ in Example 5.4.1.3 129

5.29 Synthesis filters for $\Delta = 33$ in Example 5.4.1.3 129

5.30 Analysis filters for $\Delta = 25$ in Example 5.4.1.3 130

5.31 Synthesis filters for $\Delta = 25$ in Example 5.4.1.3 130

6.1 Analysis bank implementation of the 3 level DWT 136

6.2 Synthesis bank implementation of the 3 level IDWT 136

6.3 Equivalent filter bank implementation of the wavelets 137

6.4 Typical magnitude responses of the wavelets 137

6.5 Magnitude response of the orthonormal wavelets 141

6.6 Magnitude response in dB of the orthonormal wavelets 141

6.7 Impulse response of the orthonormal wavelets; high-pass(top) to low-pass(bottom) 142

6.8 (a)(b) Impulse and magnitude response of the time domain wavelet; (c)(d) Impulse and magnitude response of the Daubechies wavelet for N=16 and L=5 142

6.9 Magnitude response of the bi-orthogonal wavelets 144

6.10 Impulse response of the bi-orthogonal wavelets; high-pass(top) to low-pass(bottom) 144

6.11 Magnitude response of the low delay wavelets 146

6.12 Impulse response of the low delay wavelets; high-pass(top) to low-pass(bottom) 146

Chapter 1

Introduction and Motivation

1.1 Introduction

Multirate digital signal processing has played a major role in the development of signal processing theory and design, especially with the growing need for fast and efficient algorithms, that deal with very large data sets.

Triggered by the first book in multirate signal processing in the mid 1980's [23], the research has grown rapidly.

Perhaps the single most important development in multirate systems was the introduction of the two-channel filter bank by Croisier et. al [24]. They introduced the QMF(Quadrature Mirror Filter) in speech coding, where a signal could be split into channels using non-ideal filters, subsampled and then reconstructed without spectral overlap(aliasing). The subband signals can be individually coded to suit its characteristics.

Smith and Barnwell [93], and also Mintzer [73] showed that the QMF can be designed to achieve Perfect Reconstruction(PR). Subsequently the theory has been extended to an arbitrary number of channels, with various solutions and structures. [106][116][118][109].

Vitterli [117] demonstrated the possibility of using multirate filter banks in multiple dimensions for applications in subband coding of images. Woods and O'Niel [124] applied multirate filter banks to image compression in a separable fashion, where the filters are applied to each dimension at a time. Karlsson and Vitterli [49] demonstrated the use of filter banks in three-dimensional coding of video. Subsequently multidimensional theory was generalized to arbitrary sampling patterns, where the filtering is nonseparable [122][53][101].

Independent of the work on multirate filter banks, families of functions obtained from a single prototype function by dilation and translation have emerged in applied mathematics in the work of Grossman and Morlet [37], and have since become known as wavelets.

Wavelets are a more efficient tool for analyzing non-stationary signals, where high-frequency short wavelets are used for high resolution time analysis, and long ones for high resolution frequency analysis.

The wavelet transform basically overcomes the drawbacks of the Short-Time Fourier Transform(STFT) introduced by Gabor[32], where the analysis is performed at a fixed time-frequency resolution [9]. The Continuous Wavelet Transform(CWT) can be discretized so that the set of basis functions form an orthonormal set, leading to the Discrete Wavelet Transform(DWT).

Daubechies[25] showed that the DWT can be viewed as a particular subband scheme, one in which the low-pass branch is iterated leading to octave band splitting. This was also demonstrated by Mallat and Meyer [59][68] within the concept of multiresolution analysis of signals. Multirate filter banks also find applications in signal scrambling [22] , spectral analysis [95], and adaptive filtering [50][34][30].

Research in this area has focussed on developing the reconstruction theory, identifying and classifying the various solutions, developing filter design procedures and algorithms, and the realization of efficient structures for implementation. The research literature mostly assumes that there is no processing of the subbands signals, such as quantization. This approach is adopted in this thesis.
Most of the theoretical development and design procedures have been based on frequency domain(z-domain) analysis of the systems.

The goal of this thesis is to develop algorithms relating both the z-domain and the time-domain. Standard digital filter design techniques are used directly in the design procedures. The designs are based on linear optimization techniques, since most of the designs in the literature use non-linear optimization, which is computationally intensive and does not always produce optimal results.

1.2 Overview of the Thesis

Chapter 2, develops the background material required for the remainder of the thesis. The fundamental building blocks of multirate systems are first reviewed. Next the analysis and design of two-channel filter banks are discussed. The general filter bank with arbitrary number of channels is reviewed. The discussion is based on the z-domain formulation. Although other techniques are briefly discussed. Finally the wavelet transform and its relation to multirate filter banks is reviewed.

Chapter 3 considers the spectral factorisation method for designing multirate filter banks. The technique is reviewed for the two-channel case, where it is the most common design method. Previous attempts to design arbitrary channel systems using spectral factorization are discussed. A new approach to the design of three channel FIR analysis/synthesis systems is then presented. This approach is based on frequency symmetry and does not require numerical optimisation.

Chapter 4 is concerned with the time-domain analysis and design of FIR multirate filter banks. The analysis is based on a block matrix formulation. Conditions for alias cancellation and perfect reconstruction are presented. The relationship between the block matrix time-domain formulation and the polyphase lossless conditions are established. A novel time-domain technique for designing multirate filter banks using standard digital filter design methods is presented.

Chapter 5 discusses the concept of low delay filter banks. A direct z-domain analysis and design of the two-channel system is first investigated. The time-domain formulation is then used to design low-delay filter banks. With a simple

modification to the time-domain technique developed in chapter 4, efficient low delay filter banks can be designed.

Chapter 6 the wavelet transform and its relation to multirate filter banks is discussed. Orthonormal and bi-orthogonal wavelets are designed using the time-domain technique. A new family of wavelets are introduced termed 'Low Delay' wavelet transforms, which addresses the problem of the growing delay in iterated filter banks. Chapter 7 concludes the work, and future research directions are discussed.

1.2.1 New Research Results

The main contributions of this thesis are summarized as follows :

- A new z-domain spectral factorization approach for designing 3-Channel based FIR Analysis/Synthesis Systems [5].
- Design of M-Channel FIR filter banks based on a general time domain framework, where the filter lengths and system delays are arbitrary [6].
- The design of low delay filter banks both in the z-domain and the time-domain [8].
- The design of a large class of Discrete Wavelet Transforms, based on the new time-domain approach [7].

Chapter 2

Review of Multirate Filter Banks

2.1 Introduction

In this chapter the necessary groundwork for the newer material developed in the subsequent chapters is presented. The chapter begins by reviewing basic multirate operations and relationships which are fundamental concepts in the area of multirate signal processing. Multirate filter banks, are then discussed starting with the two-channel filter bank, which is the most widely used. For the M-channel system the conditions for alias cancellation and perfect reconstruction are much more complicated. The general theory for perfect reconstruction and the concept of losslessnes within the polyphase structure of the filter bank is discussed.

A class of systems termed modulated filter banks, with the property that all the

filters are derived from a single prototype filter is then reviewed.

Finally the relation between filter banks and the wavelet transform theory is discussed.

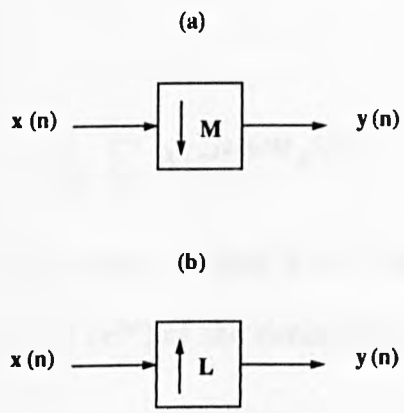

Figure 2.1: (a) Downsampling (b) Upsampling

2.2 Multirate Signal Processing

In multirate systems the sampling rate is varying throughout the various parts of the system, the basic building blocks and operations are presented in this section.

2.2.1 Downsampling

Downsampling is a linear periodically time varying operation denoted by a down-going arrow shown in Figure (2.1(a)), where M is a positive integer. Downsampling by a factor M has the effect of retaining one out of every M-th sample of the input sequence [23].

$$y(n) = x(Mn) \tag{2.1}$$

The operation is illustrated in Figure (2.2) for M=2.

The frequency domain relationship is

$$Y(e^{j\omega}) = \frac{1}{M}\sum_{k=0}^{M-1} X(e^{j(\omega+2\pi k)/M}) \tag{2.2}$$

and in the z-domain

$$Y(z) = \frac{1}{M}\sum_{k=0}^{M-1} X(e^{j2\pi k/M} z^{1/M}) \tag{2.3}$$

The relationship between the frequency response $X(e^{j\omega})$ of the original sequence $x(n)$ and the frequency response $Y(e^{j\omega})$ of the decimated sequence $y(n)$ is illustrated in Figure (2.3).

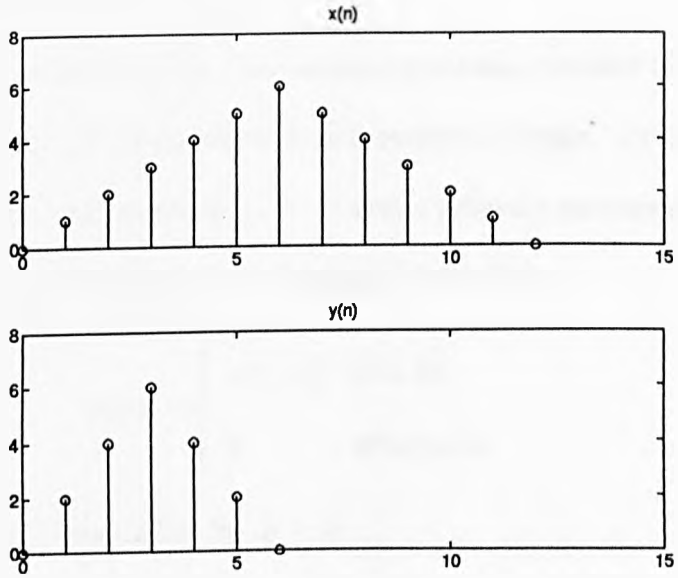

Figure 2.2: Downsampling in the time domain; x(n) is the input sequence; y(n) is the downsampled sequence for M=2.

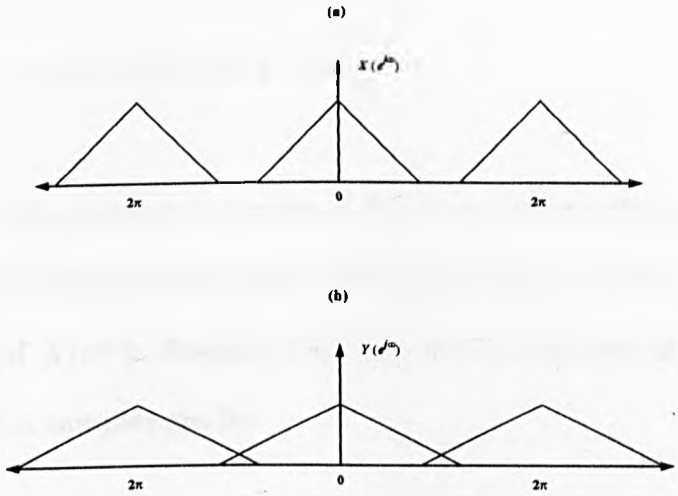

Figure 2.3: Downsampling in the frequency domain;(a) Input spectra; (b) Downsampled by 2, the spectral replicas stretch by a factor of 2

2.2.2 Upsampling

Upsampling is a linear periodically time varying operation denoted by the upgoing arrow shown in Figure (2.1(b)), where L is a positive integer. Upsampling by a factor L has the effect of inserting $(L-1)$ zeros between successive samples of the input sequence. This results in expansion in time [23].

$$y(n) = \begin{cases} x(n/L) & n = kL \\ 0 & otherwise \end{cases} \tag{2.4}$$

This is illustrated in Figure (2.4) for $L = 2$.

In the frequency domain

$$Y(e^{j\omega}) = X(e^{jL\omega}) \tag{2.5}$$

and the z-domain

$$Y(z) = X(z^M) \tag{2.6}$$

This is illustrated in Figure (2.5) for $L = 2$.

$Y(e^{j\omega})$ is an L-fold compressed version of $X(e^{j\omega})$, which results in an imaging effect. Aliasing causes loss of information, because of the possible overlap of the stretched versions of $X(e^{j\omega})$. Imaging does not lead to any loss of information since no time-domain samples are lost.

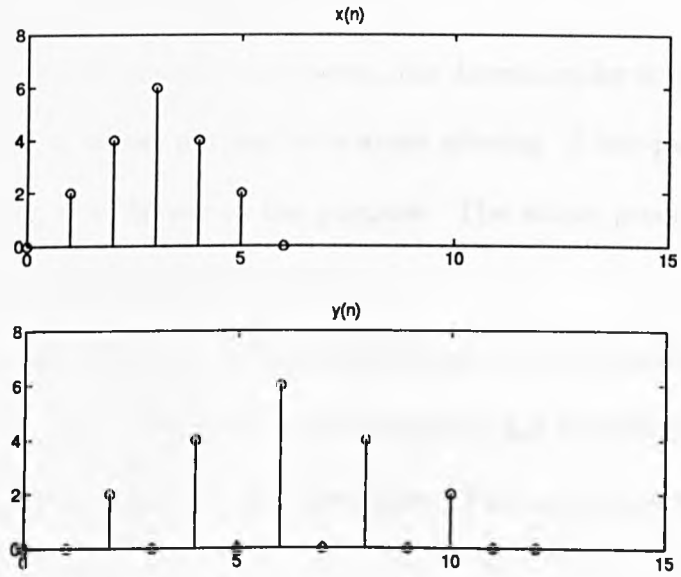

Figure 2.4: Upsampling in the time domain for $L = 2$.

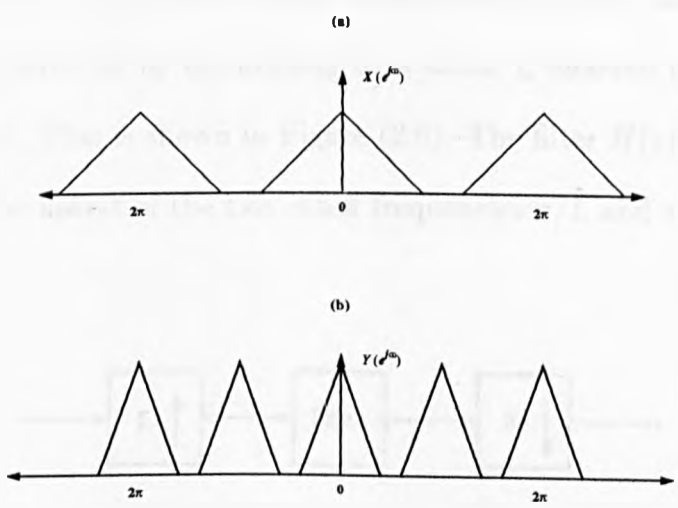

Figure 2.5: Upsampling in the frequency domain; (a) Input spectra; (b) Upsampled by 2, spectral replicas compressed by a factor of 2.

2.2.3 Decimation and Interpolation Filters

To avoid aliasing in the downsampling process, the downsampler is preceded by a bandlimiting filter $H(z)$ whose purpose is to avoid aliasing. A low-pass filter with a cutoff frequency $\omega_c = \pi/M$ serves the purpose. The whole process is termed decimation, and is illustrated in Figure.(2.7).

To eliminate the images created in the upsampling process a low-pass filter follows the upsampler. The filter is called an interpolator which has the effect of filling the zero-sampled values introduced by the upsampler. This operation is illustrated in Figure (2.8).

2.2.4 Fractional Sampling Rate Alterations

In some applications it is required to change the sampling rate by a rational factor L/M. This can be achieved by upsampling by a factor L followed by downsampling by a factor M. This is shown in Figure (2.6). The filter $H(z)$ has a cutoff frequency that is the lowest of the two cutoff frequencies π/L and π/M.

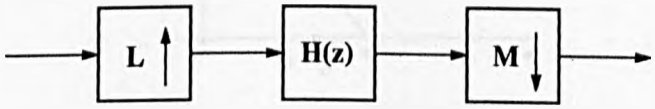

Figure 2.6: Sampling rate alteration by a factor L/M

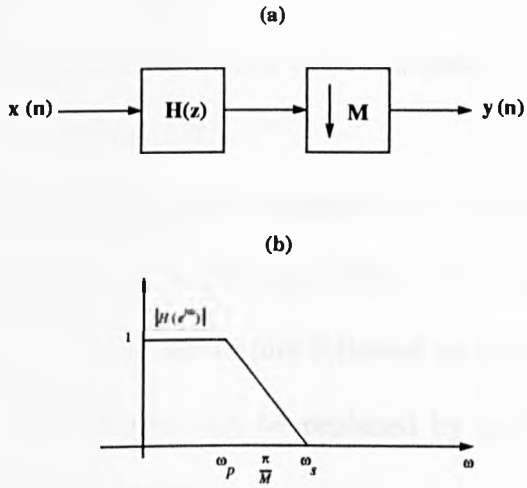

Figure 2.7: (a) The decimation operation; (b) Typical magnitude response of a decimation filter

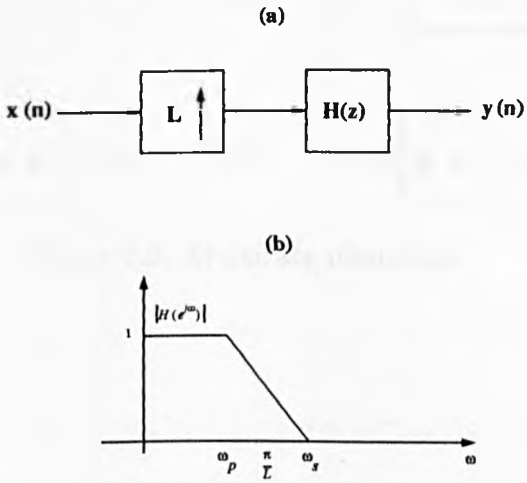

Figure 2.8: (a) The interpolation operation; (b) Typical magnitude response of an interpolation filter

2.2.5 Multirate Identities

An upsampler can be interchanged with a downsampler if and only if the sampling factors are relatively prime [108].

The order of the sampling change operation and the filtering operation can be interchanged using two important identities. A filter $G(z)$ followed by an L-fold upsampler can be replaced by the upsampler followed by $G(z^L)$ and a filter $G(z)$ preceded by a M-fold downsampler can be replaced by $G(z^M)$ followed by the downsampler as shown in Figure (2.9).

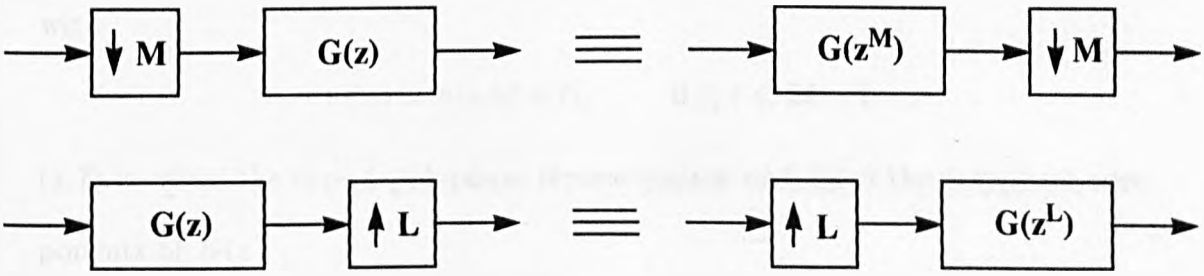

Figure 2.9: Multirate identities

2.2.6 The Polyphase Representation

The polyphase representation, first introduced by Bellanger [13], has proved to be an important advancement in multirate signal processing. This simplified many theoretical results and also leads to computationally efficient implementations of sampling rate converters, as well as filter banks [23].

For a given FIR transfer function, the M-component polyphase representation is defined as :

$$H(z) = \sum_{l=0}^{M-1} z^{-l} E_l(z^M) \tag{2.7}$$

where

$$E_l(z) = \sum_{-\infty}^{\infty} e_l(n) z^{-n}$$

with

$$e_l(n) = h(nM + l), \qquad 0 \leq l \leq M-1$$

(2.7) is called the type 1 polyphase representation and $E_l(z)$ the polyphase components of $H(z)$.

The type 2 representation is given by

$$H(z) = \sum_{l=0}^{M-1} z^{-(M-1-k)} R_l(z^M) \tag{2.8}$$

the type 2 polyphase components $R_l(z)$ are related to the type 1 components by

$$R_l(z) = E_{M-1-l}(z)$$

2.3 The Two-Channel Filter Bank

The two-channel filter bank was introduced by Croisier,et.al [24] and is shown in Figure (2.10). The input signal $x(n)$ is first filtered by two filters $H_0(z)$ and

$H_1(z)$, typically lowpass and highpass filters. Each subband signal $x_k(n)$ is then subsequently decimated by a factor of 2. In practical applications each decimated signal is then coded independently such that the properties of the subband are exploited.

At the receiver end, the received signals are decoded, upsampled, and then passed through the filters $F_0(z)$ and $F_1(z)$ to produce the output signal $\hat{x}(n)$.

$H_0(z)$ and $H_1(z)$ are called the analysis filters, $F_0(z)$ and $F_1(z)$ are called the synthesis(reconstruction) filters. Figure (2.10) ignores the coding and decoding which takes place between the downsampling and upsampling, since this is application specific.

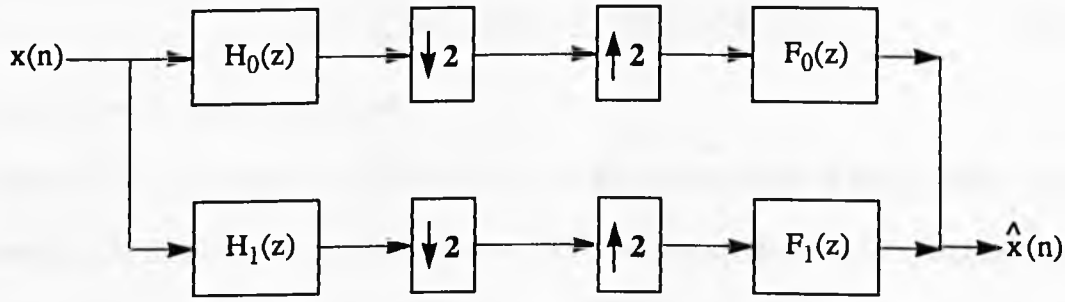

Figure 2.10: The two Channel Filter Bank

The input/output relationship can be derived using the multirate building blocks presented in section(2.2)

$$\begin{aligned}\hat{X}(z) &= \frac{1}{2}[H_0(z)F_0(z) + H_1(z)F_1(z)]X(z) \\ &+ \frac{1}{2}[H_0(-z)F_0(z) + H_1(-z)F_1(z)]X(-z) \qquad (2.9)\end{aligned}$$

The linear time invariant term $X(z)$ corresponds to the signal modified by the filters, and the linear time varying term $X(-z)$ corresponds to the aliasing component which originates because of the decimation.

The aliasing component is canceled by the suitable choice of synthesis filters :

$$F_0(z) = H_1(-z), \qquad F_1(z) = -H_0(-z) \tag{2.10}$$

Given $H_0(z)$ and $H_1(z)$, it is possible to completely cancel aliasing by this choice of synthesis filters regardless of their frequency responses.

With aliasing canceled we have

$$\hat{X}(z) = T(z)X(z)$$

where

$$T(z) = \frac{1}{2}[H_0(z)H_1(-z) - H_0(-z)H_1(z)] \tag{2.11}$$

is the overall transfer function.

Unless $T(z)$ is allpass (i.e $|T(e^{j\omega})| = c \neq 0$), we say that $\hat{X}(e^{j\omega})$ suffers from 'amplitude distortion', similarly unless $T(z)$ has linear phase $\hat{X}(e^{j\omega})$ suffers from phase distortion. If the system is free from all distortions, it is said to have Perfect Reconstruction(PR). This is equivalent to the condition $T(z) = cz^{-K}$, when

$$\begin{aligned} \hat{X}(z) &= cz^{-K}X(z) \\ \hat{x}(n) &= cx(n-K) \end{aligned} \tag{2.12}$$

where c and K are positive constants. $\hat{x}(n)$ is merely a scaled and delayed version of $x(n)$.

2.3.1 The Classical QMF

In the original formulation [24, 27] the analysis filters were related as

$$H_1(z) = H_0(-z) \tag{2.13}$$

this means $|H_1(e^{j\omega})| = |H_0(e^{j(\pi-\omega)})|$ where $|H_1(e^{j\omega})|$ is a mirror image of $|H_0(e^{j\omega})|$ with respect to the quadrature frequency $\pi/2$ (i.e 1/4 the sampling frequency), justifying the name Quadrature Mirror Filters (QMF).

With the choice of (2.10) we have

$$F_0(z) = H_0(z), \quad F_1(z) = -H_1(z)$$

Thus all the four filters are completely determined by a single filter $H_0(z)$. The overall transfer function becomes

$$T(z) = \frac{1}{2}[H_0^2(z) - H_0^2(-z)] \tag{2.14}$$

If $H_0(z)$ is a linear phase FIR filter, then $T(z)$ will also be a linear phase FIR filter, thereby eliminating any phase distortion. However amplitude distortion can not be completely removed except with a trivial choice of filters with only two coefficients [107, 108]. The most widely known method to reduce amplitude distortion is by Johnston[46], where an objective function is formulated which is a sum of the stopband error of $H_0(z)$ and the amplitude distortion function. The coefficients of $H_0(z)$ are found by minimizing the error using a non-linear optimization method.

A linear programming method is presented in [31]. More complex methods using

the minimax optimization are presented in [36][17][57].

A time-domain approach is presented in [44]. Solutions with complex coefficient filters are presented in [33]. Designs with VLSI considerations is presented in [84].

To eliminate amplitude distortion IIR filters can be used, and phase distortion is left to be minimized.

This is achieved by choosing

$$H_0(z) = \frac{1}{2}[A_0(z) + A_1(z)] \tag{2.15}$$

where $A_0(z)$ and $A_1(z)$ are all-pass filters [108] of the form

$$A_0(z) = a_0(z^2), \qquad A_1(z) = z^{-1}a_1(z^2)$$

various design methods based on this approach is presented in [107] [83][71][54].

2.3.2 Perfect Reconstruction QMF bank

The fundamental results for Perfect Reconstruction(PR) were developed by Smith and Barnwell [93], and also by Mintzer [73]. Both the amplitude and phase distortions are canceled simultaneously using a spectral factorization approach. The filter bank is termed Conjugate Quadrature Filter(CQF). The analysis filters are related by

$$H_1(z) = -z^{-(N-1)}H_0(-z^{-1}) \tag{2.16}$$

where N is an even integer.

For PR (2.11)(2.12) becomes

$$T(z) = G(z) + G(-z) = 2 \tag{2.17}$$

where $G(z) = H_0(z)H_0(z^{-1})$.

The equivalent time domain expression is

$$\sum_{n\ even} g(n)z^{-n} = 1$$

This implies that $G(z)$ is a zero phase half-band filter [72]. The analysis filters are obtained by the spectral factorisation of $G(z)$ into its respective zero terms and the appropriate zeros are assigned to $H_0(z)$ and $H_0(z^{-1})$. The analysis and synthesis filters are constrained to have non-linear phase.

The design of CQF using the binomial-Hermite sequences is presented in [3][4]. The Bernstein polynomials have been used to design CQF in [14]. An approach to match the signal statistics to the design of the CQF is presented in [115].
IIR filters can be used to achieve PR. However they require non-causal filtering in their implementation [12][39][97].

2.3.3 Linear Phase Filter Bank

In some applications linear phase filters with non-trivial forms are desirable [108]. To achieve PR with linear phase filters the mirror image constraint (2.16) on the analysis filters has to be relaxed [107].

A complementary filter method for designing linear phase PR two channel filter banks is presented in [116][118], where the filter $H_0(z)$ is chosen and the filter $H_1(z)$ is derived. This method is also used in [45].

Designs based on exploiting the algebraic structure of the two-channel filter bank, where concepts from abstract algebra such as the Bezout identity, Diophantine equations and continued fraction expansions are used in [38][121].

Lagrange multiplier optimization methods are used in [41]. Implementations that do not require the use of multiplications are presented in [42][1]. Designs based on lattice structures are presented in [78].

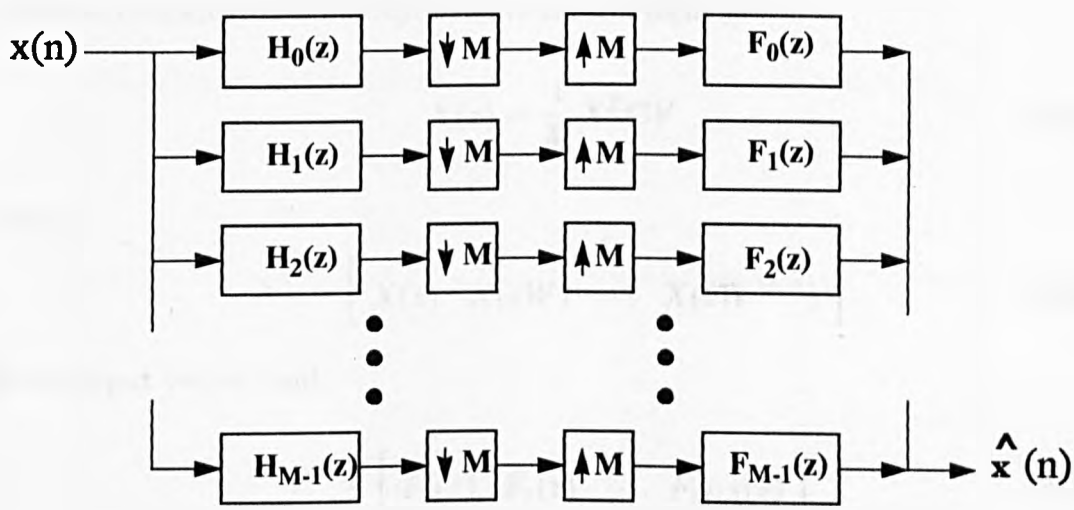

Figure 2.11: Maximally Decimated M-Channel Filter Bank

2.4 M-Channel Filter Bank

M-channel systems where M is an integer power of two can be obtained using tree structure of two channel systems [108]. However the resulting filters are sub-optimal, and the length of the filters grow exponentially with the number of tree levels.

For a general M-channel maximally decimated system shown in Figure (2.11), the output $\hat{X(z)}$ can be expressed as follows :

$$\hat{X}(z) = \frac{1}{M}\sum_{k=0}^{M-1}\sum_{l=0}^{M-1} X(zW^l)H_k(zW^l)F_k(z), \qquad W = e^{-j2\pi/M} \tag{2.18}$$

which equivalently can be expressed in matrix form as :

$$\hat{X}(z) = \frac{1}{M}X^T\mathbf{C}V \tag{2.19}$$

where

$$X^T = \begin{bmatrix} X(z) & X(zW) & \cdots & X(zW^{M-1}) \end{bmatrix} \tag{2.20}$$

is the input vector, and

$$V^T = \begin{bmatrix} F_0(z) & F_1(z) & \cdots & F_{M-1}(z) \end{bmatrix} \tag{2.21}$$

is the vector of the synthesis filters, and

$$\mathbf{C} = \begin{bmatrix} H_0(z) & H_1(z) & \cdots & H_{M-1}(z) \\ H_0(zW) & H_1(zW) & \cdots & H_{M-1}(zW) \\ \vdots & \vdots & \cdots & \vdots \\ H_0(zW^{M-1}) & H_1(zW^{M-1}) & \cdots & H_{M-1}(zW^{M-1}) \end{bmatrix} \tag{2.22}$$

is the aliasing component matrix or AC matrix [94].

The system is free from aliasing if the $l \neq 0$ terms are equal to zero

$$CV = \begin{bmatrix} MT(z) & 0 & \cdots & 0 \end{bmatrix}^T \tag{2.23}$$

and the system has PR if

$$T(z) = \frac{1}{M} \sum_{k=0}^{M-1} H_k(z) F_k(z) = cz^{-K} \tag{2.24}$$

where c and K are positive integers.

Although in theory the synthesis filters can be obtained by inverting the AC matrix, this would lead to PR. However this leads to IIR solutions which are often unstable even if the analysis filters are FIR.

FIR filters are guaranteed [94] if

$$det[\mathbf{C}] = cz^{-K}$$

This motivates solutions that do not involve the inverse of the AC matrix.

2.4.1 Lossless, paraunitary filter banks

The multirate filter bank can be implemented in a more efficient form using the Polyphase representation presented in section (2.2.6).

Figure (2.12) shows the polyphase representation of the maximally decimated filter bank. The polyphase filter bank can be transformed as in Figure (2.13) using the multirate identities in Figure (2.9) where

$$\mathbf{E}(z) = [E_{kl}(z)] \qquad \mathbf{R}(z) = [R_{lk}(z)] \quad 0 \leq l, k \leq M-1$$

The filtering operations are now carried out at the lowest possible sampling rate. Defining a matrix $\mathbf{P}(z) = \mathbf{E}(z)\mathbf{R}(z)$, a necessary condition for aliasing cancellation is that the matrix $\mathbf{P}(z)$ be pseudo-circulant [111].

The necessary and sufficient conditions for perfect reconstruction is shown to be [106]

$$\mathbf{P}(z) = \frac{\alpha}{M}\begin{bmatrix} \mathbf{O} & z^{k_{01}}\mathbf{I_1} \\ z^{-(k_{01}+1)}\mathbf{I_2} & \mathbf{O} \end{bmatrix} \tag{2.25}$$

k_{01} is such that $k_0 = k_{00} + k_{01}M$ and $k_{00} = k_0 \bmod M$ for some integer k_0 that determines the system delay [106] such that

$$\hat{X}(z) = \frac{\alpha}{M} z^{-(k_0+M-1)} X(z) \tag{2.26}$$

The matrix $\mathbf{I_1}$ is the $(M - k_{00}) \times (M - k_{00})$ identity matrix, and $\mathbf{I_2}$ is the $k_{00} \times k_{00}$ identity matrix and α is an arbitrary constant.

Vaidyanathan [106] has introduced the concept of losslessnes into the analysis of multirate filter banks. A lossless transfer matrix $\mathbf{H}(z)$ (assuming real coefficients) satisfies

$$\mathbf{H}^T(z)\mathbf{H}(z) = \mathbf{H}(z)\mathbf{H}^T(z) = \mathbf{I}$$

if $\mathbf{H}^T(e^{j\omega})\mathbf{H}(e^{j\omega}) = \mathbf{H}(e^{j\omega})\mathbf{H}^T(e^{j\omega}) = \mathbf{I}$, then matrix $\mathbf{H}(z)$ is called paraunitary (unitary on the unit circle). The most important property of the paraunitary matrix is that

$$\mathbf{H}^{-1}(z) = \mathbf{H}^T(z^{-1}) \tag{2.27}$$

which implies that if the AC matrix is paraunitary then perfect reconstruction filters can be obtained using (2.27). Returning to the polyphase form, if $\mathbf{E}(z)$ is

paraunitary then $\mathbf{R}(z) = \mathbf{E}^T(z^{-1})$, and the resulting synthesis filters are identical to the analysis filters within time reversal [119]. The design of paraunitary systems proposed in [106] is based on the structural parameterization approach where the perfect reconstruction conditions are structurlly imposed. The matrix $\mathbf{E}(z)$ is implemented as a cascade of $M \times M$ orthogonal matrices K_i and diagonal blocks of delays $\Lambda_i(z)$.

A non-linear optimisation method is then used to optimize the parameters that yield good quality analysis filters. The advantage is that perfect reconstruction is preserved under quantisation. Details can be found in [106][110][26]. Paraunitary filter banks are also known as orthogonal filter banks [2]. The paraunitary property can be quite a constraining condition. For example a paraunitary linear phase two channel solution does not exist. Paraunitary linear phase M-channel ($M > 2$) solutions and structures are presented in [100].

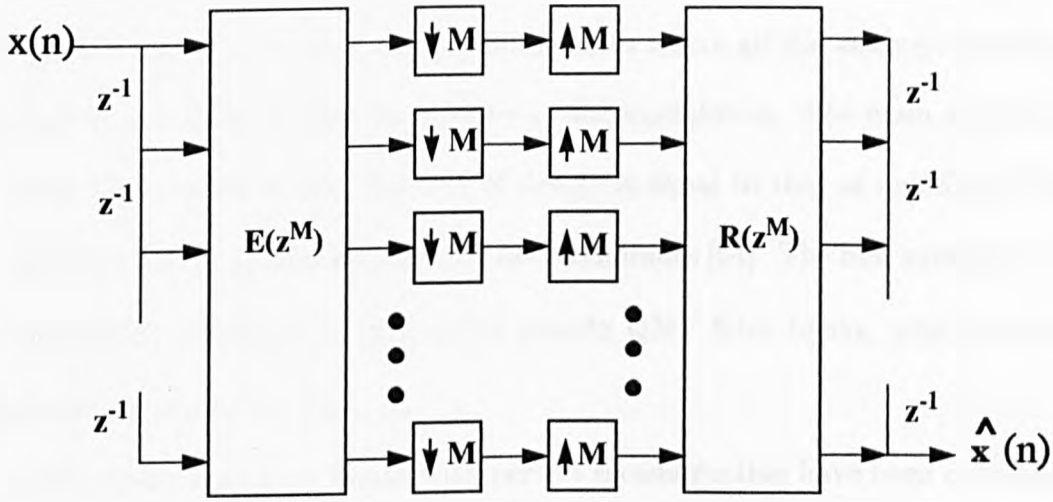

Figure 2.12: The Polyphase structure of the filter bank

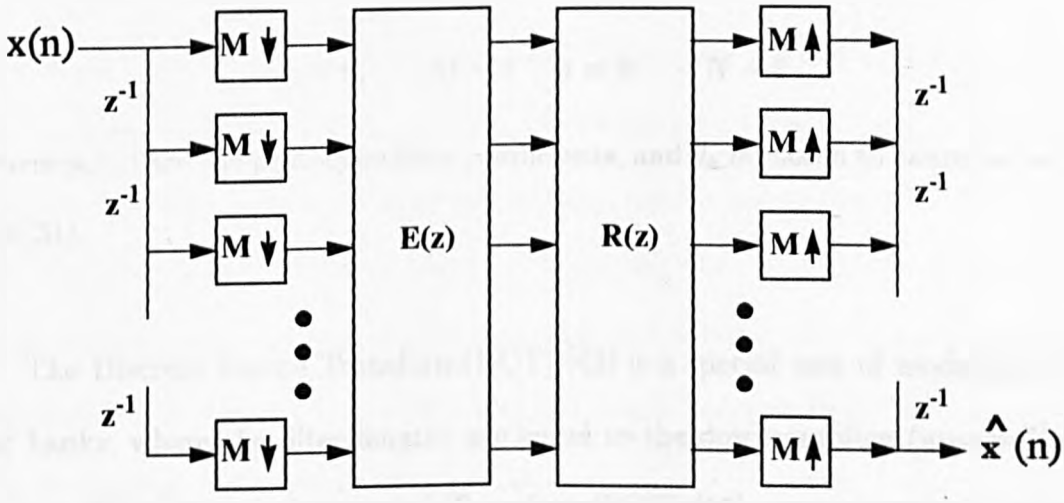

Figure 2.13: Transformed Polyphase structure of the filter bank

2.4.2 Modulated filter banks

Modulated filter banks are a class of filter banks where all the analysis filters are derived from a single prototype filter by cosine modulation. The main advantage of these filter banks is that the cost of design is equal to that of one filter. The modulation can be implemented using fast techniques [64]. The first systems were introduced by Nussbaumer [82], called pseudo QMF filter banks, which achieve approximate reconstruction.

Recently modulated filter banks with perfect reconstruction have been developed in [63][64][87][52][51] which all have the paraunitary property. In general the analysis filter coefficients have the form

$$h_k(n) = 2p_0(n)cos(\pi/M(k+0.5)(n-N/2)+\theta_k) \tag{2.28}$$

$$k = 0, \cdots, M-1 \quad n = 0, \cdots, N-1$$

where $p_0(n)$ are the prototype filter coefficients, and θ_k is chosen to cancel aliasing [64][51].

The Discrete Cosine Transform(DCT) [43] is a special case of modulated filter banks, where the filter lengths are equal to the downsampling (upsampling) factor. The Lapped Orthogonal Transform(LOT) [65] was subsequently introduced, where the filter lengths are twice the downsampling (upsampling factor). PR modulated filter banks have the paraunitary property, and the filters are constrained to have non-linear phase.

2.4.3 Time-domain techniques

Analysis of multirate filter banks in the time-domain are presented in [119][75]. The perfect reconstruction conditions are expressed in a block matrix form of equations. These equations are a set of conditions on the impulse response of the filters. Time-domain analysis is discussed in detail in Chapter 4. An optimisation technique is used to optimise the coefficients of the filters subject to the conditions for perfect reconstruction. In [56], a simulated annealing algorithm is used for the optimisation.

2.5 Wavelets and Filter Banks

The theory of multirate filter banks and the wavelet transform have recently converged to form a single theory [59][25]. Wavelet transforms have found applications in several areas such as speech coding, data compression, edge detection, and the detection of transient signals [21][55][59][104]. Also wavelets have been used extensively in image processing applications [11][60][123]. A signal processing overview of wavelet transform theory will now be presented. Further details can be found in [19][20][68][21][11][37].

The continuous time wavelet transform can be obtained from infinite level binary tree structured QMF banks, with the same filters on each level. This infinite recursion gives rise to two continuous time functions $\psi(t)$ and $\phi(t)$, which are termed the wavelet function and the scaling function respectively. The wavelet

basis is then obtained by dyadic scaling and shifting of the wavelet function $\psi(t)$ [25].

For a signal $x(t)$, the continuous wavelet transform is

$$X_{CWT}(p,q) = \frac{1}{\sqrt{p}} \int_{-\infty}^{\infty} f(\frac{t-q}{p})x(t)dt \tag{2.29}$$

the family of functions $f((t-q)/p)$ are generated from a single function $f(t)$ by translations and dilations where p is the dilation parameter and q is the translation parameter. This is a mapping from a one-dimensional continuous variable, t, to two-dimensional continuous variables (p,q).

The CWT is highly redundant when the parameters (p,q) are continuous, therefore if p and q are restricted to discrete values, the Discrete Wavelet Transform(DWT) is obtained.

For discrete-time signals

$$y_k(n) = \sum_m h_k(n)x(I_k n - m), \qquad 0 \le k \le L \tag{2.30}$$

is the DWT of the signal $x(n)$. By choosing $I_k = 2^{k+1}$, $k = 0, \cdots, L-1$, the binary DWT is obtained [105]. $y_k(n)$ are the wavelet coefficients of $x(n)$. (2.30) is a convolution followed by downsampling by a factor I_k. This can be obtained by passing the signal through a bank of $(L+1)$ filters $h_k(n)$, and downsampling the filter outputs by I_k. The system is maximally decimated if $\sum(1/I_k) = 1$ [99]. Figure (2.14) shows the implementation of the binary DWT. The signal can be recovered from its wavelet coefficients as

$$\hat{x}(n) = \sum_{k=0}^{L} \sum_m y_k(m)\eta_{km}(n) \tag{2.31}$$

This is the inverse discrete wavelet transform(IDWT) and $\eta_{km}(n)$ are termed the wavelet basis functions [120][105]. Figure (2.15) shows the filter bank implementation of the IDWT.

The synthesis filters are related to the functions η_{km} as [105]

$$\eta_{km} = f_k(n - 2^{k+1}m), \qquad k = 0, \cdots, L-1$$

$$\eta_{Lm} = f_L(n - 2^L m) \tag{2.32}$$

From a signal processing point of view, a wavelet is a bandpass filter. In the dyadic case, it is an octave band filter. Therefore the wavelet transform can be interpreted as a constant-Q filtering with a set of octave-band filters, followed by sampling at the respective Nyquist frequency. It is thus clear that by adding higher octave bands, one adds detail, or resolution to the signal.

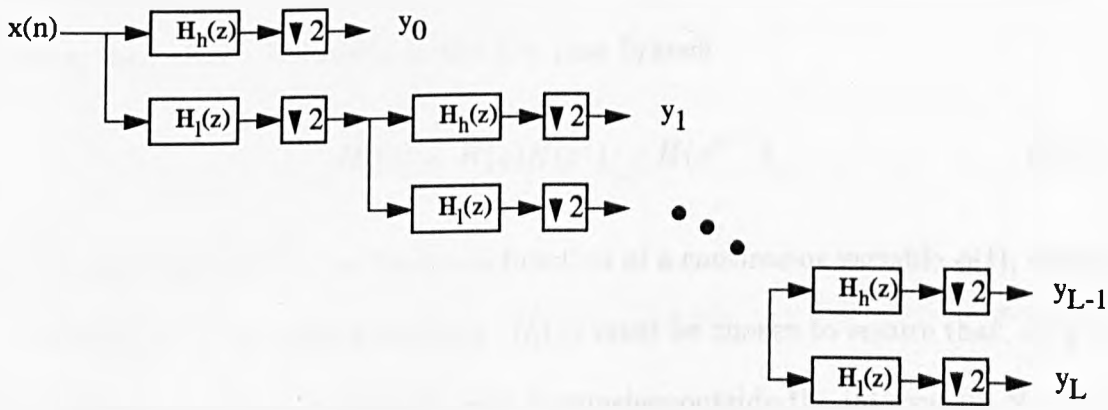

Figure 2.14: Filter bank implementation of the DWT; $H_l(z)$ and $H_h(z)$ are low-pass and high-pass analysis filters respectively.

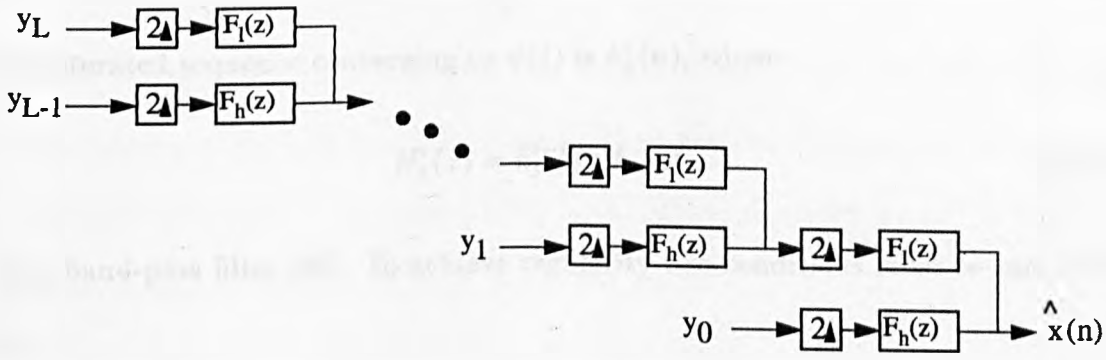

Figure 2.15: Filter bank implementation of the IDWT; $F_l(z)$ and $F_h(z)$ are low-pass and high-pass synthesis filters respectively.

2.5.1 Regularity

The construction of continuous time wavelets simply consists of iterating the two channel filter bank indefinitely. If $H_l(z)$ and $H_h(z)$ are the low-pass and high-pass filters, then after i iterations in the low-pass branch

$$H_l^i(z) = H(z)H(z^2)\cdots H(z^{2^{i-1}}) \tag{2.33}$$

$H^i(z)$ may converge in the limit to a function of a continuous variable $\phi(t)$, which is referred to as the scaling function. $H_l(z)$ must be chosen to ensure that, $\phi(t)$ is a smooth or regular function of t which vanishes outside the interval $(0, N-1)$. So regularity can be thought of as a smoothness requirement on a continuous time function, and can be mathematically defined as the continuity of this function and its derivatives [90][25].

The idea is to look at the impulse responses of $h^i(n)$ as i increases. The wavelet is constructed from

$$\psi(t) = \sum_n h_h(n)\phi(2t-n) \tag{2.34}$$

the iterated sequence converging to $\psi(t)$ is $h_h^i(n)$, where

$$H_h^i(z) = h_l^{i-1}(z)h_h(z^{2^{i-1}}) \tag{2.35}$$

is a band-pass filter [89]. To achieve regularity two conditions must be met, one is

$$\sum_n h_l(n) = \sqrt{2}$$

which is a normalization requirement.

The second states that the low-pass filter frequency response $H(e^{j\omega})$ vanishes at

the Nyquist frequency $\omega = \pi$ (i.e $H(z = -1) = 0$) which is crucial for regularity [25].

In general the low-pass filter must have at least $(R+1)$ zeros at $z = -1$ to achieve regularity of order R. This amounts to requiring that the frequency response of $H(e^{j\omega})$ is flat about $\omega = \pi$. Regularity of $H_l(z)$ is inversely proportional to the stopband attenuation. So as regularity increases, the the stopband attenuation becomes weaker [89].

The design of orthonormal and bi-orthogonal wavelets is discussed in detail in chapter.6.

Recently the binary wavelet transform have been generalized to M-channel wavelets related to nonuniform filter banks with nondyadic decimation ratios, these have been referred to as wavelet packets [90][103].

2.6 Summary

The theory of multirate filter banks has been reviewed in this chapter, and the basic multirate building blocks discussed. Then the two-channel filter bank was described. The general M-channel filter bank has been reviewed, and the wavelet transform and its relation to filter banks discussed.

Chapter 3

A Spectral Factorisation Approach to 3-Channel Filter Banks

3.1 Introduction

One of the most commonly used multirate filter banks is a cascaded tree structure of two channel prototype systems. This obviously can implement any filter bank with a power of two number of channels. One of the advantages of such cascaded structures is that the prototype filter bank can be determined without the need for numerical optimisation [73] [93]. Complex optimisation procedures are generally required to design analysis/synthesis systems whose orders are not powers of two [108].

A new technique is presented in this chapter which enables tree structures of three

channel systems to be obtained, without resorting to optimisation. The proposed method is based upon the application of standard digital filter techniques to design a low-pass filter, from which the required bandpass and high-pass filters are derived subject to symmetry constraints. This method produces filter banks in which the magnitude and phase distortions are completely eliminated, and with aliasing errors comparable to other techniques [52].

The virtue of the method outlined is its inherent simplicity, and it now becomes possible to design any analysis/synthesis filter bank with orders of powers of 2 or 3 number of channels without resorting to any complex procedures [5].

3.2 Review of Spectral Factorization

3.2.1 The Two-Channel System

Consider the two channel filter bank in Figure.(2.10)

$$\begin{aligned}\hat{X}(z) &= \frac{1}{2}[H_0(z)F_0(z) + H_1(z)F_1(z)]X(z) \\ &+ \frac{1}{2}[H_0(-z)F_0(z) + H_1(-z)F_1(z)]X(-z) \qquad (3.1)\end{aligned}$$

The term involving $X(-z)$ is the aliasing term and is required to be made zero. In [93][73] the following relations between the filters are enforced

$$\begin{aligned}H_1(z) &= z^{-(N-1)}H_0(-z^{-1}) \\ F_0(z) &= z^{-(N-1)}H_0(z^{-1}) \\ F_1(z) &= z^{-(N-1)}H_1(z^{-1}) \qquad (3.2)\end{aligned}$$

where N is the length of $H_0(z)$ which is constrained to be even.

The analysis filters $H_0(z)$ and $H_1(z)$ are constrained to satisfy

$$H_0(z^{-1})H_0(z) + H_1(z^{-1})H_1(z) = 1 \tag{3.3}$$

(3.2) is sufficient to enforce the condition

$$H_0(-z)F_0(z) + H_1(-z)F_1(z) = 0 \tag{3.4}$$

and thereby canceling aliasing.

Then (3.1) becomes

$$\hat{X}(z) = \frac{1}{2}z^{-(N-1)}[H_0(z^{-1})H_0(z) + H_1(z^{-1})H_1(z)]X(z) \tag{3.5}$$

then (3.3) can be written as

$$G(z) + G(-z) = 1 \tag{3.6}$$

where $G(z)$ is constrained to be a linear-phase FIR half-band filter [93] of length $(2N-1)$.

The frequency response of $G(z)$ exhibits symmetry with respect to $\pi/2$, in particular $\omega_s = \pi - \omega_p$, where ω_p is the passband frequency and ω_s is the stopband frequency.

The design of the analysis filters now amounts to the design of the product filter $G(z)$. Then $G(z)$ is factored into its respective zero terms and appropriate zeros are assigned to $H_0(z)$ and $H_0(z^{-1})$.

3.2.2 M-Channel Filter Bank

In [112] an M-channel spectral factorization approach was discussed. The approach is based on designing an M-th band filter

$$G(z) = \sum_{n=0}^{N-1} g(n) z^{-n} \tag{3.7}$$

where $G(z)$ is a linear phase low-pass filter with cutoff π/M satisfying

$$g(n) = 0, \quad n - \frac{N-1}{2} = \text{nonzero multiples of M} \tag{3.8}$$

A zero-phase FIR filter is defined such that

$$G_1(z) = z^{(N-1)/2} G(z)$$

because of (3.8) $G_1(z)$ satisfies

$$\sum_{k=0}^{M-1} G_1(zW^{-k}) = Mg(\frac{N-1}{2}), \quad W = e^{-2\pi j/M} \tag{3.9}$$

Causal spectral factors are defined as

$$H_k(z) H_k^*(z^{-1}) = G_1(zW^{-k}), \quad 0 \leq k \leq M-1 \tag{3.10}$$

then

$$\sum_{k=0}^{M-1} H_k(z) H_k^*(z^{-1}) = Mg(\frac{N-1}{2}) \tag{3.11}$$

Accordingly designing $H_k(z)$ in the above manner, and the choice of synthesis filters as

$$F_k(z) = z^{-(N-1)} H_k(z^{-1})$$

perfect reconstruction is achieved under the assumption that aliasing is negligible. $H_k(z)$ chosen from (3.10) will have complex coefficients except with $k = 0$, and hence the subband signals would be complex, even for real signals. This would not always be desirable. In [52] a spectral factorization approach to design pseudo-QMF banks is presented, where the prototype filter is a spectral factor of a 2Mth band filter. In this design aliasing is approximately canceled , and the magnitude response has undesirable effects around $\omega = 0$ and $\omega = \pi$.

3.3 3-Channel System

Consider the maximally decimated 3-channel system shown in Figure (3.1). The overall transfer function can be written as a linear combination of a linear time varying-term $A(z)$, and a linear time invariant term $T(z)$ where

$$A(z) = \frac{1}{3}\sum_{l=1}^{2}\sum_{k=0}^{2} H_k(zW^l)F_k(z), \qquad W = e^{-j2\pi/3} \tag{3.12}$$

and

$$T(z) = \frac{1}{3}\sum_{k=0}^{2} H_k(z)F_k(z) = \frac{1}{3}\sum_{k=0}^{2} G_k(z) \tag{3.13}$$

Aliasing is eliminated if $A(z)$ is equal to zero, phase error is eliminated if $T(z)$ has linear phase, and magnitude error is eliminated if $T(z)$ is all-pass.

The system has perfect reconstruction(PR) if $T(z)$ is a pure delay such that

$$T(z) = \frac{1}{3}\sum_{k=0}^{2} G_k(z) = z^{-(N-1)} \tag{3.14}$$

where N is the analysis and synthesis filter lengths. (3.14) is satisfied if the filters $G_k(z)$ are $(2N-1)$ zero-phase third-band filters with impulse responses constrained to have every third term equal to zero and with the center term equal to 1/3 [72] i.e.

$$\begin{aligned} g_k(N-1) &= \tfrac{1}{3} \\ g_k(3n) &= 0, \qquad 0 \le n \le 2N-1 \end{aligned} \tag{3.15}$$

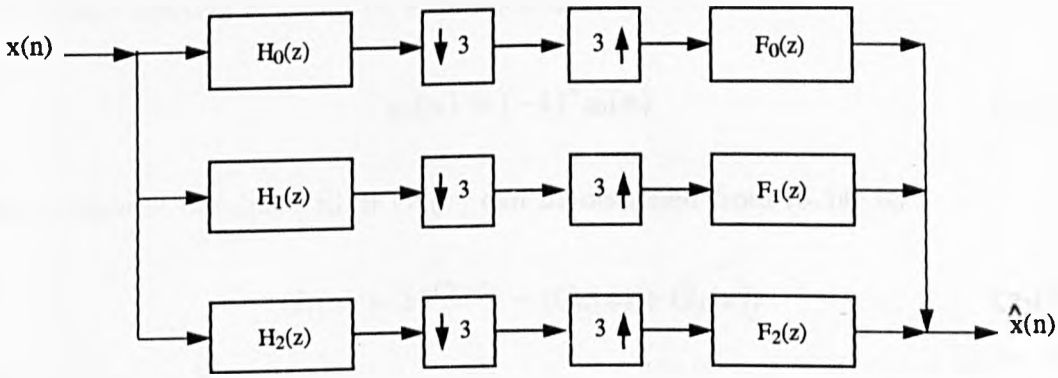

Figure 3.1: Maximally decimated 3-channel system

3.4 Product Filter Design

To design the product filters $G_k(z)$ to satisfy (3.15) and have good frequency responses, a pair-wise mirror image symmetry condition [77] is imposed on the frequency responses of the product filters. Pair-wise mirror image symmetry

states that the frequency response of the filters are symmetric about $\pi/2$, therefore

$$G_k(z) = G_{2-k}(-z) \qquad k = 0, 1, 2 \tag{3.16}$$

and

$$|G_k(e^{j\omega})| = |G_{2-k}(e^{j(\omega-\pi)})|$$

The procedure starts by designing the low-pass filter $G_0(z)$ subject to the condition in (3.15), and the high-pass filter $G_2(z)$ can be obtained by

$$G_2(z) = G_0(-z)$$

In the time-domain this can be expressed as

$$g_2(n) = (-1)^n g_0(n) \tag{3.17}$$

The composite bandpass filter $G_1(z)$ can be obtained from (3.14) by

$$G_1(z) = z^{-(N-1)} - (G_0(z) + G_2(z)) \tag{3.18}$$

The product filters are now said to be strictly complementary [108]. A signal filtered by $G_k(z)$ can be reconstructed exactly (except for a delay) simply by adding the subband signals.

3.5 Spectral Factorisation

The second stage of the procedure is to impose constraints on $H_k(z)$ and $F_k(z)$ to ensure that $T(z)$ is free from phase distortion. This is achieved by setting the

synthesis filters as time reversed versions of the analysis filters viz

$$F_k(z) = z^{-(N-1)} H_k(z^{-1}) \tag{3.19}$$

Then from (3.13) the product filters must have the form

$$G_k(z) = z^{-(N-1)} H_k(z^{-1}) H_k(z) \tag{3.20}$$

Substituting in (3.14) results in

$$T(z) = \frac{z^{-(N-1)}}{3} \sum_{k=0}^{2} H_k(z^{-1}) H_k(z) \tag{3.21}$$

Clearly

$$3T(e^{j\omega}) = e^{-j\omega(N-1)} \sum_{k=0}^{N-1} |H_k(e^{j\omega})|^2 \tag{3.22}$$

which shows that $T(z)$ has linear phase.

It is observed that the analysis filters satisfy the power complementary property

$$\frac{1}{3} \sum_{k=0}^{2} |H_k(e^{j\omega})|^2 = 1 \tag{3.23}$$

which is not necessarily sufficient for perfect reconstruction for more than two channels [107] [108]. However with a suitable choice of filters aliasing can be minimized to an acceptable level.

Since $H_k(z)$ and $F_k(z)$ must be FIR filters , then

$$G_k(z) = C \prod_{m=1}^{2N-2} (z - z_m)(z^{-1} - z_m) \tag{3.24}$$

where C is a constant. This means that for every zero of $G_k(z)$ at $re^{j\phi}$ there must be a zero at $(1/r)e^{-j\phi}$, and any zeros on the unit circle must have a multiplicity of two. Then for each zero pair in $G_k(z)$ one of the pair is included in

the analysis filter while the other is included in the synthesis filter. The analysis and synthesis filters always have identical magnitude responses, which is exactly the square root of the magnitude responses of $G_k(z)$. Therefore $G_k(z)$ must be designed to be the square of the desired analysis filters.

The number of possible factorizations of $G_0(z)$ into $H_0(z)$ and $F_0(z)$ grows exponentially with the number of zeros [118]. Assuming $G_0(z)$ is of odd length L FIR filter, the number of possible factorizations of its $L-1$ zeros into equal groups of $(L-1)/2$ zeros is equal to

$$n_i = \frac{2^{(L-1)}}{\sqrt{2\pi(L-1)}}$$

The problem is that while the product of two good low-pass filters yields a good low-pass filter, the reciprocal statement is not necessarily true [118].

All the possible factors should have identical magnitude responses but differing phase responses.

3.6 Minimum/Maximum Phase Design

Because of the large number of possible factorizations, it is preferable to use factorizations where fast algorithms exist: a unique factorization is the minimum/maximum phase filters [52]. The simplest way to design a third-band filter without the use of optimization, is to use a window based method to obtain $G_0(z)$. The impulse response of the low-pass filter $G_0(z)$ has the form

$$g_0(n) = \frac{sin(\pi n/3)}{\pi n} w(n) \tag{3.25}$$

where $g_0(n)$ has length $2N-1$, and $w(n)$ is an appropriate window function.

In order for the product filter to be factorised into FIR filters with identical magnitude response, it has to have a positive spectrum. This is achieved by applying the following transformation on the impulse responses of the filters $G_k(z)$

$$\tilde{g}_0(n) = \begin{cases} g_0(n) & n \neq 0 \\ g_0(n) + \delta_s & n = N-1 \end{cases} \tag{3.26}$$

where δ_s is the maximum stopband attenuation. The filter is no longer a third band filter, to produce a third band filter, the coefficients are re-scaled via $\tilde{g}_0(n) = \tilde{g}_0(n)/(3*\tilde{g}_0(N-1))$. This filter is a third band filter with a nonnegative frequency response. For a minimum/maximum phase design, the zeros inside the unit circle are allocated to the analysis filters, and the zeros outside the unit circle are allocated to the synthesis filters.

3.6.1 Aliasing Error

For aliasing cancellation the following two conditions must be satisfied from (3.12)

$$\begin{aligned} H_0(zW)F_0(z) + H_1(zW)F_1(z) + H_2(zW)F_2(z) &= 0 \\ H_0(zW^2)F_0(z) + H_1(zW^2)F_1(z) + H_2(zW^2)F_2(z) &= 0 \end{aligned} \tag{3.27}$$

Figure (3.2(a),(b),(c)) shows typical magnitude responses of the three analysis filters, along with their shifted versions, assuming that only adjacent filters overlap.

The signal which enters the filters $F_k(z)$ contains the terms

$$H_0(z)X(z), H_0(zW)X(zW), and \;\; H_0(zW^2)X(zW^2)$$

The purpose of $F_k(z)$ is to eliminate the terms involving $X(zW)$ and $X(zW^2)$. This is done if $F_k(z)$ attenuates the replicas $H_k(zW)$ and $H_k(zW^2)$, and retains only $H_k(z)$. For this reason, the responses of $|F_k(e^{j\omega})|$ resembles $|H_k(e^{j\omega})|$, as shown in Figure (3.2(d)). Since the filters $F_k(z)$ are not ideal in practice, they do not completely eliminate the shifted replicas $H_k(zW)$ and $H_k(zW^2)$. The terms in (3.27) are not individually equal to zero. The residual aliasing terms are shown in Figure (3.3,3.4) for $l = 1$, and $l = 2$. The responses of $H_0(zW^l)F_0(z)$ and $H_1(zW^l)F_1(z)$ has overlap, and so do the responses of $H_1(zW^l)F_1(z)$ and $H_2(zW^l)F_2(z)$. The idea is to choose the synthesis filters such all the overlapping terms are canceled out.

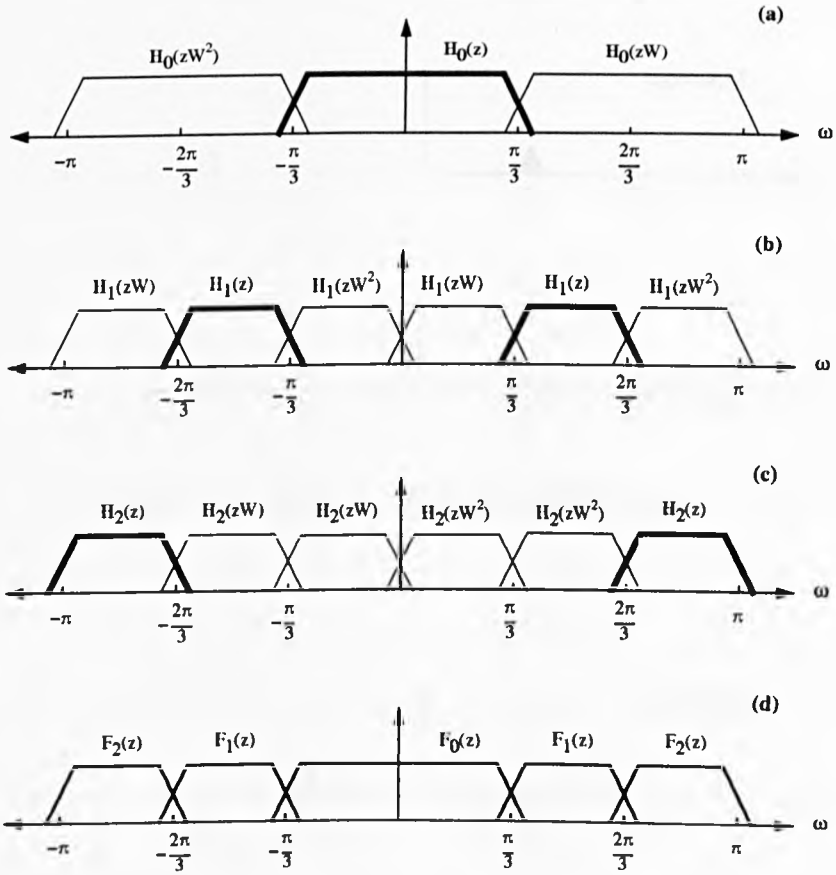

Figure 3.2: (a),(b),(c) Magnitude responses of the analysis filters (bold) and their aliasing versions. (d) Magnitude responses of the synthesis filters.

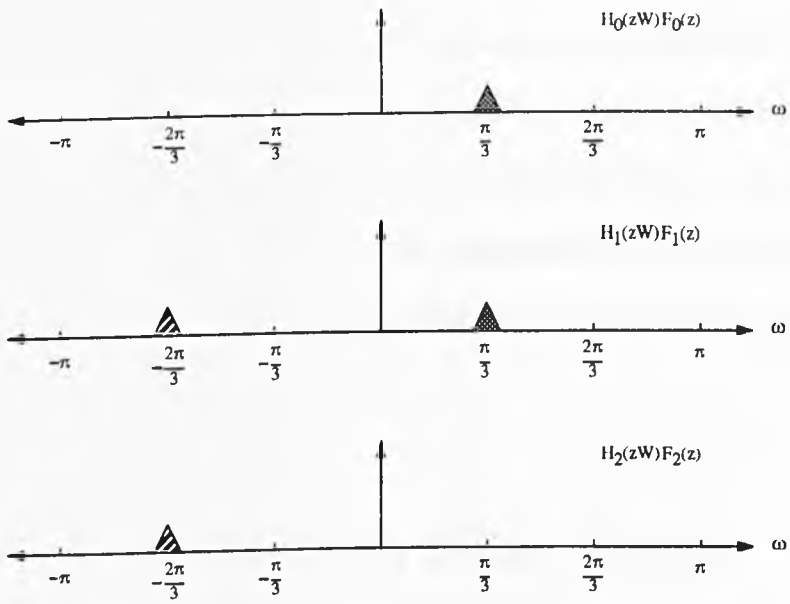

Figure 3.3: Residual alias terms with $l = 1$

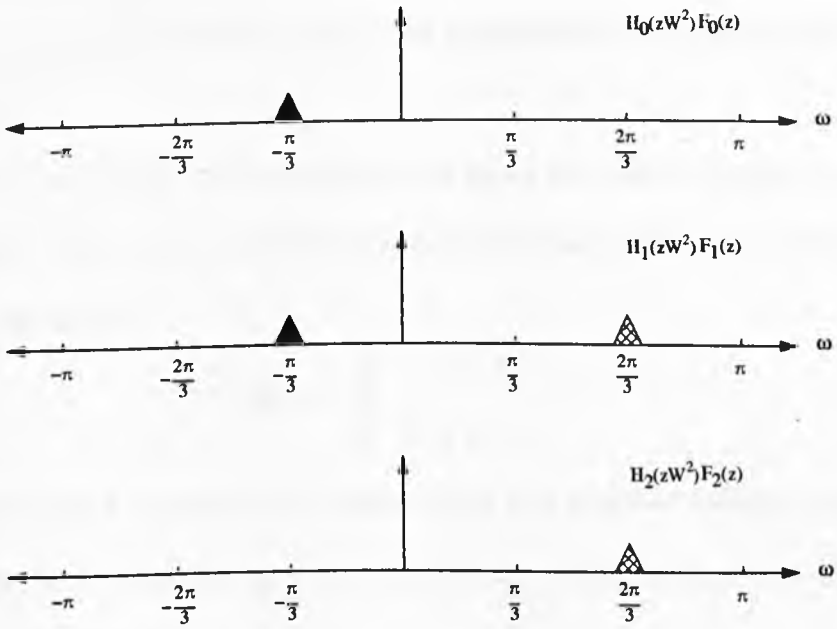

Figure 3.4: Residual alias terms with $l = 2$

In the window design the aliasing error is determined primarily by the order of the filters used, and to a smaller extent the windows used in the initial low pass filter design. To ensure that the aliasing error is minimized, the filters are constrained such that only adjacent filters overlap, and that they have opposite phase characteristics. That is $H_0(z)$ and $H_2(z)$ are constrained to be minimum phase and $H_1(z)$ to be maximum phase, which makes the choice of phase comparable with pseudo-QMF methods such as [52].

3.7 Optimal Third-Band Filter Design

The window technique described above is a very efficient method for designing third band filters, however this method does not result in filters that are optimal in any way. In this section an optimal third band filter design method is presented based on the Eigenfilter approach [113]. The Eigenfilters are optimal in the least square sense.

One of the advantages of the Eigenfilters over other FIR filters is that, they can be designed to incorporate a wide variety of time-domain constraints such as the M-th band constraint

$$b(Mn) = \begin{cases} c & n = 0 \\ 0 & n \neq 0 \end{cases}$$

The optimum filter b is equal to the eigenvector of a positive definite matrix $\mathbf{R}$ corresponding to its smallest eigenvalue λ_0 (Details of the composition of $\mathbf{R}$ can be found in Appendix A).

The third band condition is imposed by modifying the objective function as follows: define a new vector $\hat{b}$ by deleting the components $b(3n)(n \neq 0)$. Having defined $\hat{b}$, the matrix $\mathbf{R}$ is replaced with a reduced matrix $\hat{\mathbf{R}}$ obtained by deleting from $\mathbf{R}$ all the rows and columns whose indices are multiples of 3 (except the 0th row and column). The solution $\hat{b}$ is the eigenvector corresponding of $\hat{\mathbf{R}}$ corresponding to the smallest eigenvalue. The optimal third band filter b is obtained by inserting the deleted zeros in $\hat{b}$.

3.8 Design Examples

Two Examples are presented, the first example uses the window method and the second example the Eigenfilter technique.

Example 3.8.1 The illustrative example starts by designing a third-band filter $G_0(z)$ with length $2N-1$ where N is constrained to be a multiple of three.
In this example $N = 15$, and $G_0(z)$ obtained using (3.25) with an optimal prolate spheroidal [92] window with transition band equal to $.1\pi$. The filters $G_1(z)$ and $G_2(z)$ are designed according to (3.17),(3.18). Figure (3.5) shows the frequency response of the product filters $G_k(z)$, and Figure (3.6) shows their impulse responses. Figure (3.7) shows the zeros of $G_k(z)$ and Figure (3.8) shows the transformed zeros of $\tilde{G}_0(z)$ and $\tilde{G}_1(z)$, the zeros of $\tilde{G}_2(z)$ are the mirror image of $\tilde{G}_0(z)$. It is clear that the zeros on the unit circle have migrated to form mirror images of the unit circle. Figure.(3.9) shows the analysis filters.

The aliasing error is defined as

$$E(\omega) \triangleq \frac{1}{3}[\sum_{l=1}^{2} |A_l(e^{j\omega})|^2]^{1/2} \tag{3.28}$$

where

$$A_l(z) = \sum_{k=0}^{2} H_k(zW_3^l)F_k(z)$$

This aliasing error is shown in Figure (3.10), its peak value is $E_p \triangleq max_\omega E(\omega) = 7.7 \times 10^{-4}$. Clearly the aliasing error is maximum at the transition bands around $\pi/3$ and $2\pi/3$.

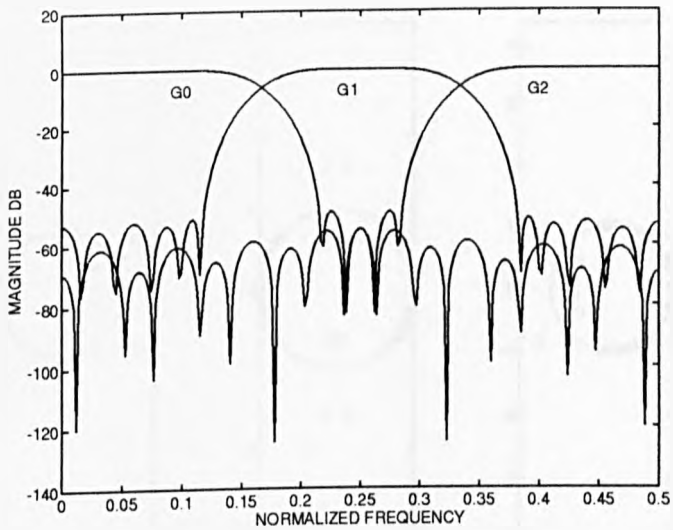

Figure 3.5: The product filters

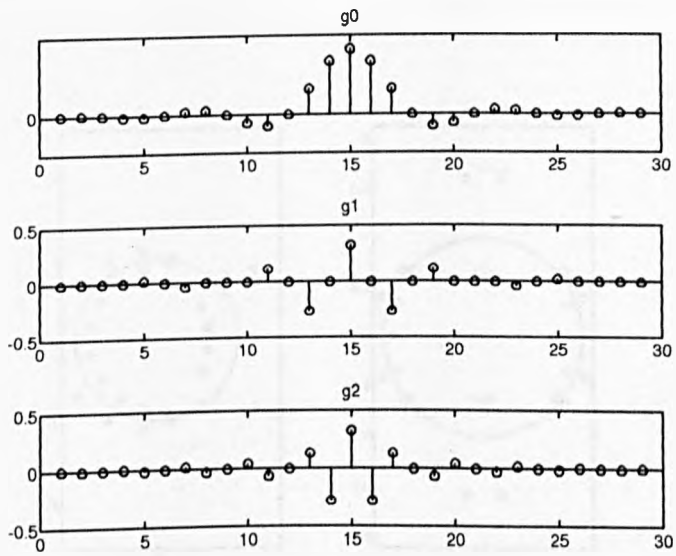

Figure 3.6: Impulse responses of the product filters (Amplitude vs Time)

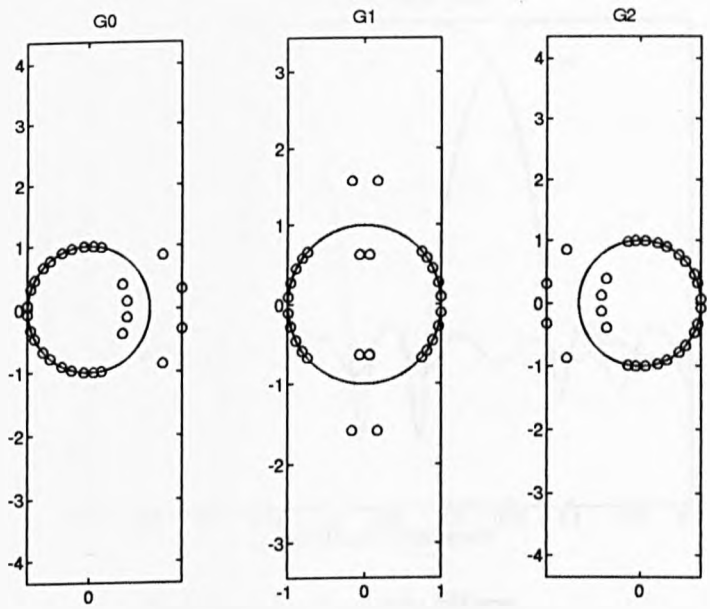

Figure 3.7: Product filters zeros

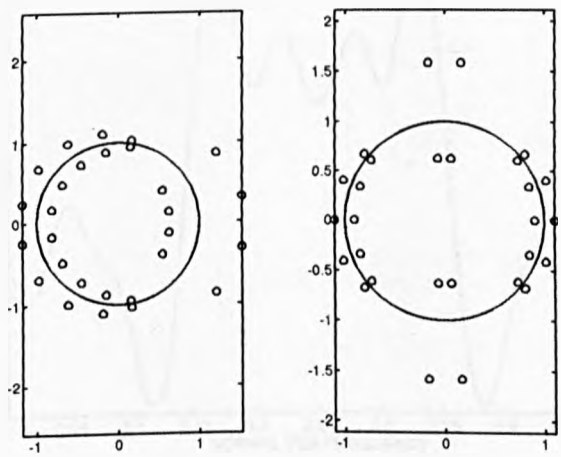

Figure 3.8: Transformed zeros

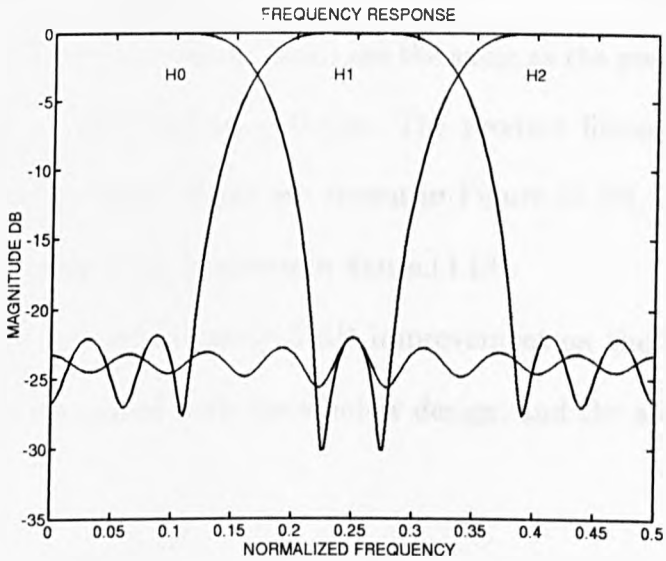

Figure 3.9: Analysis filters

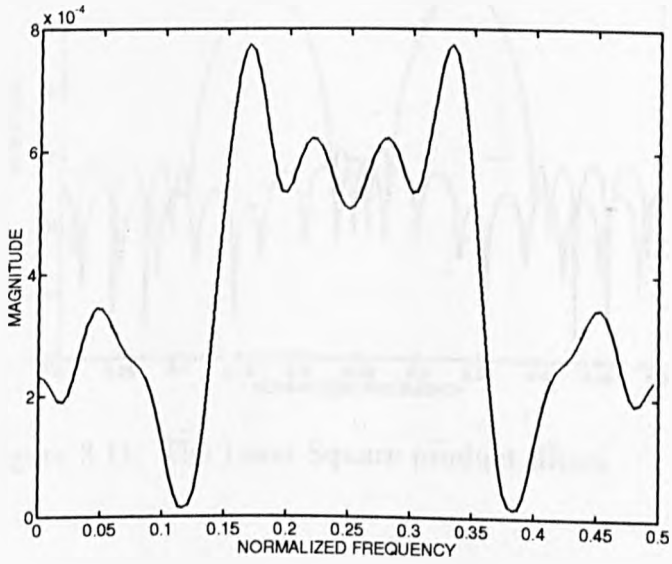

Figure 3.10: Aliasing error

Example 3.8.2 In this example the low-pass filter $G_0(z)$ is designed using the Eigenfilter method. The filter specifications are the same as the previous example where $N = 15$, $\omega_p = .23\pi$, and $\omega_s = 0.43\pi$. The product filters are shown in Figure.(3.11), and the analysis filters are shown in Figure.(3.12), its peak value is 2.9×10^{-4} The aliasing error is shown in figure.(3.13).

It is clear that there is approximately 5 dB improvement on the frequency responses of the filters compared with the window design, and the aliasing error is reduced.

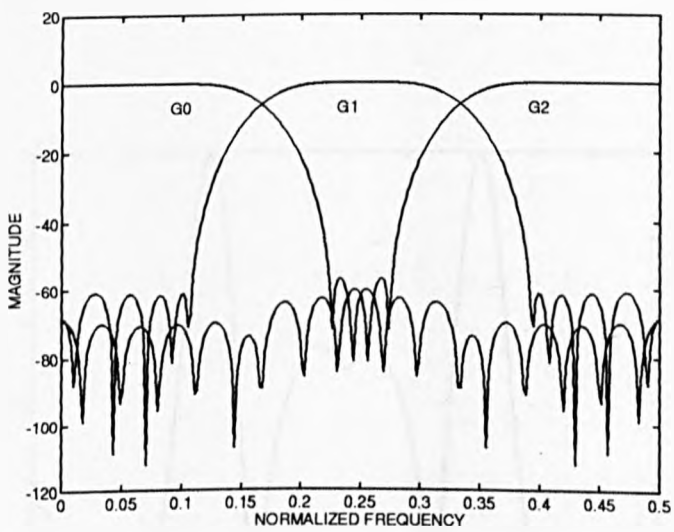

Figure 3.11: The Least Square product filters

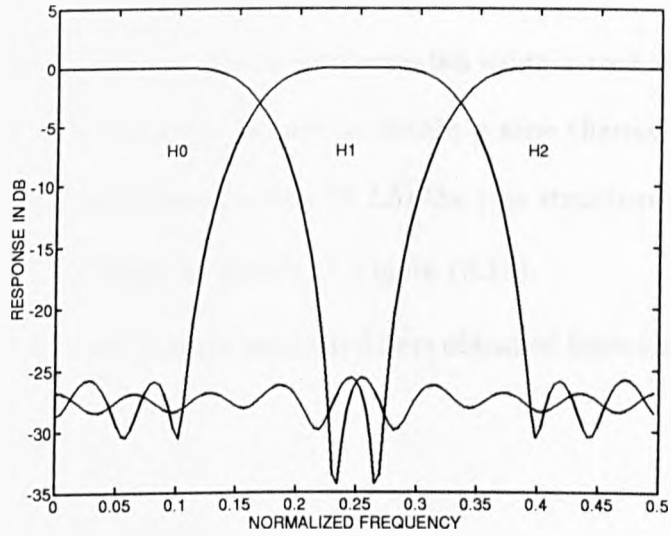

Figure 3.12: Least square Analysis filters

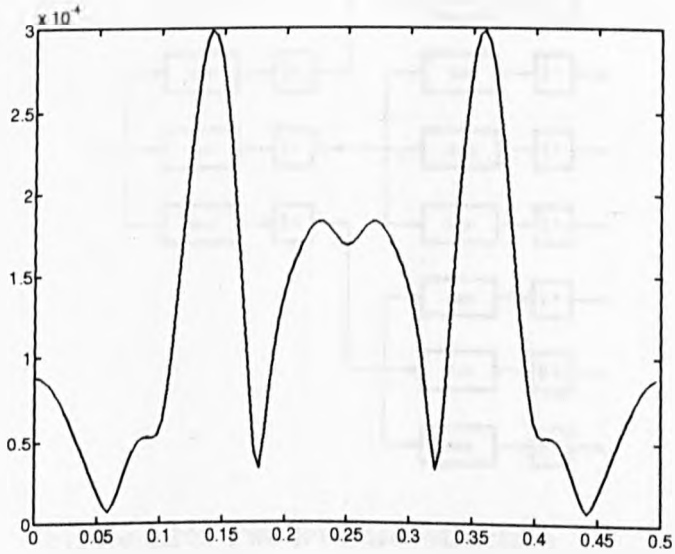

Figure 3.13: Least square aliasing error

3.9 Tree Structures

Power of three number of bands can be implemented using a tree structure. Figure (3.14) shows a two level tree structure to obtain a nine channel system.

By using the noble identities from Section (2.2.5) the tree structure can be transformed to a parallel filter bank as shown in Figure (3.15).

Figure (3.16) shows the nine-channel analysis filters obtained from the least square design example.

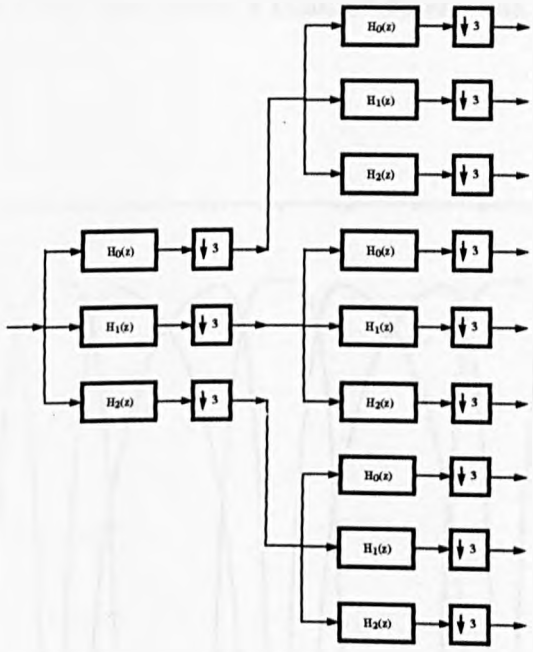

Figure 3.14: Two level tree-structure

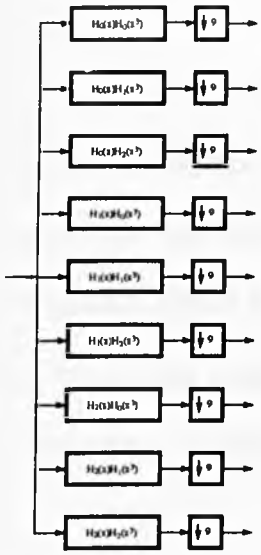

Figure 3.15: Equivalent 9 channel filter bank

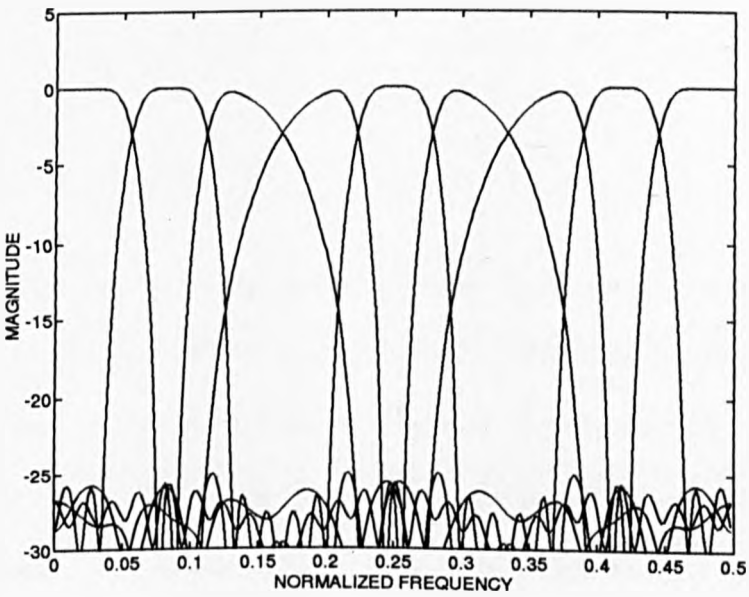

Figure 3.16: 9 Channel System (Magnitude in dB)

3.10 Conclusion

It has been known for some time that multirate filter banks where the number of channels is a power of 2 can be designed utilizing standard digital filter design techniques. This chapter has illustrated how a similar philosophy can be applied to 3-channel multirate systems. Standard digital filter techniques are used to obtain the prototype product filter. Symmetry conditions, the shifting of zeros from the unit circle and spectral factorization are then used to derive the required analysis and synthesis filters.

This technique is computationally simple, and produces aliasing errors comparable to other techniques.

Chapter 4

Time-Domain Analysis and Design of FIR Multirate Filter Banks

4.1 Introduction

The analysis and design of multirate filter banks has been dominated by frequency domain techniques. For the two-channel QMF filter bank, Smith and Barnwell [93] as well as Mintzer [73] provided the fundamental results for Perfect Reconstruction (PR) designs. In the M-channel case, Nussbaumer [82] pioneered the work on pseudo QMF banks, which provide approximate alias cancellation. Smith and Barnwell [94][96] as well as Ramstad[88] independently showed how to formulate the PR conditions in matrix form. It was recognized by Vetterli [116] and then Vaidyanathan [106] that the polyphase component approach results in

considerable simplification of the theory. Subsequently, a class of systems called the cosine modulated filter banks were developed [63][87][51]. These have the advantage that the cost of design as well as implementation is largely determined by the cost of one prototype filter, since all the other filters are derived from it.

In this chapter a general time-domain formulation for FIR multirate filter banks is derived. The analysis and synthesis filters are constrained to have equal lengths. Starting from the z-domain PR conditions, first the two-channel time domain conditions are derived in detail. Subsequently the M-channel conditions are derived for arbitrary length filters and arbitrary decimation rates.

The power of this formulation lies in the fact that the whole problem is embedded in a matrix system of equations, which turns out to be overdetermined for arbitrary length filters. A unique property of this system of equations is the ability to control the system delay with ease, which is not the case for z-domain techniques. An iterative design algorithm is presented based on the time-domain formulation, by designing a suitable choice of initial analysis filters which satisfy the frequency specifications required. The system of equations is solved using the least square method. The synthesis filters produced are used to update the analysis filters for the next iteration.

This method can be considered as a general time-frequency design technique where a large class of FIR near perfect and perfect reconstruction multirate filter banks can be designed within a single design context.

4.2 Time-Domain Analysis

4.2.1 The Two-Channel Filter Bank

Consider the two-channel filter filter bank shown in figure.(4.1), the output $\hat{X}(z)$ can be expressed as:

$$\begin{aligned}\hat{X}(z) &= \frac{1}{2}[H_0(z)F_0(z) + H_1(z)F_1(z)]X(z) \\ &+ \frac{1}{2}[H_0(-z)F_0(z) + H_1(-z)F_1(z)]X(-z) \\ &= T(z)X(z) + A(z)X(-z) \end{aligned} \tag{4.1}$$

which is a linear combination of the LTI system transfer function $T(z)$ and the aliasing term $A(z)$. For aliasing cancellation $A(z)$ is required to be zero, and for perfect reconstruction T(z) must be a pure delay.

In matrix form the PR conditions can be written as:

$$\frac{1}{2}\begin{bmatrix} H_0(z) & H_1(z) \\ H_0(-z) & H_1(-z) \end{bmatrix}\begin{bmatrix} F_0(z) \\ F_1(z) \end{bmatrix} = \begin{bmatrix} z^{-\Delta} \\ 0 \end{bmatrix} \tag{4.2}$$

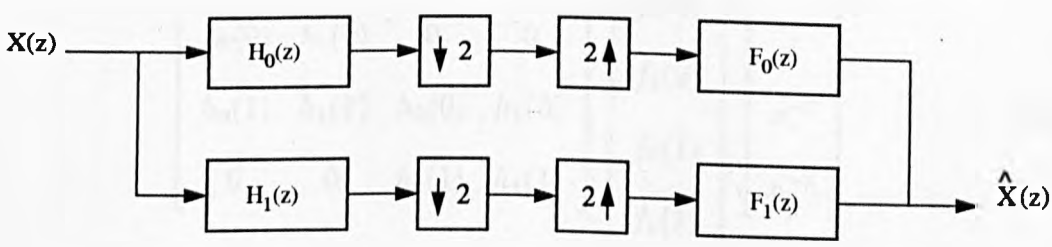

Figure 4.1: Two-channel filter bank

Denoting the impulse response of the filter $H_k(z)$ by $h_k(n)$, $H_k(z)$ can be expressed in terms of $h_k(n)$ by:

$$H_k(z) = h_k(0) + h_k(1)z^{-1} + \cdots + h_k(N-1)z^{-(N-1)}$$

To illustrate the analysis process, we start by assuming that the length of the filters N is equal to 2, then

$$\begin{aligned} H_k(z) &= h_k(0) + h_k(1)z^{-1} \\ H_k(-z) &= h_k(0) - h_k(1)z^{-1} \end{aligned}$$

In matrix form $H_0(z)F_0(z)$ can be expressed as

$$\begin{bmatrix} h_0(0) & 0 \\ h_0(1) & h_0(0) \\ 0 & h_0(0) \end{bmatrix} \begin{bmatrix} f_0(0) \\ f_0(1) \end{bmatrix} \begin{bmatrix} 1 \\ z^{-1} \\ z^{-2} \end{bmatrix}^T \tag{4.3}$$

then $H_0(z)F_0(z) + H_1(z)F_1(z)$ can be formed by interleaving the columns of the analysis matrix and the rows of the synthesis matrix

$$\begin{bmatrix} h_0(0) & h_1(0) & 0 & 0 \\ h_0(1) & h_1(1) & h_0(0) & h_1(0) \\ 0 & 0 & h_0(1) & h_1(1) \end{bmatrix} \begin{bmatrix} f_0(0) \\ f_1(0) \\ f_0(1) \\ f_1(1) \end{bmatrix} \begin{bmatrix} 1 \\ z^{-1} \\ z^{-2} \end{bmatrix}^T \tag{4.4}$$

Define the matrices **H** and **F** from the coefficients of the analysis and the synthesis filters respectively:

$$\mathbf{H} = \begin{bmatrix} h_0(0) & h_0(1) \\ h_1(0) & h_1(1) \end{bmatrix} \qquad \mathbf{F} = \begin{bmatrix} f_0(0) & f_0(1) \\ f_1(0) & f_1(1) \end{bmatrix} \tag{4.5}$$

which can be written in terms of (2×1) block matrices as:

$$\mathbf{H} = \begin{bmatrix} \mathbf{H}_0 & \mathbf{H}_1 \end{bmatrix} \qquad \mathbf{F} = \begin{bmatrix} \mathbf{F}_0 & \mathbf{F}_1 \end{bmatrix} \tag{4.6}$$

substituting (4.6) in (4.4) results in

$$\begin{bmatrix} \mathbf{H}_0^T & \mathbf{0}_2^T \\ \mathbf{H}_1^T & \mathbf{H}_0^T \\ \mathbf{0}_2^T & \mathbf{H}_1^T \end{bmatrix} \begin{bmatrix} \mathbf{F}_0 \\ \mathbf{F}_1 \end{bmatrix} \begin{bmatrix} 1 \\ z^{-1} \\ z^{-2} \end{bmatrix}^T \tag{4.7}$$

where $\mathbf{0}_2^T$ is a (2×1) zero matrix.

From (4.1) aliasing is eliminated by forcing $A(z)$ to zero

$$[H_0(-z)F_0(z) + H_1(-z)F_1(z)] = 0 \tag{4.8}$$

using (4.7), (4.8) can be expressed in the time-domain as

$$\begin{bmatrix} \mathbf{H}_0^T & \mathbf{0}_2^T \\ -\mathbf{H}_1^T & \mathbf{H}_0^T \\ \mathbf{0}_2^T & -\mathbf{H}_1^T \end{bmatrix} \begin{bmatrix} \mathbf{F}_0 \\ \mathbf{F}_1 \end{bmatrix} = \begin{bmatrix} 0 \\ 0 \\ 0 \end{bmatrix} \tag{4.9}$$

Phase and magnitude errors are canceled by forcing $T(z)$ to be pure delay

$$T(z) = z^{-\Delta}$$

Then all the elements in (4.7) are forced to zero except the $z^{-\Delta}$ term, from (4.2)

$$\begin{bmatrix} \mathbf{H}_0^T & \mathbf{0}_2^T \\ \mathbf{H}_1^T & \mathbf{H}_0^T \\ \mathbf{0}_2^T & \mathbf{H}_1^T \end{bmatrix} \begin{bmatrix} \mathbf{F}_0 \\ \mathbf{F}_1 \end{bmatrix} = \begin{bmatrix} 0 \\ 2 \\ 0 \end{bmatrix} \tag{4.10}$$

where $\Delta = 1$.

With no sampling rate alteration in the filter bank, (4.10) is sufficient for PR. The system is alias-free if (4.9) is enforced. If the following condition is imposed on (4.10)

$$\mathbf{H}_0^T F_1 = \mathbf{H}_1^T \mathbf{F}_0 \tag{4.11}$$

then the PR conditions for $N = 2$ can be expressed as:

$$\begin{bmatrix} \mathbf{H}_0^T \\ \mathbf{H}_1^T \end{bmatrix} \begin{bmatrix} \mathbf{F}_0 & \mathbf{F}_1 \end{bmatrix} = \begin{bmatrix} 0 & 1 \\ 1 & 0 \end{bmatrix} \tag{4.12}$$

Example (4.2.1) Choose $H_0(z)$ and $H_1(z)$ as

$$H_0(z) = \frac{1}{\sqrt{2}}(1 + z^{-1}) \qquad H_1(z) = \frac{1}{\sqrt{2}}(1 - z^{-1})$$

solving (4.12) results in

$$F_0(z) = \frac{1}{\sqrt{2}}(1 + z^{-1}) \qquad F_1(z) = \frac{1}{\sqrt{2}}(-1 + z^{-1})$$

The above example represents the simplest PR system where the filters are orthogonal and have linear phase [108].

For arbitrary length filters, N will be assumed to be even, without loss of generality since the value of the coefficients are not constrained to be zero.

The block matrices in (4.6) become

$$\mathbf{H} = \begin{bmatrix} \mathbf{H}_0 & \mathbf{H}_1 & \cdots & \mathbf{H}_{N-1} \end{bmatrix} \qquad \mathbf{F} = \begin{bmatrix} \mathbf{F}_0 & \mathbf{F}_1 & \cdots & \mathbf{F}_{N-1} \end{bmatrix} \tag{4.13}$$

and (4.7) becomes

$$\begin{bmatrix} \mathbf{H}_0^T & \mathbf{0}_2^T & \cdots & \mathbf{0}_2^T \\ \mathbf{H}_1^T & \mathbf{H}_0^T & \ddots & \vdots \\ \vdots & \mathbf{H}_1^T & \ddots & \vdots \\ \mathbf{H}_{N-1}^T & \vdots & \ddots & \mathbf{H}_0^T \\ \mathbf{0}_2^T & \mathbf{H}_{N-1}^T & \ddots & \mathbf{H}_1^T \\ \vdots & \ddots & \ddots & \vdots \\ \mathbf{0}_2^T & \cdots & \mathbf{0}_2^T & \mathbf{H}_{N-1}^T \end{bmatrix} \begin{bmatrix} \mathbf{F}_0 \\ \mathbf{F}_1 \\ \vdots \\ \mathbf{F}_{N-1} \end{bmatrix} \begin{bmatrix} 1 \\ z^{-1} \\ \vdots \\ z^{-(2N-2)} \end{bmatrix}^T \tag{4.14}$$

Aliasing is eliminated if :

$$\begin{bmatrix} \mathbf{H}_0^T & \mathbf{0}_2^T & \cdots & \mathbf{0}_2^T \\ -\mathbf{H}_1^T & \mathbf{H}_0^T & \ddots & \vdots \\ \vdots & -\mathbf{H}_1^T & \ddots & \vdots \\ \mathbf{H}_{N-1}^T & \vdots & \ddots & \mathbf{H}_0^T \\ \mathbf{0}_2^T & \mathbf{H}_{N-1}^T & \ddots & -\mathbf{H}_1^T \\ \vdots & \ddots & \ddots & \vdots \\ \mathbf{0}_2^T & \cdots & \mathbf{0}_2^T & \mathbf{H}_{N-1}^T \end{bmatrix} \begin{bmatrix} \mathbf{F}_0 \\ \mathbf{F}_1 \\ \vdots \\ \mathbf{F}_{N-1} \end{bmatrix} = \begin{bmatrix} 0 \\ 0 \\ \vdots \\ 0 \end{bmatrix} \tag{4.15}$$

Magnitude and phase errors are eliminated if

$$\begin{bmatrix} \mathbf{H}_0^T & \mathbf{0}_2^T & \cdots & \mathbf{0}_2^T \\ \mathbf{H}_1^T & \mathbf{H}_0^T & \ddots & \vdots \\ \vdots & \mathbf{H}_1^T & \ddots & \vdots \\ \mathbf{H}_{N-1}^T & \vdots & \ddots & \mathbf{H}_0^T \\ \mathbf{0}_2^T & \mathbf{H}_{N-1}^T & \ddots & \mathbf{H}_1^T \\ \vdots & \ddots & \ddots & \vdots \\ \mathbf{0}_2^T & \cdots & \mathbf{0}_2^T & \mathbf{H}_{N-1}^T \end{bmatrix} \begin{bmatrix} \mathbf{F}_0 \\ \mathbf{F}_1 \\ \vdots \\ \mathbf{F}_{N-1} \end{bmatrix} = \begin{bmatrix} 0 \\ \vdots \\ 2 \\ \vdots \\ 0 \end{bmatrix} \tag{4.16}$$

where $\Delta = N - 1$, from (4.15) and (4.16) ,it can be seen that

$$\mathbf{H}_0^T \mathbf{F}_0 = \mathbf{H}_{N-1}^T \mathbf{F}_{N-1} = 0$$

and Δ is bounded by

$$1 \leq \Delta \leq 2N - 3 \tag{4.17}$$

For the classical case ($\Delta = N - 1$), the following is imposed

$$\sum_{n=0}^{\lfloor (N-1)/2 \rfloor} \mathbf{H}_{N-1-2n}^T \mathbf{F}_{2n} = \sum_{n=0}^{\lceil (N-1)/2 \rceil} \mathbf{H}_{N-1-(2n+1)}^T \mathbf{F}_{2n+1} \tag{4.18}$$

where $\lfloor x \rfloor$ is the integer less or equal to x. For $N = 2$ this condition reduces to equation (4.11).

Then the PR conditions for the two Channel system can be expressed as:

$$\begin{bmatrix} \mathbf{H}_0^T & \mathbf{0}_2^T & \cdots & \mathbf{0}_2^T \\ \mathbf{H}_1^T & \mathbf{0}_2^T & \ddots & \vdots \\ \vdots & \mathbf{H}_0^T & \ddots & \vdots \\ \mathbf{H}_{N-1}^T & \mathbf{H}_1^T & \ddots & \vdots \\ \mathbf{0}_2^T & \vdots & \ddots & \mathbf{H}_1^T \\ \mathbf{0}_2^T & \vdots & \ddots & \vdots \\ \vdots & \mathbf{H}_{N-1}^T & \ddots & \vdots \\ \mathbf{0}_2^T & \cdots & \mathbf{0}_2^T & \mathbf{H}_{N-1}^T \end{bmatrix} \begin{bmatrix} \mathbf{F}_0 & \mathbf{F}_1 \\ \mathbf{F}_2 & \mathbf{F}_3 \\ \vdots & \vdots \\ \mathbf{F}_{N-2} & \mathbf{F}_{N-1} \end{bmatrix} = \begin{bmatrix} \mathbf{0}_2^T \\ \vdots \\ \mathbf{J}_2 \\ \vdots \\ \mathbf{0}_2^T \end{bmatrix} \tag{4.19}$$

where $\mathbf{J}_2$ is a (2×2) anti-diagonal identity (Exchange) matrix. The system of equations in (4.19) represents the necessary and sufficient conditions for PR.

4.2.2 The M-Channel System

The M-channel filter bank with arbitrary decimation rate $R \leq M$ is shown in Figure (4.2), the output $\hat{X(z)}$ can be expressed as follows

$$\hat{X}(z) = \frac{1}{M} \sum_{k=0}^{M-1} \sum_{l=0}^{R-1} X(zW^l) H_k(zW^l) F_k(z), \qquad W = e^{-j2\pi/R} \tag{4.20}$$

which equivalently can be expressed in matrix form as :

$$\hat{\mathbf{X}}(z) = \frac{1}{M} \mathbf{X}^T \mathbf{C} \mathbf{V} \tag{4.21}$$

where

$$\mathbf{X}^T = \begin{bmatrix} X(z) & X(zW) & \cdots & X(zW^{R-1}) \end{bmatrix} \tag{4.22}$$

is the input vector

$$\mathbf{V}^T = \begin{bmatrix} F_0(z) & F_1(z) & \cdots & F_{M-1}(z) \end{bmatrix} \tag{4.23}$$

is the vector of the synthesis filters, and

$$\mathbf{C} = \begin{bmatrix} H_0(z) & H_1(z) & \cdots & H_{M-1}(z) \\ H_0(zW) & H_1(zW) & \cdots & H_{M-1}(zW) \\ \vdots & \vdots & \cdots & \vdots \\ H_0(zW^{R-1}) & H_1(zW^{R-1}) & \cdots & H_{M-1}(zW^{R-1}) \end{bmatrix} \tag{4.24}$$

is the aliasing component matrix or AC matrix [94].

The system is free from aliasing if the $l \neq 0$ terms are equal to zero

$$\mathbf{CV} = \begin{bmatrix} MT(z) & 0 & \cdots & 0 \end{bmatrix}^T \tag{4.25}$$

and the system has PR if

$$T(z) = \frac{1}{M} \sum_{k=0}^{M-1} H_k(z) F_k(z) = z^{-\Delta} \tag{4.26}$$

We begin by assuming that $N = R = 3$.

Define $\mathbf{H}$ and $\mathbf{F}$ from the coefficients of the analysis and the synthesis filters

$$\mathbf{H} = \begin{bmatrix} \mathbf{H}_0 & \mathbf{H}_1 & \mathbf{H}_2 \end{bmatrix} \qquad \mathbf{F} = \begin{bmatrix} \mathbf{F}_0 & \mathbf{F}_1 & \mathbf{F}_2 \end{bmatrix} \tag{4.27}$$

where $\mathbf{H}_k$ and $\mathbf{F}_k$ are third order vectors.

The aliasing terms can be expressed as($l = 1, 2$)

$$\begin{bmatrix} \mathbf{H}_0^T & \mathbf{0}_3^T & \mathbf{0}_3^T \\ W^1\mathbf{H}_1^T & \mathbf{H}_0^T & \mathbf{0}_3^T \\ W^2\mathbf{H}_2^T & W^1\mathbf{H}_1^T & \mathbf{H}_0^T \\ \mathbf{0}_3^T & W^2\mathbf{H}_2^T & W^1\mathbf{H}_1^T \\ \mathbf{0}_3^T & \mathbf{0}_3^T & W^2\mathbf{H}_2^T \end{bmatrix} \begin{bmatrix} \mathbf{F}_0 \\ \mathbf{F}_1 \\ \mathbf{F}_2 \end{bmatrix} \begin{bmatrix} 1 \\ z^{-1} \\ \vdots \\ z^{-5} \end{bmatrix}^T \tag{4.28}$$

aliasing is eliminated if

$$\begin{bmatrix} \mathbf{H}_0^T & \mathbf{0}_3^T & \mathbf{0}_3^T \\ W^1\mathbf{H}_1^T & \mathbf{H}_0^T & \mathbf{0}_3^T \\ W^2\mathbf{H}_2^T & W^1\mathbf{H}_1^T & \mathbf{H}_0^T \\ \mathbf{0}_3^T & W^2\mathbf{H}_2^T & W^1\mathbf{H}_1^T \\ \mathbf{0}_3^T & \mathbf{0}_3^T & W^2\mathbf{H}_2^T \end{bmatrix} \begin{bmatrix} \mathbf{F}_0 \\ \mathbf{F}_1 \\ \mathbf{F}_2 \end{bmatrix} = \begin{bmatrix} 0 \\ 0 \\ 0 \\ 0 \\ 0 \end{bmatrix} \tag{4.29}$$

and magnitude and phase errors are canceled if

$$\begin{bmatrix} \mathbf{H}_0^T & \mathbf{0}_3^T & \mathbf{0}_3^T \\ \mathbf{H}_1^T & \mathbf{H}_0^T & \mathbf{0}_3^T \\ \mathbf{H}_2^T & \mathbf{H}_1^T & \mathbf{H}_0^T \\ \mathbf{0}_3^T & \mathbf{H}_2^T & \mathbf{H}_1^T \\ \mathbf{0}_3^T & \mathbf{0}_3^T & \mathbf{H}_2^T \end{bmatrix} \begin{bmatrix} \mathbf{F}_0 \\ \mathbf{F}_1 \\ \mathbf{F}_2 \end{bmatrix} = \begin{bmatrix} 0 \\ 0 \\ 3 \\ 0 \\ 0 \end{bmatrix} \tag{4.30}$$

where $\Delta = 2$.

By examining the z^{-2} term in (4.29) and (4.30) we have

$$W^l\mathbf{H}_2^T\mathbf{F}_0 + W^l\mathbf{H}_1^T\mathbf{F}_1 + \mathbf{H}_0^T\mathbf{F}_2 = 0, \quad (l = 1, 2) \tag{4.31}$$

and

$$\mathbf{H}_2^T\mathbf{F}_0 + \mathbf{H}_1^T\mathbf{F}_1 + \mathbf{H}_0^T\mathbf{F}_2 = 3 \tag{4.32}$$

Since

$$\sum_{k=0}^{M-1} W^k = \sum_{k=0}^{M-1} e^{j2\pi k/M} = 0$$

then from (4.31) and (4.32)

$$\mathbf{H}_2^T\mathbf{F}_0 = \mathbf{H}_1^T\mathbf{F}_1 = \mathbf{H}_0^T\mathbf{F}_2$$

Then PR conditions reduce to

$$\begin{bmatrix} \mathbf{H}_0^T \\ \mathbf{H}_1^T \\ \mathbf{H}_2^T \end{bmatrix} \begin{bmatrix} \mathbf{F}_0 & \mathbf{F}_1 & \mathbf{F}_2 \end{bmatrix} = \begin{bmatrix} 0 & 0 & 1 \\ 0 & 1 & 0 \\ 1 & 0 & 0 \end{bmatrix} \tag{4.33}$$

which reduces to (4.12) when $N = M = 2$.

Without loss of generality assuming than $N = SR$ (S integer) it can be shown the PR conditions for arbitrary number of channels can be expressed as ($R \leq M$)

$$\begin{bmatrix} \mathbf{H}_0^T & \mathbf{0}_R^T & \cdots & \mathbf{0}_R^T \\ \vdots & \ddots & \ddots & \vdots \\ \mathbf{H}_{N-1}^T & \vdots & \ddots & \mathbf{H}_0^T \\ \mathbf{0}_R^T & \mathbf{H}_{N-1}^T & \ddots & \vdots \\ \vdots & \ddots & \ddots & \vdots \\ \mathbf{0}_R^T & \cdots & \mathbf{0}_R^T & \mathbf{H}_{N-1}^T \end{bmatrix} \begin{bmatrix} \mathbf{F}_0 & \mathbf{F}_1 & \cdots & \mathbf{F}_{S-1} \\ \mathbf{F}_S & \ddots & \ddots & \vdots \\ \vdots & \ddots & \ddots & \vdots \\ \cdots & \cdots & \cdots & \mathbf{F}_{SR-1} \end{bmatrix} = \begin{bmatrix} \mathbf{0}_R^T \\ \vdots \\ \mathbf{J}_R \\ \vdots \\ \mathbf{0}_R^T \end{bmatrix} \tag{4.34}$$

This system can be expressed in a more compact form in terms of $(M \times R)$ submatrices $\mathbf{P}_j$ and $\mathbf{Q}_j (j = 0, \cdots, S-1)$

$$\underbrace{\begin{bmatrix} \mathbf{P}_0^T & \mathbf{O} & \cdots & \mathbf{O} \\ \mathbf{P}_1^T & \mathbf{P}_0^T & \ddots & \vdots \\ \vdots & \mathbf{P}_1^T & \ddots & \vdots \\ \mathbf{P}_{L-1}^T & \ddots & \ddots & \mathbf{P}_0^T \\ \mathbf{O} & \mathbf{P}_{S-1}^T & \ddots & \mathbf{P}_1^T \\ \vdots & \ddots & \ddots & \vdots \\ \mathbf{O} & \cdots & \mathbf{O} & \mathbf{P}_{S-1}^T \end{bmatrix}}_{\mathbf{A}} \underbrace{\begin{bmatrix} \mathbf{Q}_0 \\ \mathbf{Q}_1 \\ \vdots \\ \mathbf{Q}_{S-1} \end{bmatrix}}_{\mathbf{s}} = \underbrace{\begin{bmatrix} \mathbf{0}_R^T \\ \vdots \\ \mathbf{J}_R \\ \vdots \\ \mathbf{0}_R^T \end{bmatrix}}_{\mathbf{B}} \tag{4.35}$$

where $\mathbf{O}$ is an $(R \times M)$ zero matrix.

The $(2S-1)R \times SR$ matrix $\mathbf{A}$ is defined from the coefficients of the analysis filters. The $(2S-1)R \times R$ matrix $\mathbf{B}$ has all zero elements except one $(R \times R)$ matrix $\mathbf{J}_R$. The $(SR \times R)$ matrix $\mathbf{s}$ is defined from the coefficients of the synthesis filters.

The first M columns of $\mathbf{A}$ are the transpose of the analysis filters matrix $\mathbf{P}$ followed by $(S-1)$ blocks of $(R \times M)$ zero matrices. The other columns of $\mathbf{A}$ are circularly shifted versions of the first M columns.

The necessary and sufficient conditions for the system to PR is to satisfy the linear system of equations

$$\mathbf{A}\mathbf{s} = \mathbf{B} \tag{4.36}$$

The M-band system can have a minimum delay of $(R-1)$ samples and a maximum delay of $(2S-1)R-1$ samples.

This time-domain formulation has been independently derived by Nayebi et. al. [75] using a direct time-domain analysis of the system, where the FIR filtering was considered to be a time-domain operation in which the output at any instant of time is a linear combination of present and past input samples, and the decimation operation is simply used to remove the redundant information which is not necessary for PR.

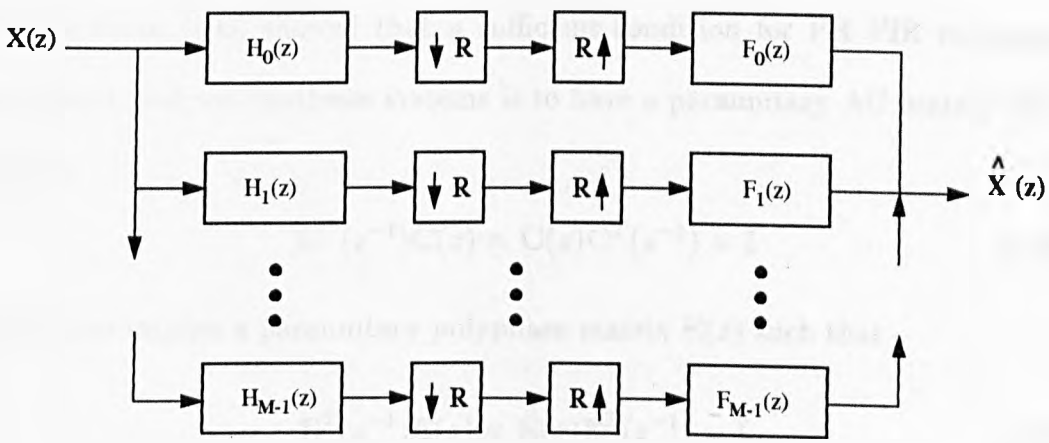

Figure 4.2: M-channel filter bank

4.3 Paraunitary Time-Domain Conditions

For maximally decimated systems, designing paraunitary(lossless) AC-matrices [106] results in a special form of the matrix $\mathbf{A}$ in which the columns of $\mathbf{A}$ are orthonormal [75] that is

$$\mathbf{A}^T\mathbf{A} = \mathbf{I} \tag{4.37}$$

In this section the time-domain paraunitary conditions are established in terms of the block matrices in (4.35).

Vaidyanathan [106] showed that a sufficient condition for PR FIR maximally decimated analysis/synthesis systems is to have a paraunitary AC matrix which implies

$$\mathbf{C}^T(z^{-1})\mathbf{C}(z) = \mathbf{C}(z)\mathbf{C}^T(z^{-1}) = \mathbf{I} \tag{4.38}$$

(4.38) also implies a paraunitary polyphase matrix $\mathbf{E}(z)$ such that

$$\mathbf{E}^T(z^{-1})\mathbf{E}(z) = \mathbf{E}(z)\mathbf{E}^T(z^{-1}) = \mathbf{I} \tag{4.39}$$

where $\mathbf{E}(z)$ is defined from the analysis filters as

$$H_k(z) = \sum_{l=0}^{M-1} z^{-l}E_{kl}(z^M), \qquad 0 \le k \le M-1 \tag{4.40}$$

and

$$E_{kl}(z^M) = \sum_{l=0}^{\infty} h_{k(l+nM)}z^{-nM} \tag{4.41}$$

Denoting the matrix $\mathbf{p}$ in terms of the analysis filter coefficients as

$$\mathbf{p}_{kn} = \begin{bmatrix} h_0(0) & \cdots & h_0(N-1) \\ \vdots & \vdots & \vdots \\ h_{M-1}(0) & \cdots & h_{M-1}(N-1) \end{bmatrix} \tag{4.42}$$

and writing (4.42) in terms of $(M \times M)$ block matrices as

$$\mathbf{P}_j = \begin{bmatrix} \mathbf{P}_0 & \mathbf{P}_1 & \cdots & \mathbf{P}_{S-1} \end{bmatrix} \tag{4.43}$$

The polyphase matrix can be written in terms of (4.42) as

$$\mathbf{E}_{kl} = \sum_{n=0}^{S-1} \mathbf{p}_{k(N-n)M-1-l} z^{-n} \tag{4.44}$$

and from (4.43) $\mathbf{E}(\mathbf{z})$ becomes

$$\mathbf{E}(z) = \sum_{j=0}^{S-1} \mathbf{P}_j \mathbf{J} z^{-(N-1-j)} \tag{4.45}$$

The time-domain paraunitary conditions can be obtained by using (4.45) in (4.39), we have

$$\sum_{j=0}^{S-1} \sum_{r=0}^{S-1} \mathbf{P}_j \mathbf{P}_r^T = \sum_{j=0}^{S-1} \sum_{r=0}^{S-1} \mathbf{P}_j^T \mathbf{P}_r = \delta(r-j)\mathbf{I} \tag{4.46}$$

Paraunitary filter banks belong to the class of PR FIR filter banks with identical analysis and synthesis filters (within time reversal) [119], where

$$F_k(z) = z^{-(N-1)} H_k(z)$$

These conditions can only be satisfied in (4.35) when the synthesis filters are time reversed versions of the analysis filters and system delay Δ is equal to $N-1$.

The time-domain conditions are reduced to a set of cross orthogonality conditions of analysis and synthesis filter coefficients. These conditions provide a powerful set of constraints which can be utilized in the direct design of multirate filter banks. Paraunitary transfer matrices were applied to the design of PR systems in [106][109]. It turns out that the two channel PR QMF bank termed conjugate quadrature filters(CQF) has the paraunitary property [93]. Also it has been shown [119] that some of the earlier filter bank designs [86] also have the paraunitary property. The Lapped Orthogonal Transform(LOT) [15] [65], has been shown later to have the paraunitary property. Subsequently, paraunitary systems have been used in the design of cosine modulated filter banks, which offer great simplicity of design as well as implementation [63] [51] [87].

4.4 Least Square Minimization

The system in (4.36) has more equations than unknowns for $N > R$, so the system is said to be overdetermined. Usually an overdetermined system has no exact solution, since $\mathbf{b}$ must be an element of range space $\mathbf{A}$ [35]. This suggests we strive to minimize $\| \mathbf{As} - \mathbf{B} \|_p$ for some suitable value of p.

Minimization of the 1-norm and the ∞-norm is complicated by the fact that the function $f(s) = \| \mathbf{As} - \mathbf{B} \|_p$ is not differentiable for these values of p.

In contrast to general p-norm minimization the *Least Square(LS)* problem [35]

$$\min \| \mathbf{As} - \mathbf{B} \|_2 \tag{4.47}$$

is more tractable for two reasons:

- $\phi(s) = \frac{1}{2} \parallel \mathbf{As} - \mathbf{B} \parallel_2^2$ is differentiable with respect to s and so the minimizers of ϕ satisfy the gradient equation $\nabla\phi(s) = 0$.

  This turns out to be an easily constructed symmetric linear system which is positive definite if **A** has full column rank.

- The 2-norm is preserved under orthogonal transformation.

Thus if **A** has full rank then there is a unique *LS* solution to **s** and it solves the symmetric positive definite linear system

$$\mathbf{A}^T\mathbf{A}\mathbf{s}_{LS} = \mathbf{A}^T\mathbf{B} \tag{4.48}$$

Solving this equation is tantamount to solving the gradient equation $\nabla\phi = 0$ where

$$\epsilon_{LS} = \parallel \mathbf{As} - \mathbf{B} \parallel_2 \tag{4.49}$$

is minimized. Note that if ϵ_{LS} is small we can predict **B** with the columns of **A**. In [75] the design algorithm was based on defining a cost function which is used in an iterative procedure. This cost function consists of two error components which are minimized. The first component of the cost function is the reconstruction error, and the second component is a function which describes the frequency domain properties of the system filters which is usually nonlinear.

A conjugate gradient optimisation procedure is used to update the matrix **A**. At each iteration the *Least Square* system of (4.48) is solved and the cost function is evaluated, if the error is below a certain value, the algorithm is stopped.

This algorithm is quite intensive, and does not guarantee optimal solutions. Therefore the starting filters are chosen to have similar frequency characteristics as the cost function.

4.5 Design Algorithm

In this section an efficient technique for designing multirate filter banks based on the time-domain formulation is presented. The proposed technique is based on an iterative process to find the coefficients of the analysis and synthesis filters that minimizes the related error measure. By solving (4.48) an approximate solution is found. After obtaining the coefficients of the synthesis filter $f_k^i(n)$ from the first iteration, we set the coefficients of the analysis filters equal to

$$h_k^{i+1}(n) = (-1)^n f_k^i(N-1-n) \tag{4.50}$$

where $n = 0, \cdots, N-1$ and $k = 0, \cdots, M-1$. The modulation by -1 and the time reversal ensures that the properties of the filters are preserved throughout the design process [6]. A stopping criteria can then be set to terminate the iterative algorithm.

For each iteration, the reconstruction error measure is defined as the distance of $\mathbf{B}$ from the range space of $\mathbf{A}$. This distance is the size of the minimum residual vector $\mathbf{e}$ given as

$$\mathbf{e} = \mathbf{A}\mathbf{s}_{\mathrm{LS}} - \mathbf{B} \tag{4.51}$$

The 2-norm of the i-th minimum residual vector $\mathbf{e}$ is a measure of the reconstruction quality of the i-th iteration.

$$\epsilon = \| \mathbf{e} \|^2 \tag{4.52}$$

Therefore (4.52) is used as a stopping criteria. If ϵ reaches the desired reconstruction error the process is terminated. A zero-norm value (within the numerical accuracy of the computer) for ϵ means that the system is exactly solvable, and

PR is achieved.

Frequency domain characteristics of the filter bank are only imposed on the starting filters, therefore the problem is reduced to solving a set of linear equations at each iteration, this reduces the required computational complexity considerably during the design process.

This method allows one to trade off frequency-domain and time-domain properties of the filter bank, thus optimizing the design for a given application [6].

The design flowgraph is shown in Figure (4.3).

This method can be considered as a general time-frequency design technique where a large class of FIR near perfect and perfect reconstruction multirate filter banks can be designed within a single design context. In this chapter only traditional filter bank design is considered $\Delta = N - 1$. The design of low delay filter banks will be discussed in chapter 5.

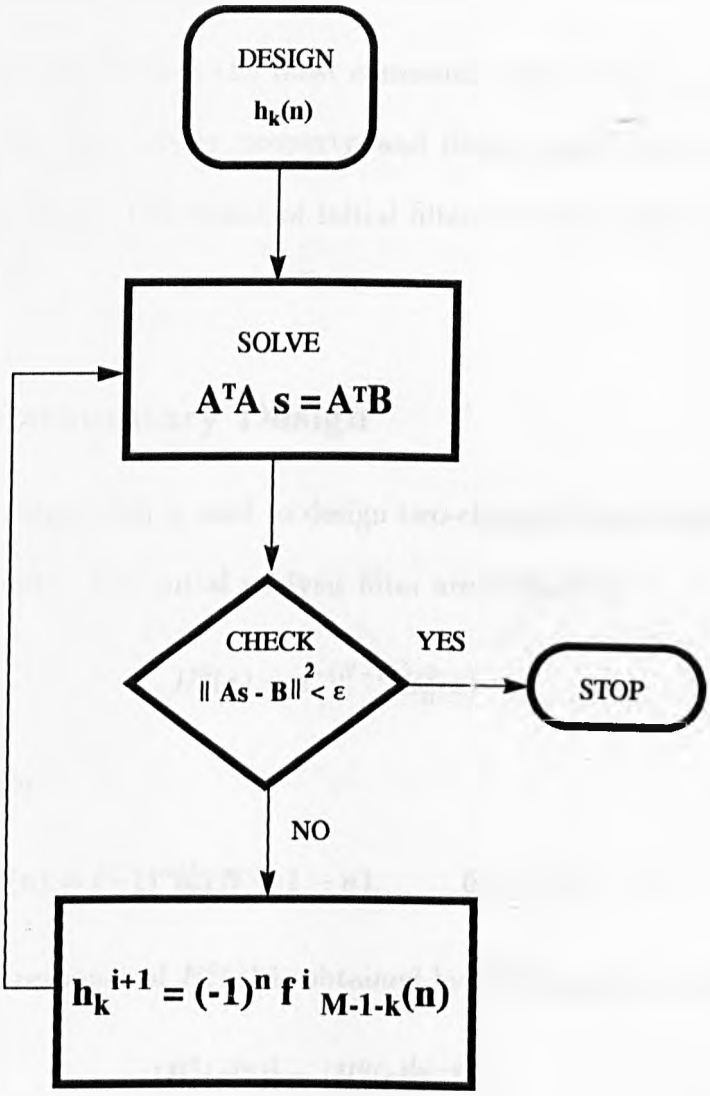

Figure 4.3: Design Flowgraph

4.6 Two Channel Filter Bank Design

The two channel filter bank is the most commonly used system, in this section systems having the paraunitary property, and linear phase filters are designed within a single context. The choice of initial filters determine the type of filters and filter bank.

4.6.1 PR Paraunitary Design

The time-domain algorithm is used to design two-channel filter banks having the paraunitary property. The initial analysis filter are related by

$$H_1^0(z) = z^{-(N-1)} H_0^0(z) \tag{4.53}$$

in the time domain

$$h_1^0(n) = (-1)^n h_0^0(N-1-n), \qquad 0 \leq n \leq N-1 \tag{4.54}$$

so the magnitude response of $H_1^0(z)$ is obtained by shifting that of $H_0^0(z)$ by π

$$|H_1^0(e^{j\omega})| = |H_0^0(e^{j(\omega-\pi)}|$$

both filters have the same ripple sizes, and transition band widths. The filter $h_0^0(n)$ is constrained to be a non-linear phase filter, so the first step is to design a non-linear phase filter with cutoff frequency $\pi/2$.

Non-linear Phase Filter Design

Non-linear phase filters can be obtained by the spectral factorization of a linear phase filter, this approach was shown in chapter 3.

In this section a zero reflection method is used to design non-linear phase filters, that do not require spectral factorization. This method is based on designing a linear phase filter, and then obtaining a minimum phase counterpart by reflecting the zeros located outside the unit circle to their mirror image locations inside the unit circle, this ensures that the magnitude response remains exactly the same. This simple transformation is used

$$z_m(n) = \begin{cases} 1/z_l^*(n) & |z_l(n)| > 0 \\ z_l(n) & \text{otherwise} \end{cases} \tag{4.55}$$

where $z_l(n)$ are the zeros of the linear phase filter, and $z_m(n)$ are the zeros of the minimum phase filter. Figure (4.4(a),(b)) shows a typical linear phase filter and it's zeros respectively. Figure (4.5(a),(b)) shows the minimum phase counter part. The zeros inside the unit circle are all double zeros.

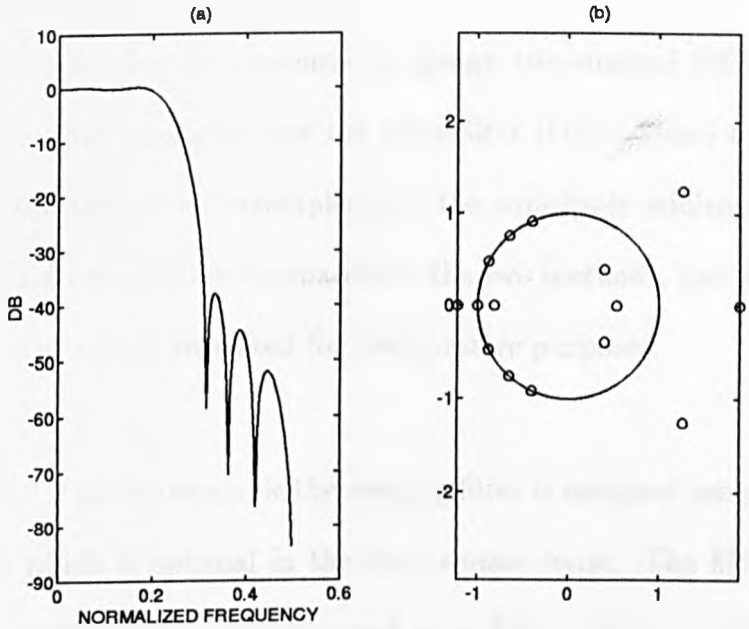

Figure 4.4: (a) Linear phase filter (b)Linear phase zeros

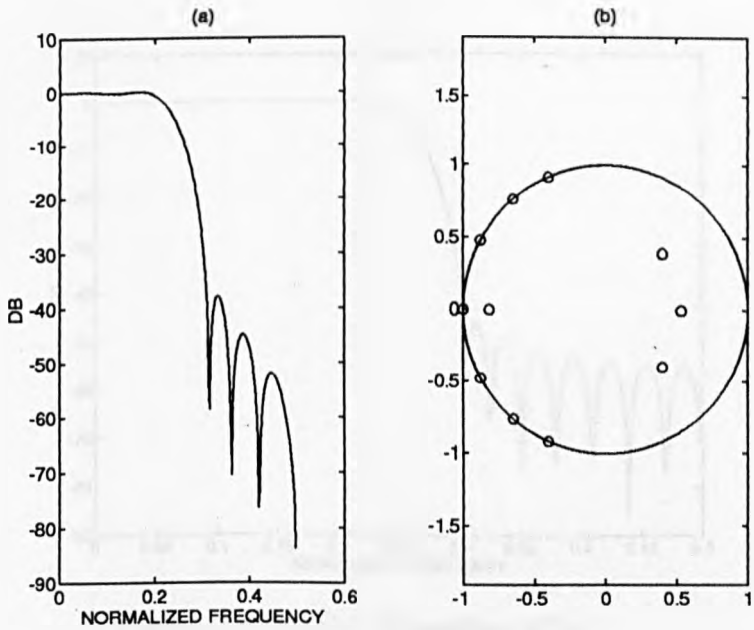

Figure 4.5: (a) Minimum phase filter (b) Minimum phase zeros

Design Examples

Two illustrative examples are presented to design two-channel PR paraunitary filter banks. The first examples uses the Eigenfilter [113] method to design the starting filter, and the second examples uses the equiripple minimax filter [66]. Convergence characteristics are compared for the two methods, and Aliasing and magnitude error plots are presented for comparative purposes.

Example 4.6.1.1 In this example the starting filter is designed using the Eigenfilter technique which is optimal in the least square sense. The filter length is chosen to be $N = 32$ with $\omega_p = 0.44\pi$, and $\omega_s = 0.6\pi$. $H_0^0(z)$ is obtained using the non-linear phase technique described above. The high pass filter is related to the low pass filter by (4.54).

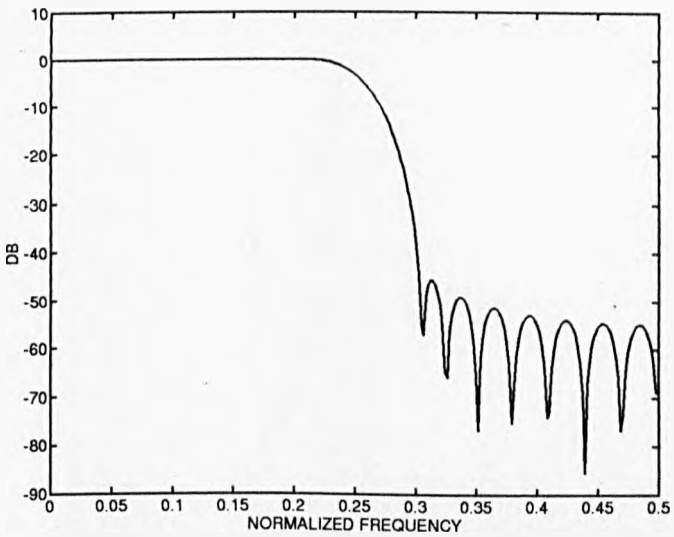

Figure 4.6: Initial Eigenfilter $h_0^0(n)$

Figure.(4.6) shows the starting low-pass minimum phase Eigenfilter. Figure (4.7) and Figure (4.8) shows the resulting analysis and synthesis filters respectively. The magnitude and aliasing errors are shown in Figure (4.9), and Figure (4.10), which confirms that the errors are practically zero. The algorithm was stopped at a reconstruction error of 2×10^{-16}, which is practically zero. The synthesis filters are time reversed versions of the analysis filters.

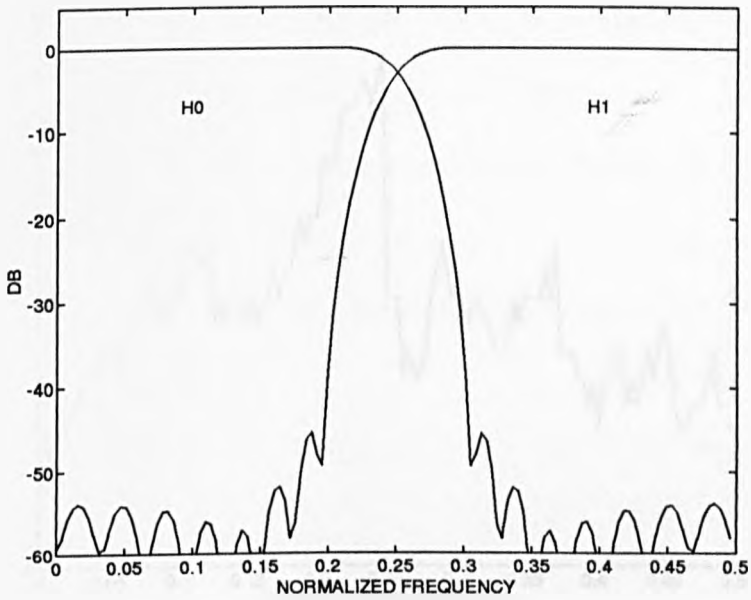

Figure 4.7: Analysis Filters for Example 4.6.1.1

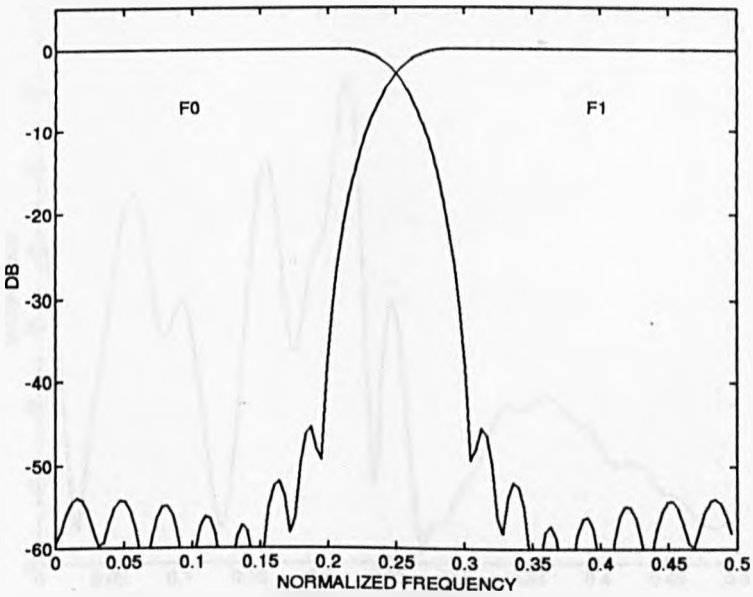

Figure 4.8: Synthesis filters for Example 4.6.1.1

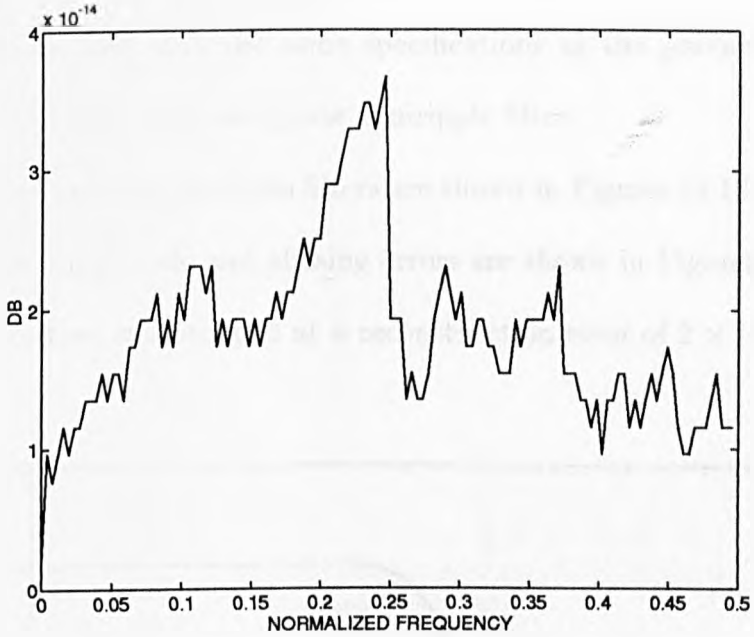

Figure 4.9: Magnitude error for Example 4.6.1.1

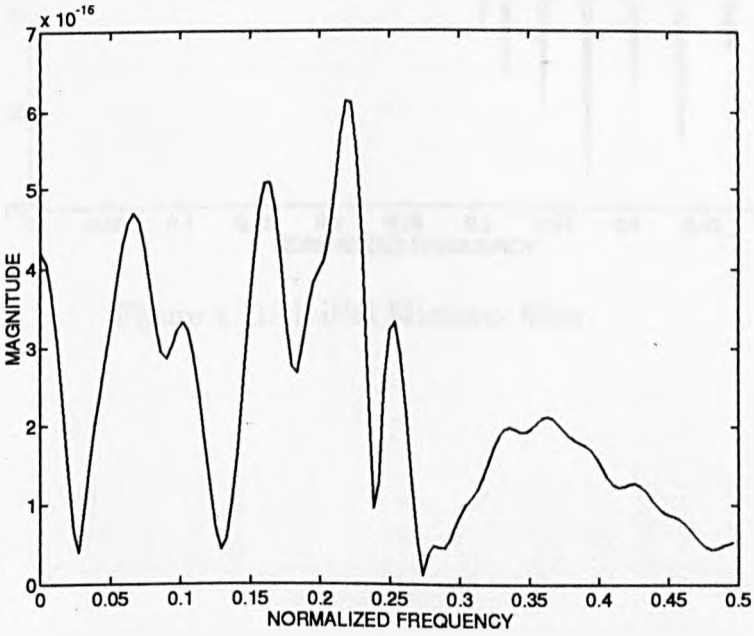

Figure 4.10: Aliasing error for Example 4.6.1.1

Example 4.6.1.2 In this example the starting filter is designed using equiripple minimax technique [66] with the same specifications as the previous example. Figure(4.11) shows the minimum phase equiripple filter.

The resulting analysis and synthesis filters are shown in Figures (4.12) and (4.13) respectively. The magnitude and aliasing errors are shown in Figures (4.14) and (4.15). The algorithm was stopped at a reconstruction error of 2×10^{-16}.

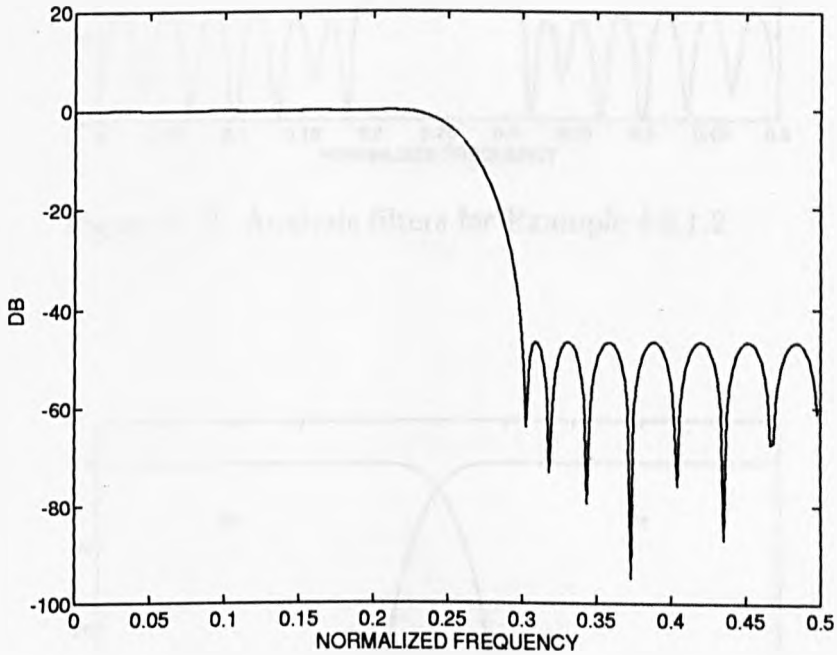

Figure 4.11: Initial Minimax filter

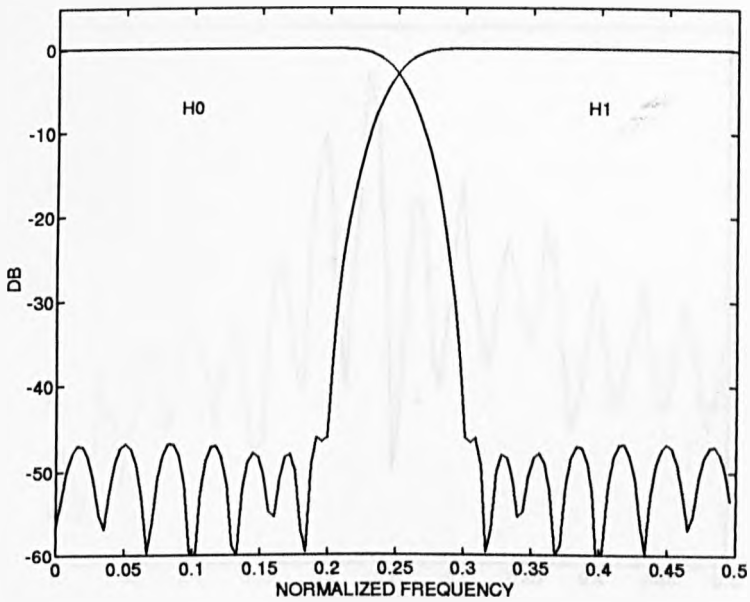

Figure 4.12: Analysis filters for Example 4.6.1.2

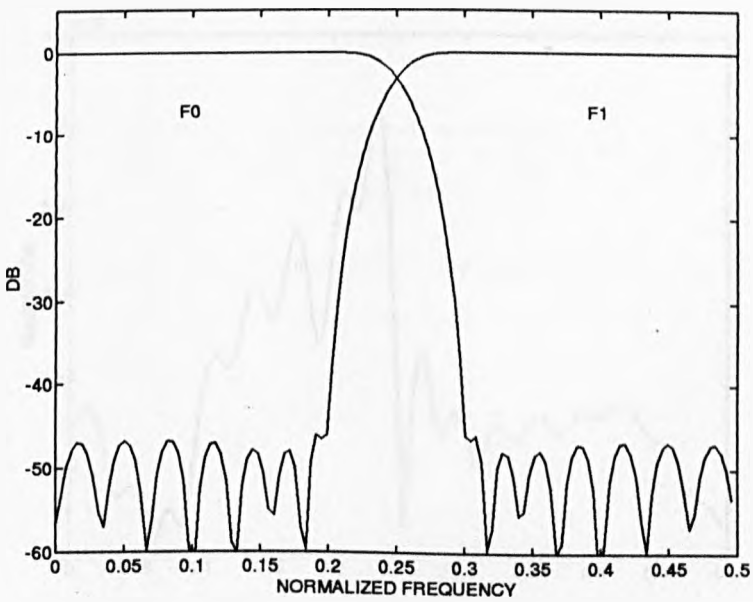

Figure 4.13: Synthesis filters for Example 4.6.1.2

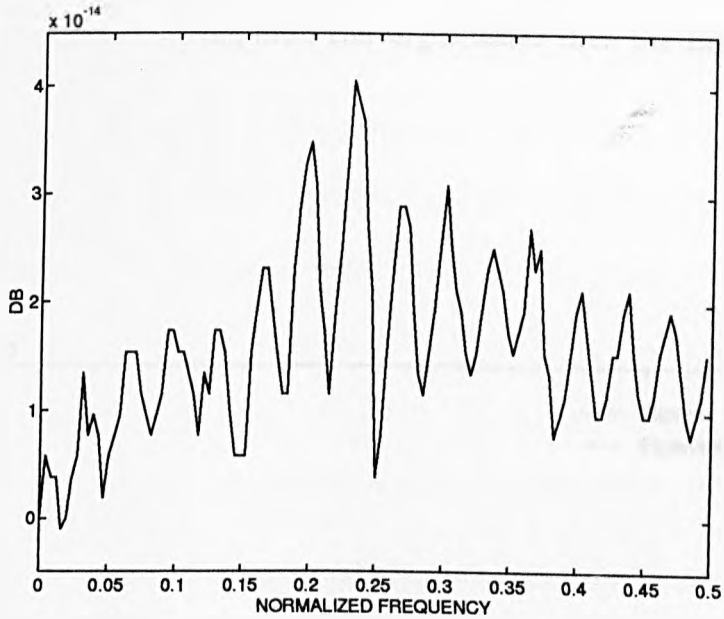

Figure 4.14: Magnitude error for Example 4.6.1.2

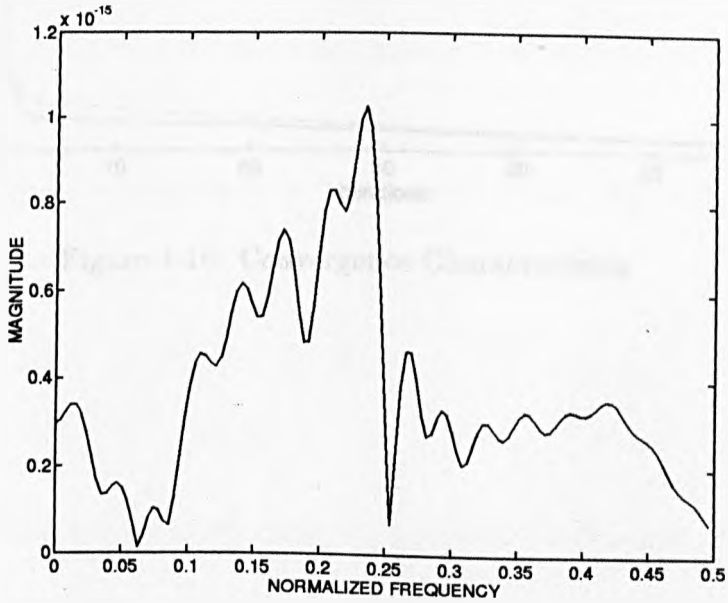

Figure 4.15: Aliasing error for Example 4.6.1.2

Convergence characteristics are compared for both examples. Figure (4.16) shows that the minimax starting filter converges faster than the Eigenfilter.

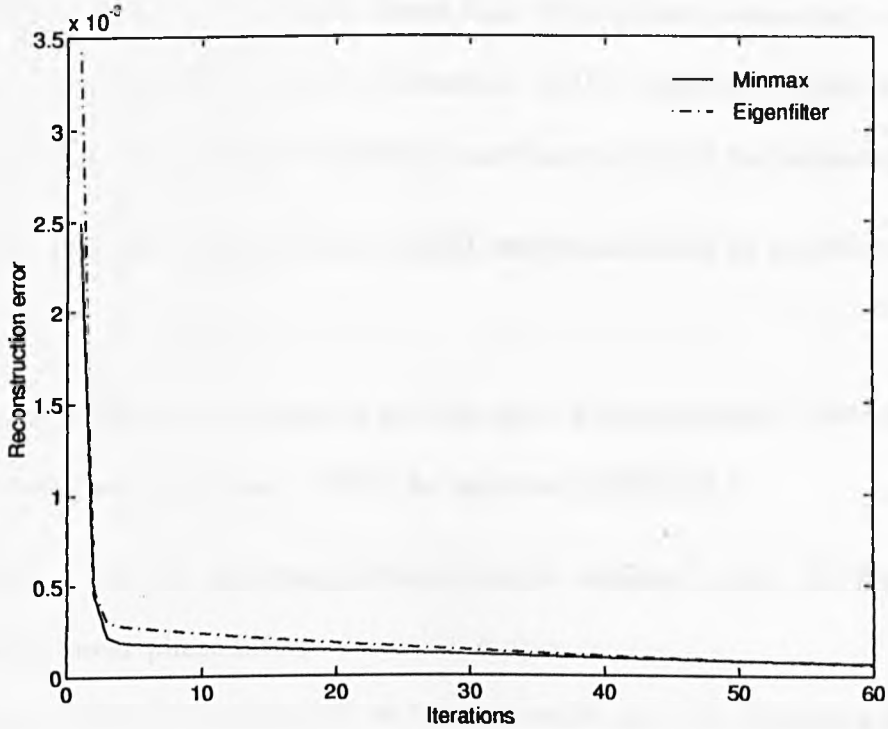

Figure 4.16: Convergence Characteristics

4.6.2 Linear Phase Design

In this section the design of linear phase two channel filter banks is presented. In the paraunitary case the analysis filters are constrained to be non-linear phase filters related by (4.54). It turns out [78][119], that in order to design nontrivial FIR linear-phase PR two-channel filter banks, it is necessary to give up the paraunitary property. It has been shown that linear-phase paraunitary systems cannot have PR unless $N = 2$ [107]. Vetterli et. al [121] had shown that to obtain linear-phase PR FIR solutions the filters must have either of the following forms

- Both filters are symmetric and of odd lengths, differing by an odd multiple of 2.
- One of the filters is symmetric and the other is antisymmetric: both lengths are even, and are equal or differ by an even multiple of 2.

Example 4.6.2.1 A two-channel filter bank is designed where the filters are equal length linear-phase filters.

The low-pass filter is constrained to be symmetric and the high-pass filter is antisymmetric such that

$$\begin{aligned} h_0^0(n) &= h_0^0(N-1-n) \\ h_1^0(n) &= -h_1^0(N-1-n) \qquad 0 \le n \le N-1 \end{aligned} \tag{4.56}$$

The starting filters are designed using the equiripple technique, with $N = 32$, the low-pass filter has $\omega_p = 0.44\pi$, and $\omega_s = 0.6\pi$. The high-pass filter has $\omega_s = 0.42\pi$, and $\omega_p = 0.6\pi$. Figure (4.17) shows the starting filters.

The algorithm converges much slower than the paraunitary design, and it was

stopped at a reconstruction error of 2×10^{-7}. The resulting analysis and synthesis filters are shown in Figures (4.18) and (4.19). The trade off is obvious in the quality if the filters compared with the paraunitary design. The magnitude and aliasing errors are shown in Figures (4.20) and (4.21).

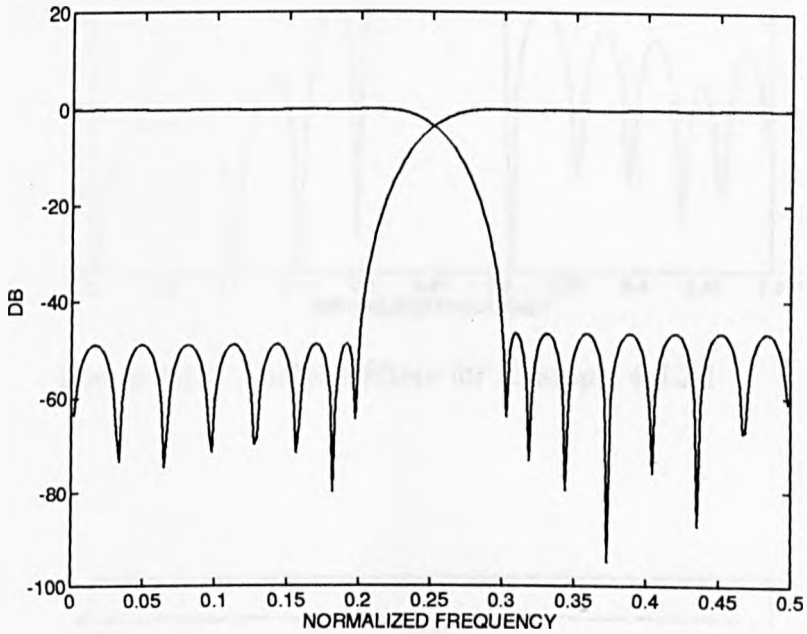

Figure 4.17: Initial linear phase filters

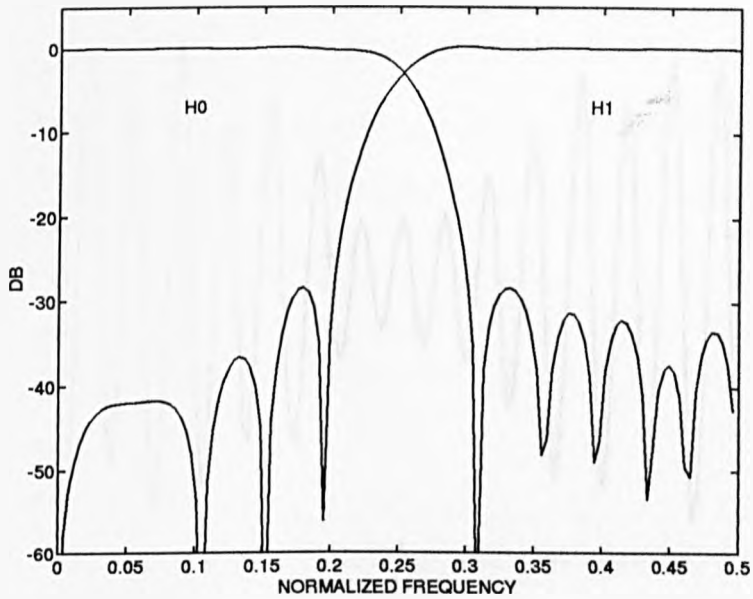

Figure 4.18: Analysis filters for Example 4.6.2.1

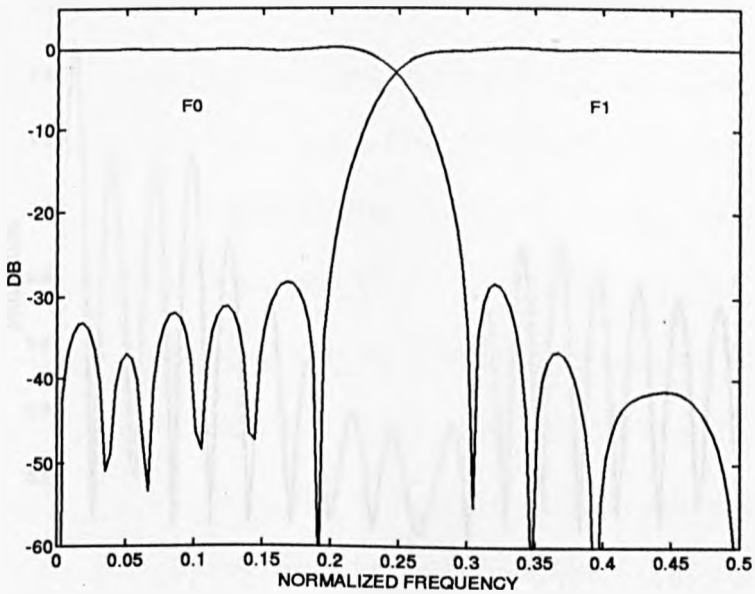

Figure 4.19: Synthesis filters for Example 4.6.2.1

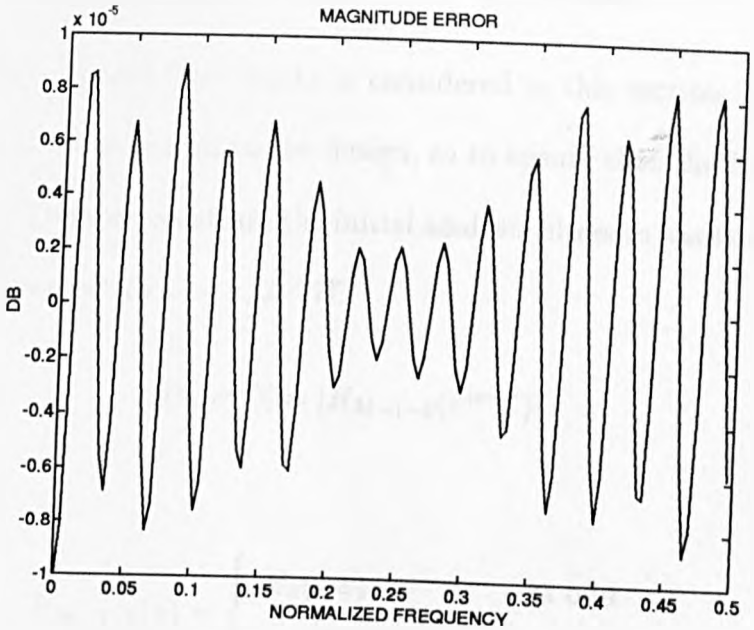

Figure 4.20: Magnitude error for Example 4.6.2.1

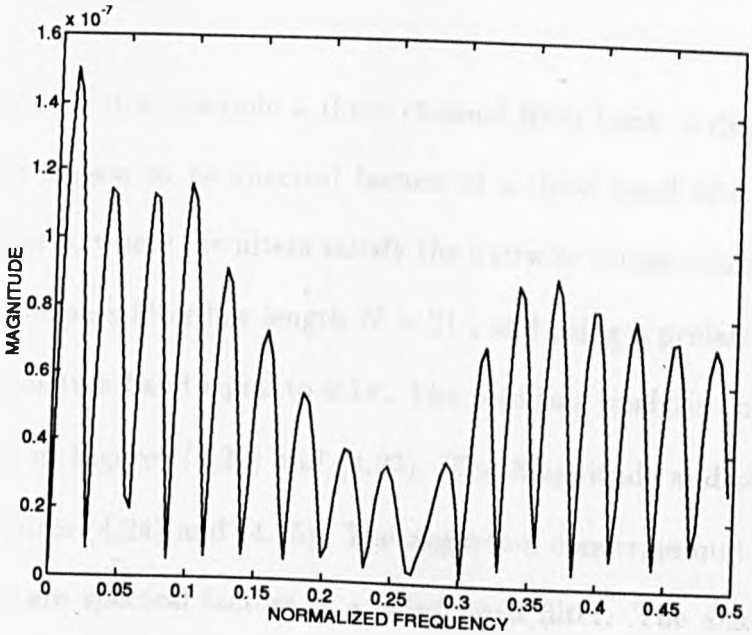

Figure 4.21: Aliasing error for Example 4.6.2.1

4.7 M-channel Filter Bank Design

The design of M-channel filter banks is considered in this section. The quality of the starting filters is crucial to the design, so to ensure that the filters remain good band pass filters we constrain the initial analysis filters to have mirror image symmetry with respect to $\omega = \pi/2$ [77].

$$|H_k(e^{j\omega})| = |H_{M-1-k}(e^{j\omega+\pi})| \tag{4.57}$$

in the z-domain

$$H_{M-1-k}(z) = \begin{cases} H_k(-z) & \text{M odd} \\ z^{-(N-1)}H_k(-z^{-1}) & \text{M even} \end{cases} \tag{4.58}$$

Maximally decimated examples are presented ($R = M$) for three and five channel systems.

Example 4.7.1 In this example a three channel filter bank is designed. The initial filters are chosen to be spectral factors of a third band filter, using the method in chapter 3, where the filters satisfy the pairwise image condition (4.58). The prototype low-pass filter has length $N = 21$, and using a prolate spheroidal window with transition band equal to 0.1π. The resulting analysis and synthesis filters are shown in Figures (4.22) and (4.23). The Magnitude and phase errors are shown in Figures (4.24) and (4.25). The algorithm converges quite fast since the initial filters are spectral factors of a third band filter. The algorithm was stopped at a reconstruction error of 2×10^{-12}.

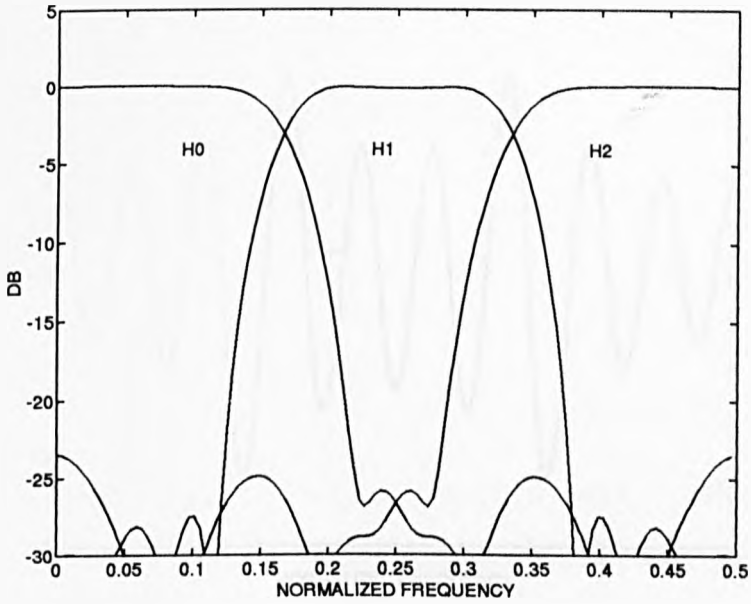

Figure 4.22: Analysis filters for Example 4.7.1

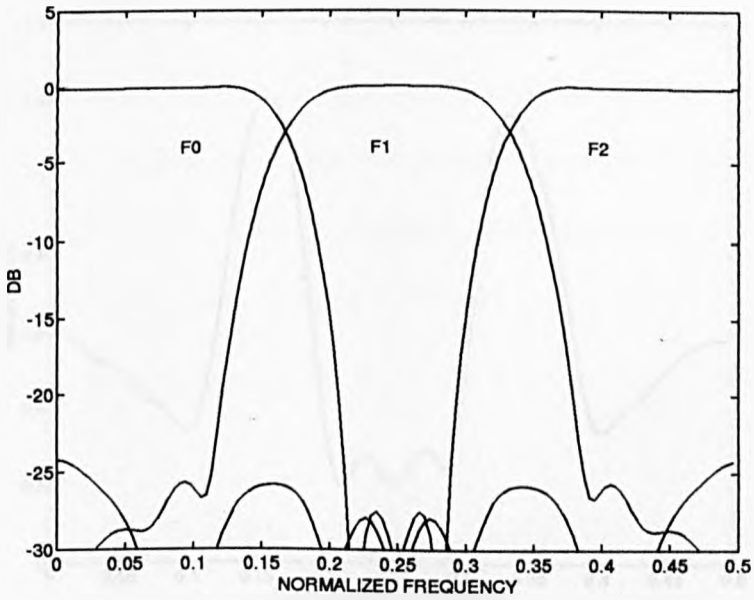

Figure 4.23: Synthesis filters for Example 4.7.1

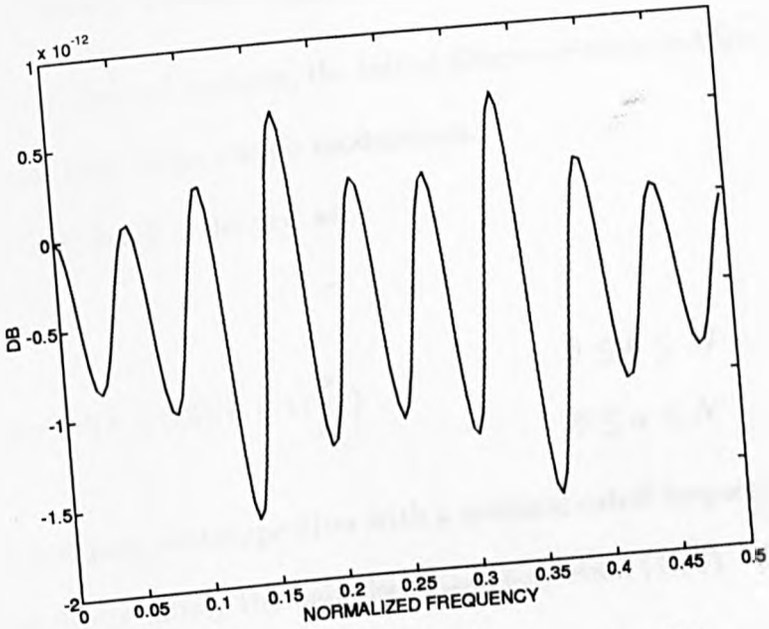

Figure 4.24: Magnitude error for Example 4.7.1

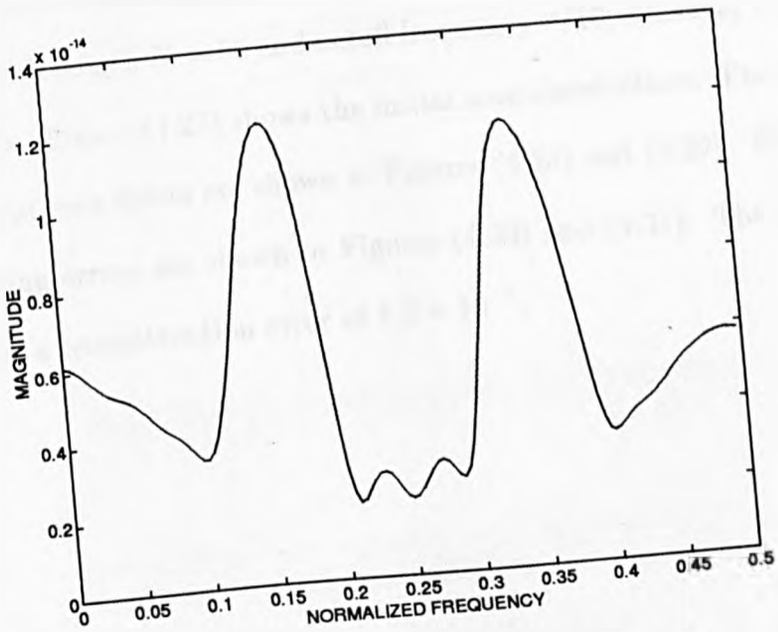

Figure 4.25: Aliasing error for Example 4.7.1

4.7.1 Modulated Filter Bank

For more than three channel systems, the initial filters are obtained from a single prototype low-pass filter using cosine modulation.

The modulated filter bank is defined as

$$h_k^0(n) = b(n)cos((k+0.5)(n+1)\frac{\pi}{M}) \qquad \begin{array}{l} 0 \leq k \leq M-1 \\ 0 \leq n \leq N-1 \end{array} \tag{4.59}$$

where $b(n)$ is a low-pass prototype filter with a nominal cutoff frequency of $\pi/2M$. The modulated filters satisfy the pairwise image condition (4.58).

Example 4.7.1.1 A five channel filter bank is designed. The initial filters are obtained using (4.59). The prototype filter is an equiripple minimax filter shown in Figure (4.26), with length $N = 55$ and cutoff frequency $\pi/10$, where $\omega_p = 0.008\pi$, and $\omega_s = 0.228\pi$. Figure (4.27) shows the initial modulated filters. The resulting analysis and synthesis filters are shown in Figures (4.28) and (4.29). The magnitude and aliasing errors are shown in Figures (4.30) and (4.31). The algorithm was stopped at a reconstruction error of 1.3×10^{-7}.

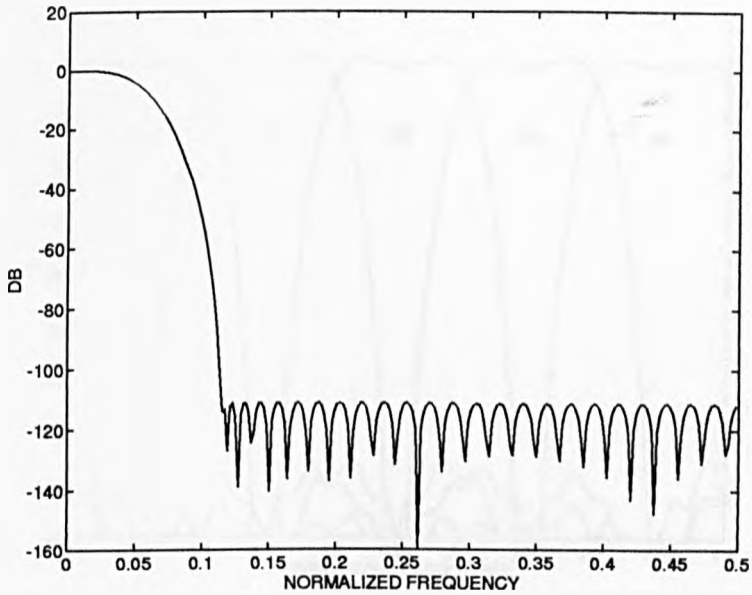

Figure 4.26: Prototype filter

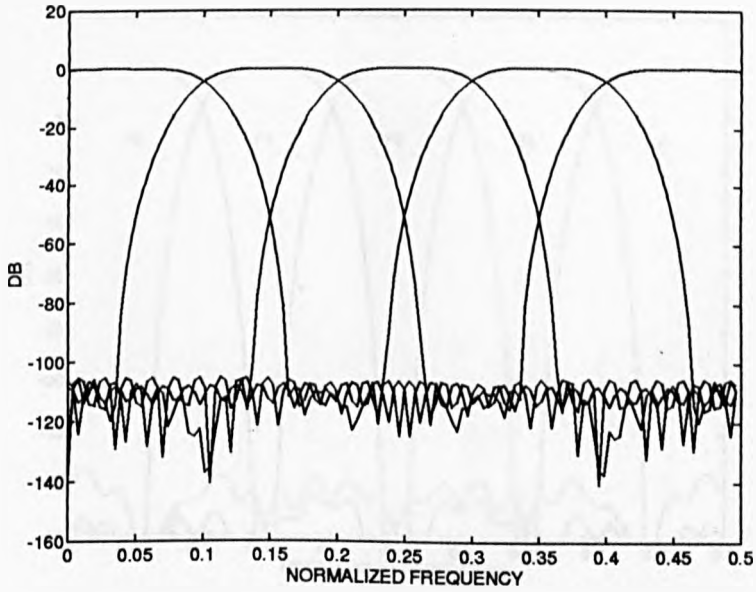

Figure 4.27: Modulated filter bank

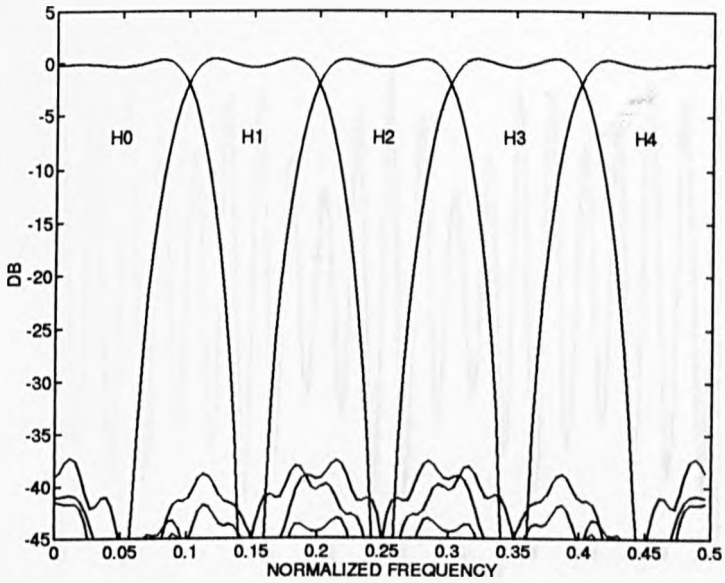

Figure 4.28: Analysis filters for Example 4.7.1.1

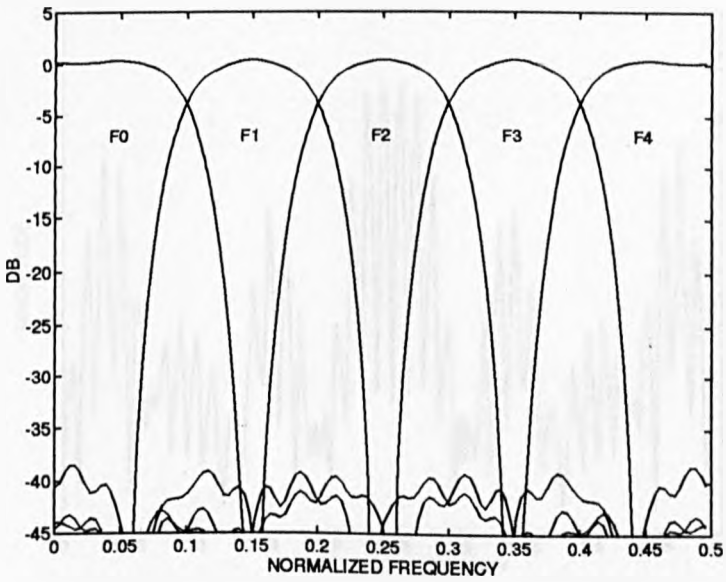

Figure 4.29: Synthesis filters for Example 4.7.1.1

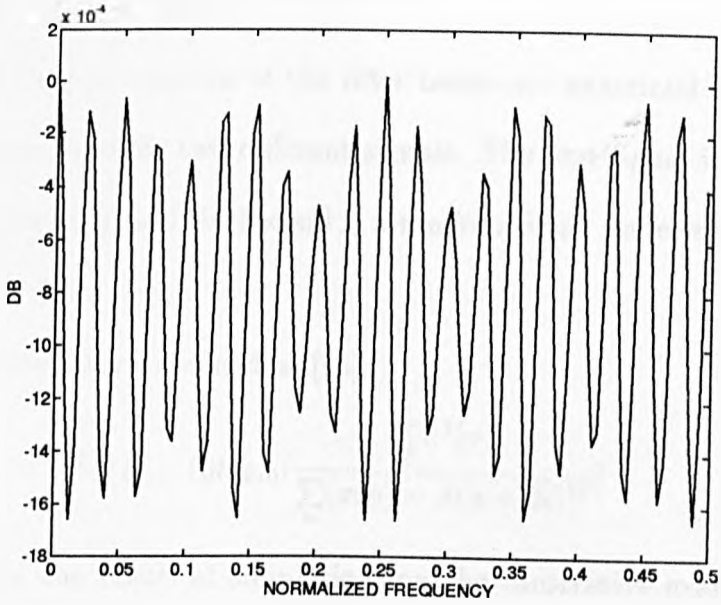

Figure 4.30: Magnitude error for Example 4.7.1.1

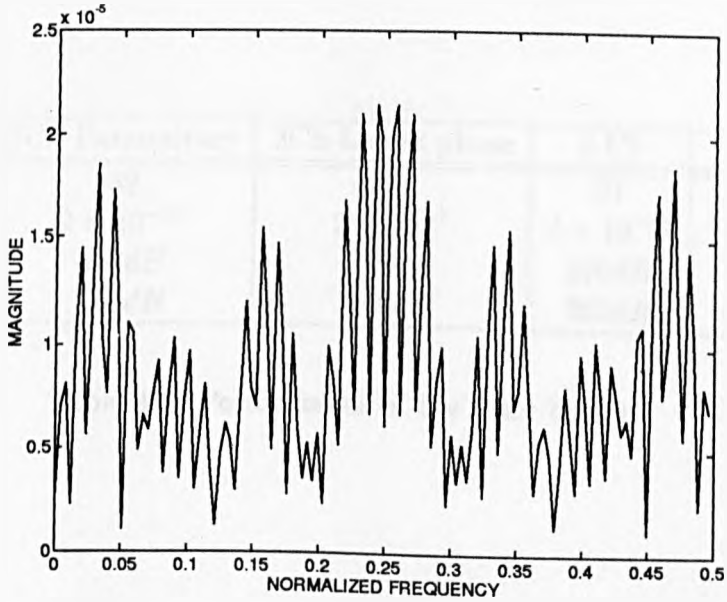

Figure 4.31: Aliasing error for Example Example 4.7.1.1

4.8 Performance Analysis

The reconstruction performance of the filter banks are examined by computing the signal to noise ratio for two different signals. The first signal is a unit ramp signal 100 samples long, and the second is a random signal uniformly distributed between -100 and 100.

The signal to noise ratio is defined as [75]

$$SNR = 10log_{10}(\frac{\sum_n x^2(n)}{\sum_n (x(n) - \hat{x}(n+\Delta))^2}) \tag{4.60}$$

Table (4.1) shows the result of simulations on the illustrative examples shown earlier. SNR1 denoted the signal to noise ratio of the ramp signal, and SNR2 denotes the signal-to-noise ratio of the random signal.

	2Ch-Paraunitary	2Ch-Linear phase	3-Ch	5-Ch
N	32	32	21	55
Rec. error	2×10^{-16}	2×10^{-7}	2×10^{-12}	1.3×10^{-6}
SNR1	$310dB$	$150dB$	$290dB$	$89dB$
SNR2	$306dB$	$146dB$	$282dB$	$85dB$

Table 4.1: Performance of the filter banks

4.9 Conclusions

A general time-domain formulation for FIR multirate filter banks has been derived. Starting from the z-domain perfect reconstruction conditions, a set of matrix system of equations are obtained. The paraunitary (lossless) time-domain conditions has been derived. These conditions represent a set of cross orthogonality conditions of filter coefficients in the analysis and synthesis filters.

The time-domain formulation has been utilized to design a wide class of multirate filter banks. The design is simplified by the fact that the analysis and synthesis filters are interrelated, and using the previous values of the synthesis filters to update the analysis filters from the next iteration of a least square minimisation algorithm.

All the simulation results show that a high signal-to-noise ratio can be easily achieved, which is sufficient for most practical applications. The results shown were obtained using MATLAB on a SUN SPARC workstation.

Chapter 5

Low Delay Multirate Filter Banks

5.1 Introduction

In this chapter, the issue of system delay is explicitly addressed. Delay is an important issue that has been recognized previously as a source of distortion in real-time subband coding systems [69][58][70].

In most perfect reconstruction systems addressed previously, the overall delay has been fixed by the length of the filters [108]. However Nayebi et. al. [75] recognised that low delay perfect reconstruction systems can be designed relatively independent of the length of the filters.

Tree structured systems based on the two channel filter bank has been used extensively in subband coding [27][93]. These systems have inherently long delays that can be objectionable in real implementations and applications of subband

coders. Also non-uniform filter banks such as the wavelet transform also suffer from long delays [90].

In this chapter, the design of low delay two channel filter banks is initially considered using direct z-domain analysis and design. This procedure is simple and achieves perfect reconstruction. The main disadvantage is that it requires the spectral factorization of a non-linear phase filter, which consequently does not guarantee good quality analysis and synthesis filters, Also the system delay is constrained to be odd. Next, the design of low delay M-channel filter banks using the time-domain formulation is investigated. The design involves a simple modification of the algorithm presented in chapter 4. The algorithm is modified to overcome the unsymmetric nature of the system of equations when the system delay is forced to be less than $N-1$.

This procedure produces low delay systems with good quality analysis and synthesis filters, with arbitrary values of the system delay Δ [8].

5.2 The Two Channel Low Delay System

The two channel filter bank is analyzed in the classical z-domain formulation with arbitrary system delay. Initially consider the two-channel filter bank of Figure (4.1), the output $\hat{X}(z)$ can be expressed as

$$\hat{X}(z) = T(z)X(z) + A(z)X(-z) \tag{5.1}$$

where $A(z)$ is the aliasing term

$$A(z) = \frac{1}{2}[H_0(-z)F_0(z) + H_1(-z)F_1(z)] \tag{5.2}$$

and $T(z)$ is the system transfer function

$$T(z) = \frac{1}{2}[H_0(z)F_0(z) + H_1(z)F_1(z)] \tag{5.3}$$

To eliminate aliasing distortion, the synthesis filters are chosen as

$$\begin{aligned} F_0(z) &= H_1(-z) \\ F_1(z) &= -H_0(-z) \end{aligned} \tag{5.4}$$

then (5.2) is equal to zero, and (5.3) becomes

$$T(z) = \frac{1}{2}[H_0(z)H_1(-z) - H_1(z)H_0(-z)] \tag{5.5}$$

Define the product filter $G(z)$ as

$$G(z) = H_0(z)H_1(-z) \tag{5.6}$$

then (5.5) can be expressed as

$$T(z) = G(z) + G(-z) \tag{5.7}$$

For perfect reconstruction $T(z)$ must be a pure delay

$$T(z) = z^{-\Delta}$$

where Δ is the system delay.

In the time-domain the PR conditions can be written as

$$t(n) = g(n) + (-1)^n g(n) = \delta(n - \Delta) \tag{5.8}$$

this means that all except one of the even samples of $g(n)$ are zero

$$g(2n) = \begin{cases} 0.5 & n = \Delta \\ 0 & \text{otherwise} \end{cases} \tag{5.9}$$

In the classical two channel QMF design [93][73], Δ is constrained to be $N-1$, where N is even, and the product filter is now constrained to be an odd length linear phase half-band filter, where

$$G(z) = H_0(z)H_0(z^{-1})$$

A low delay system is defined to be a system with filters of length N and with a delay Δ, which is less than $N-1$. To design low delay two-channel systems, Δ is defined as

$$\Delta = N - 1 - d$$

where d is a positive even integer. Clearly from (5.9), the filter is no longer symmetric, and the maximum value is shifted from the center. A direct design of $G(z)$ is presented in the next section based on a truncated half-band filter to obtain the required non-linear phase filter.

5.2.1 Design Procedure

The procedure starts by designing a half-band product filter $G_1(z)$ with length $(2N-1+2d)$, and then discarding the first $2d$ coefficients to obtain a non-linear phase filter $G(z)$. This will shift the maximum coefficient from $(N-1)$ to $(N-1-d)$.

Subsequently the product filter $G(z)$ is factorised to its appropriate factors according to (5.6).

The difficulty lies in the spectral factorisation, since $G(z)$ is a non-linear phase filter, and its zeros are unsymmetric. The following design examples demonstrates

Example 5.2.1

Product filters are designed and the value of d is varied for comparison. The value of N is chosen to be 8. Figure (5.1) shows the product filters for values of $d = 0, 2, 4$ respectively, and Figure (5.2) shows their zeros. Clearly by increasing the value of d the filter response in the stopband is degraded, and the filter becomes dominantly minimum phase.

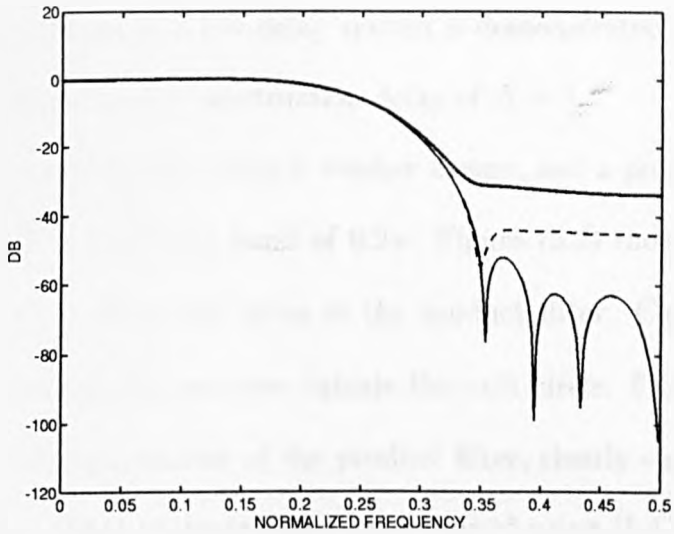

Figure 5.1: Magnitude responses of the product filters for d=0 (solid line), d=2 (dashed line), d=4 (dotted line)

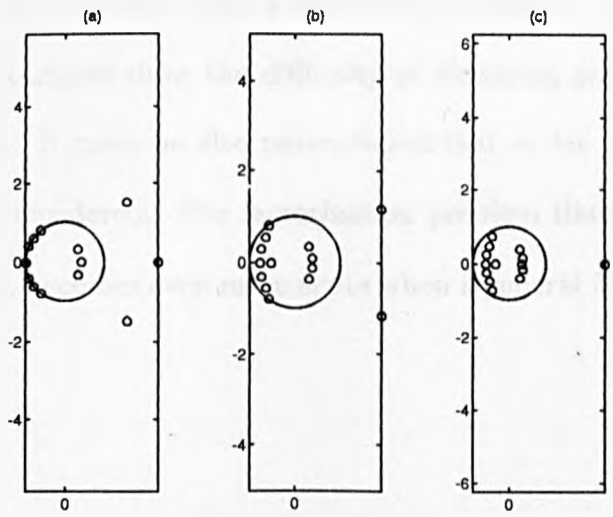

Figure 5.2: Zeros of the product filters for (a) d=0, (b) d=2, (c) d=4

Example 5.2.2

In this example the design of a low delay system is demonstrated for $N = 8$ and $d = 4$, thus the system has a reconstruction delay of $\Delta = 3$.

The product filter was designed using a window design, and a prolate spheroidal window is used with a transition band of 0.2π. Figure (5.3) shows the product filter, and Figure (5.4) shows the zeros of the product filter. Clearly the filter is minimum phase except for one zero outside the unit circle. Figures (5.5) and (5.6) show a possible factorisation of the product filter, clearly one of the filters has a good response. The synthesis filters are obtained using (5.4).

Example 5.2.3

The same product filter is designed as in the previous example, but the analysis and synthesis filters are obtained using a different factorisation. Figures (5.7) and (5.8). Clearly the examples show the difficulty of obtaining good quality filters using this procedure. It must be also remembered that so far only two channel systems have been considered. The factorization problem illustrated above for the two channel case, becomes even more acute when a general M-channel system is considered.

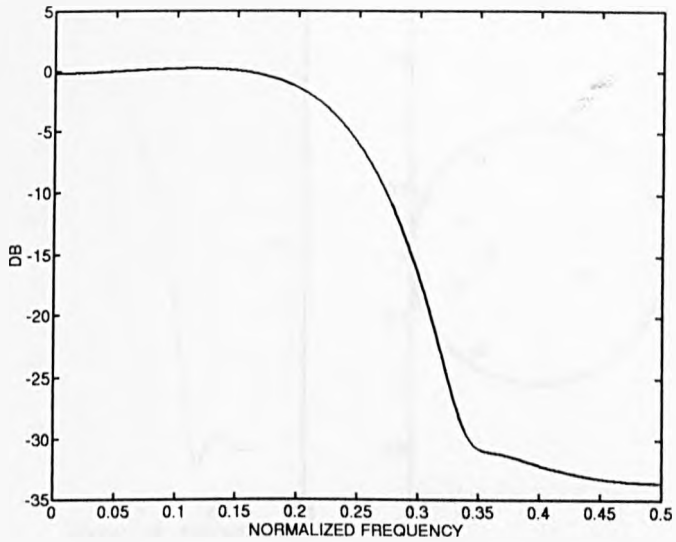

Figure 5.3: Magnitude response of the product filter

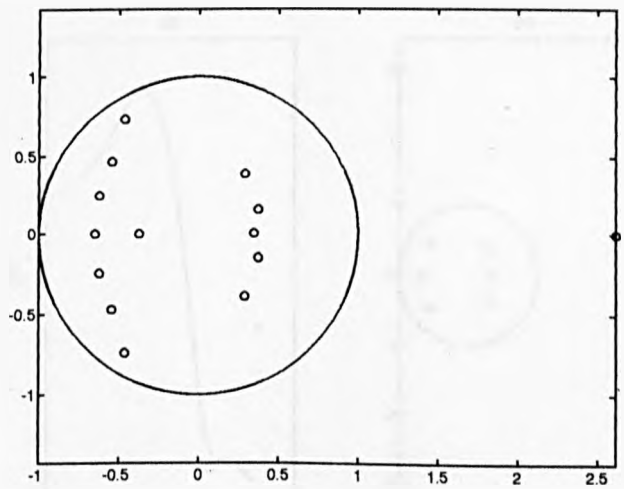

Figure 5.4: zeros of the product filter

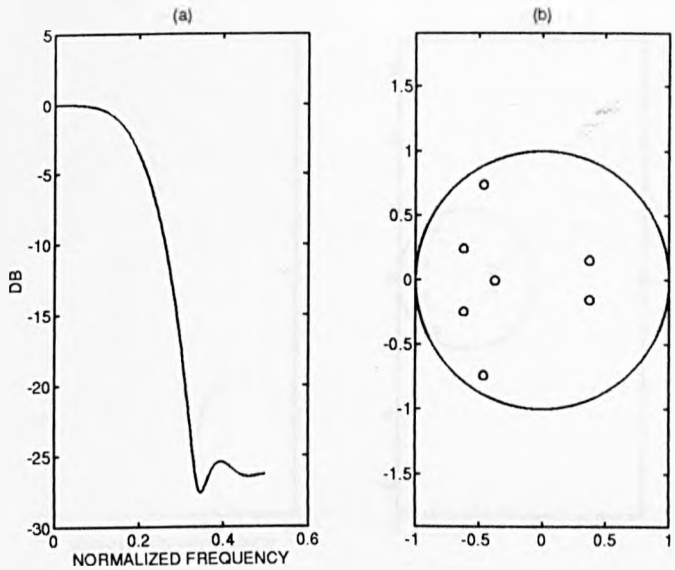

Figure 5.5: (a) Magnitude response of $H_0(z)$ (b) zeros of $H_0(z)$ for Example 5.2.2

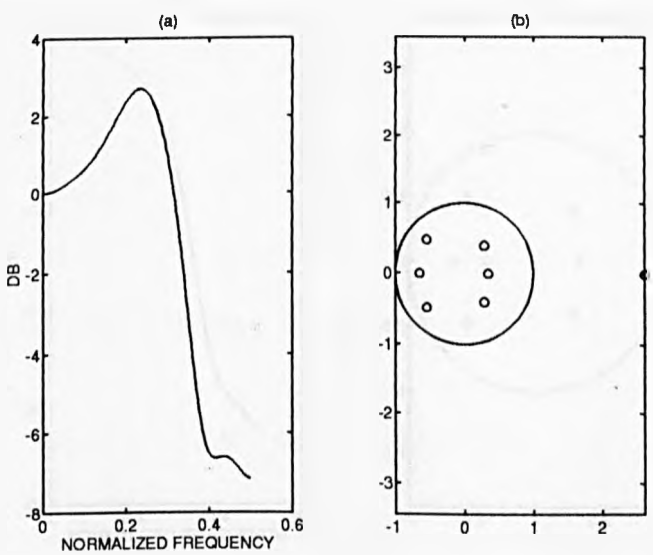

Figure 5.6: (a) Magnitude response of $H_1(-z)$ (b) zeros of $H_1(-z)$ for Example 5.2.2

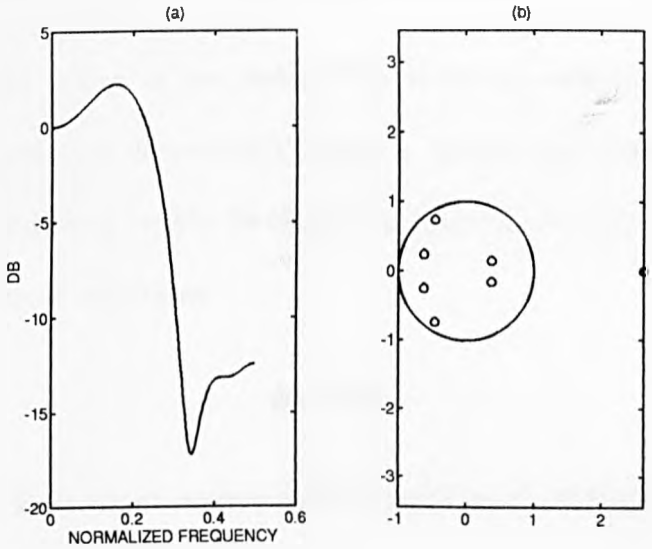

Figure 5.7: (a) Magnitude response of $H_0(z)$ (b) zeros of $H_0(z)$ for Example 5.2.3

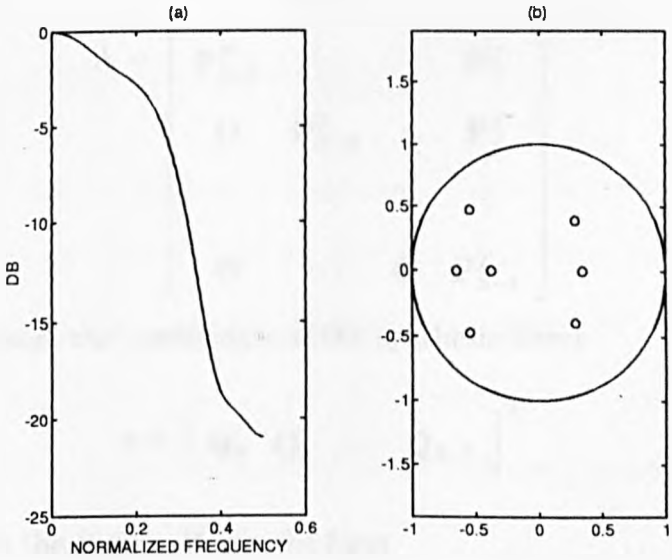

Figure 5.8: (a) Magnitude response of $H_1(-z)$ (b) zeros of $H_1(-z)$ for Example 5.2.3

5.3 Time-Domain Formulation

In this section the design of low delay filter banks is considered based on the time domain formulation derived in Chapter 4. Recall that time-domain perfect reconstruction conditions for the M-channel system figure.(4.2) can be expressed as a matrix system of equations

$$\mathbf{A}\mathbf{s} = \mathbf{B} \tag{5.10}$$

where $\mathbf{A}$ is a block circulant matrix derived from the coefficients of the analysis filters

$$\mathbf{A} = \begin{bmatrix} \mathbf{P}_0^T & \mathbf{O} & \cdots & \mathbf{O} \\ \mathbf{P}_1^T & \mathbf{P}_0^T & \ddots & \vdots \\ \vdots & \mathbf{P}_1^T & \ddots & \vdots \\ \mathbf{P}_{L-1}^T & \ddots & \ddots & \mathbf{P}_0^T \\ \mathbf{O} & \mathbf{P}_{S-1}^T & \ddots & \mathbf{P}_1^T \\ \vdots & \ddots & \ddots & \vdots \\ \mathbf{O} & \cdots & \mathbf{O} & \mathbf{P}_{S-1}^T \end{bmatrix} \tag{5.11}$$

and $\mathbf{s}$ is derived from the coefficients of the synthesis filters

$$\mathbf{s} = \begin{bmatrix} \mathbf{Q}_0 & \mathbf{Q}_1 & \cdots & \mathbf{Q}_{S-1} \end{bmatrix}^T \tag{5.12}$$

Most importantly the matrix $\mathbf{B}$ has the form

$$\mathbf{B} = \begin{bmatrix} \mathbf{0}_R^T & \mathbf{0}_R^T & \cdots & \mathbf{J}_R & \cdots & \mathbf{0}_R^T & \mathbf{0}_R^T \end{bmatrix}^T \tag{5.13}$$

where $\mathbf{0_R}$ is an $R \times 1$ zeros matrix, and $\mathbf{J_R}$ is an $R \times R$ anti-diagonal identity matrix.

It has been shown in Chapter 4, that the position of the submatrix $\mathbf{J_R}$ in $\mathbf{B}$ is directly proportional to the total delay of the system Δ.

In general, the M-channel system in Figure.(4.2) can have a minimum delay of $R-1$ samples, and a maximum delay of $(2S-1)R-1$ samples. For example a minimum delay system with $R-1$ samples of delay, the matrix $\mathbf{B}$ should be of the form

$$\mathbf{B_{min}} = \begin{bmatrix} \mathbf{J}_R & \mathbf{0}_R^T & \cdots & \mathbf{0}_R^T \end{bmatrix}^{\mathbf{T}}$$

The design of low delay systems using the time-domain formulation has been considered by Nayebi et.al. [75][74]. The design is based on the same optimisation routine described in Chapter 4.

5.4 Time-Domain Design

The time-domain design algorithm presented in Chapter 4, exploits the fact that the linear system of equations (5.10) is symmetric when the matrix $\mathbf{B}$ is symmetric as in (5.13), this only occurs when the system delay $\Delta = N-1$. Experiments have shown that the direct application of the algorithm to low delay systems ($\Delta < N-1$) results in undesirable effects in the frequency response of the analysis and synthesis filters.

In this section a modified time-domain algorithm is proposed, where the system delay is adjusted gradually throughout the design process. Figure (5.9) shows the modified design flowgraph. The system delay is initially set to $(N-1)$ ($\Delta_0 = N-1$), and then gradually reduced with each iteration until the desired

system delay Δ_r is reached. Subsequently the reconstruction error is minimized to an acceptable level.

This process ensures that the frequency response of the analysis and synthesis filters are not severely degraded. The imposition of low delay in the system will in general require analysis and synthesis filters with non-linear phase as was shown in the two-channel low delay design in section (5.2). However experiments have shown that linear phase starting filters are more suitable and produce better quality filters.

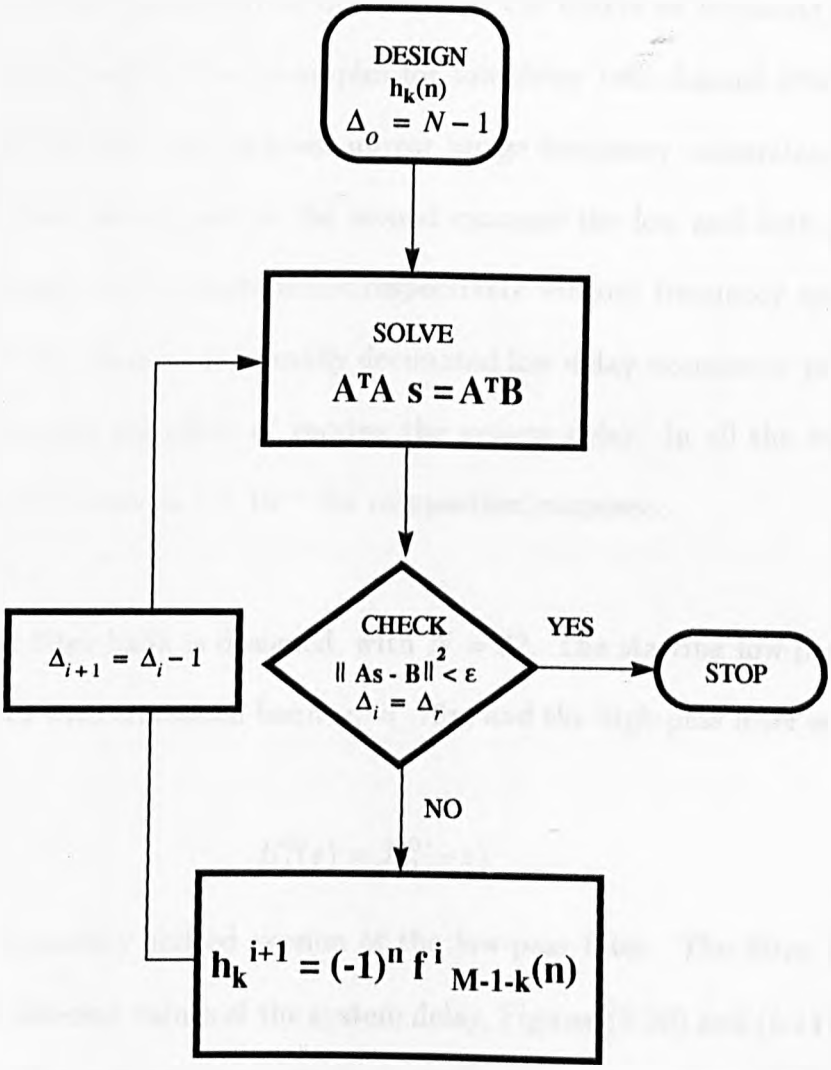

Figure 5.9: Low Delay Design Flowgraph

5.4.1 Design Examples

Design examples are presented to demonstrate the effects of imposing low delays on the filter banks. Two examples for low delay two channel filter banks are illustrated; the first one imposes mirror image frequency constraints on the low and high pass filters, and in the second example the low and high pass filters are symmetric and antisymmetric respectively without frequency symmetry constraints. A five channel maximally decimated low delay example is presented which demonstrates the effect of varying the system delay. In all the examples the reconstruction error is 1×10^{-5} for comparison purposes.

Example 5.4.1.1

A two channel filter bank is designed, with $N = 32$. The starting low-pass filter is an Eigenfilter with transition band $\omega_s = .16\pi$, and the high-pass filter is chosen as

$$H_1^0(z) = H_0^0(-z)$$

which is the frequency shifted version of the low-pass filter. The filter bank is designed with different values of the system delay, Figures (5.10) and (5.11) shows the analysis and synthesis filters when $\Delta = 31$. Figures (5.12) and (5.13) shows the analysis and synthesis filters for $\Delta = 28$. Figures (5.14) and (5.15) shows the analysis and synthesis filters for $\Delta = 23$. Lowering the delay further will result in undesirable effects in the frequency response of the filters.

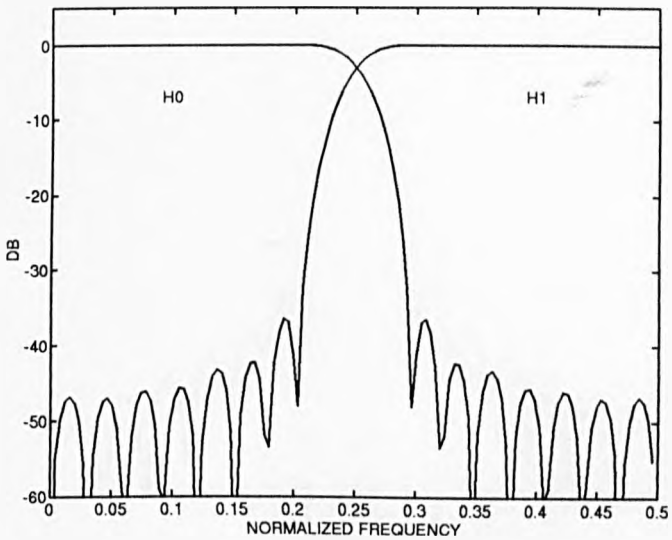

Figure 5.10: Analysis filters for $\Delta = 31$ in Example 5.4.1.1

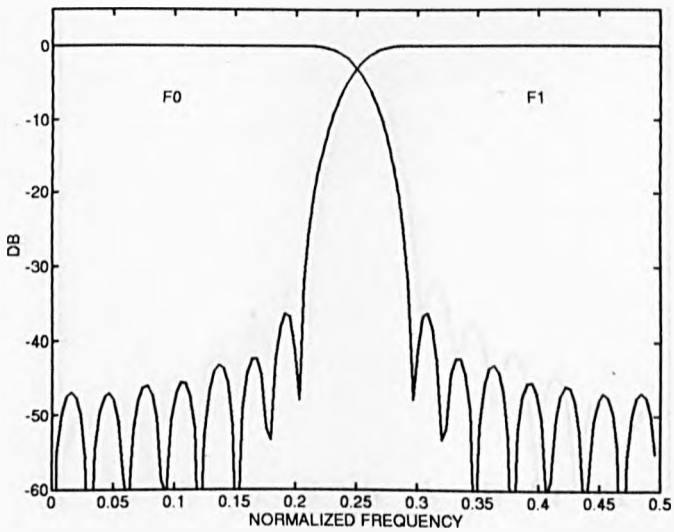

Figure 5.11: Synthesis filters for $\Delta = 31$ in Example 5.4.1.1

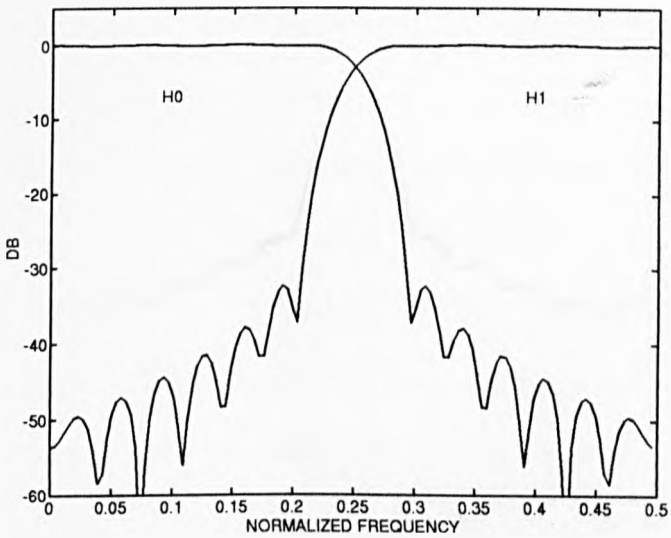

Figure 5.12: Analysis filters for $\Delta = 28$ in Example 5.4.1.1

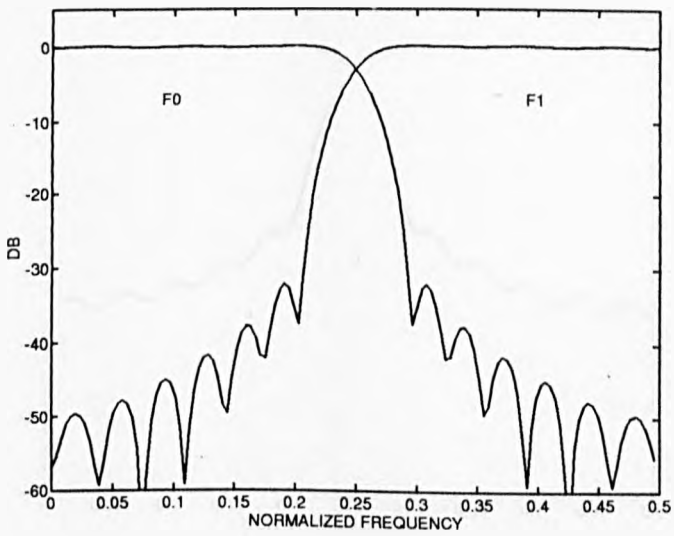

Figure 5.13: Synthesis filters for $\Delta = 28$ in Example 5.4.1.1

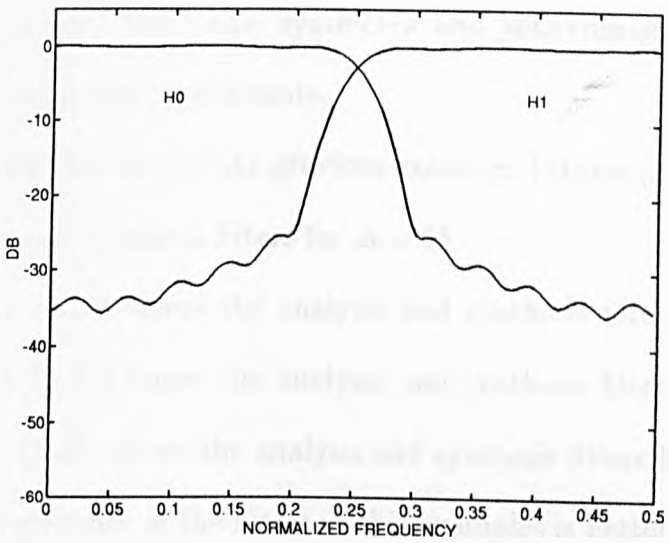

Figure 5.14: Analysis filters for $\Delta = 23$ in Example 5.4.1.1

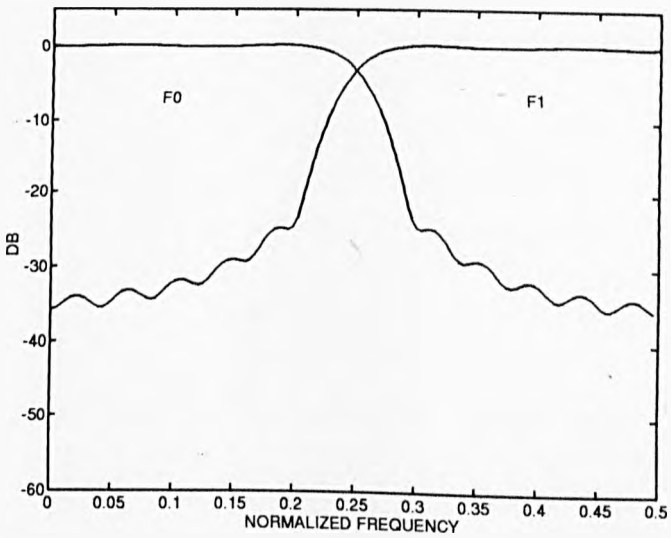

Figure 5.15: Synthesis filters for $\Delta = 23$ in Example 5.4.1.1

Example 5.4.1.2 A two channel system is designed,where the low and high pass starting filters are linear phase symmetric and antisymmetric respectively without frequency symmetry constraints.

The filter lengths are the same as the previous example. Figures (5.16) and (5.17) shows the analysis and synthesis filters for $\Delta = 25$.

Figures (5.18) and (5.19) shows the analysis and synthesis filters for $\Delta = 18$.

Figures (5.20) and (5.21) shows the analysis and synthesis filters for $\Delta = 15$.

Figures (5.22) and (5.23) shows the analysis and synthesis filters for $\Delta = 10$.

It is clear that the response of the filters in this examples is better than the previous, and a much lower delay can be achieved without severe distortion in the frequency response of the filters.

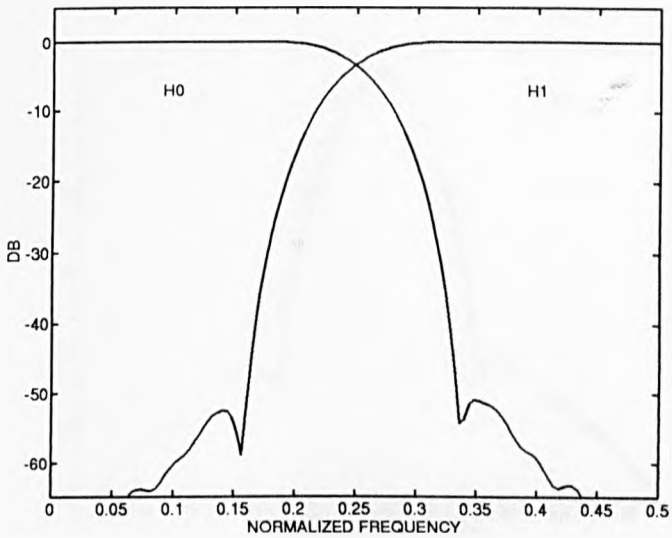

Figure 5.16: Analysis filters for $\Delta = 25$ in Example 5.4.1.2

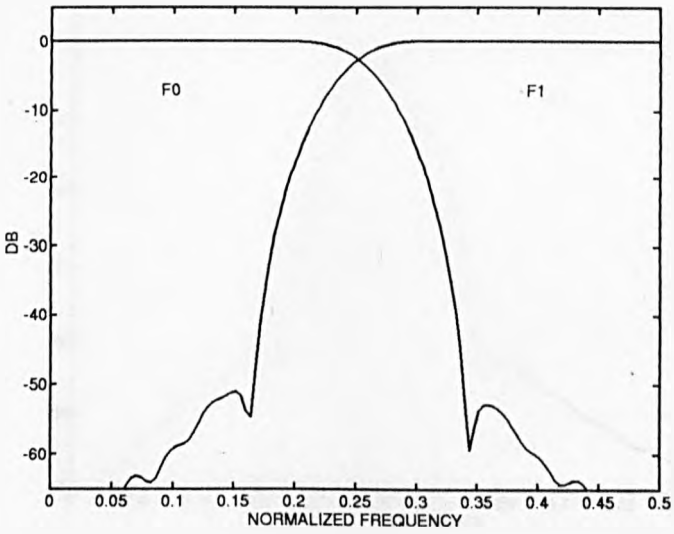

Figure 5.17: Synthesis filters for $\Delta = 25$ in Example 5.4.1.2

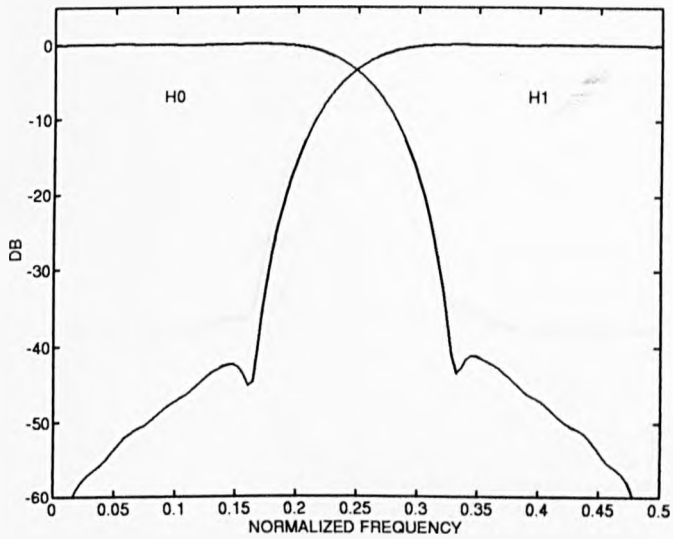

Figure 5.18: Analysis filters for $\Delta = 18$ in Example 5.4.1.2

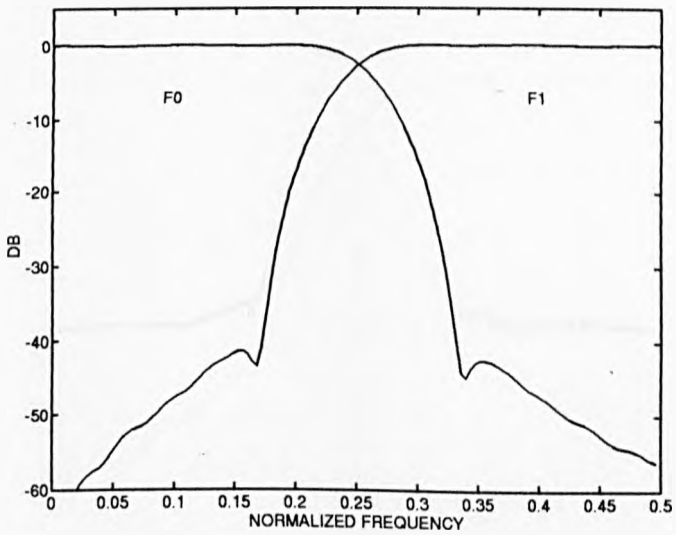

Figure 5.19: Synthesis filters for $\Delta = 18$ in Example 5.4.1.2

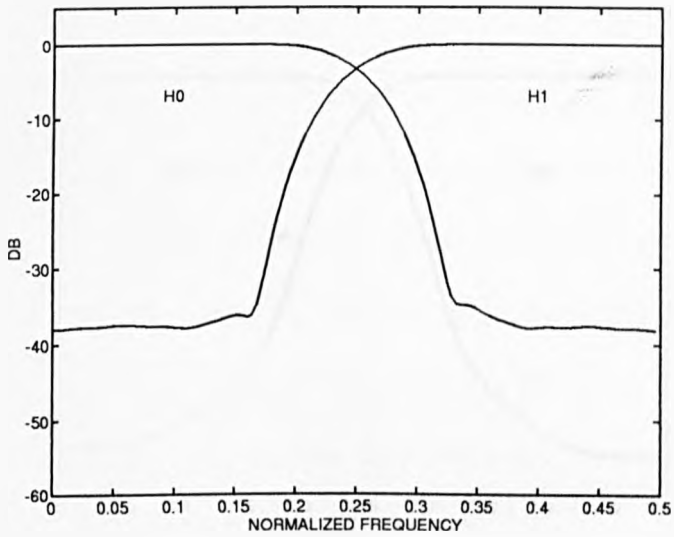

Figure 5.20: Analysis filters for $\Delta = 15$ in Example 5.4.1.2

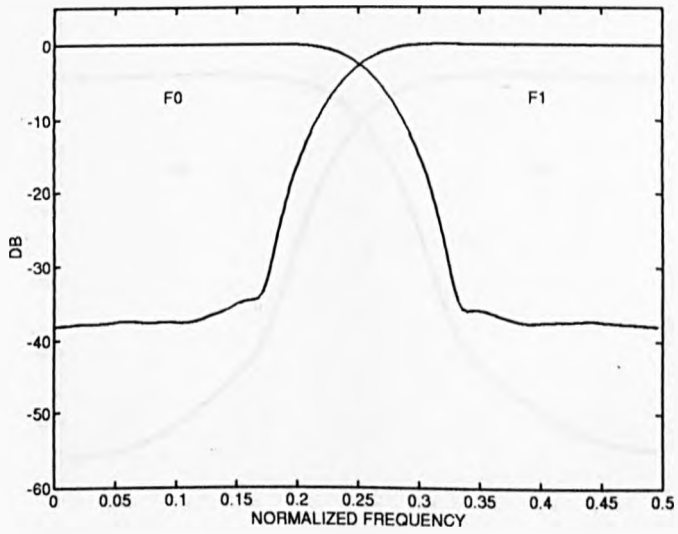

Figure 5.21: Synthesis filters for $\Delta = 15$ in Example 5.4.1.2

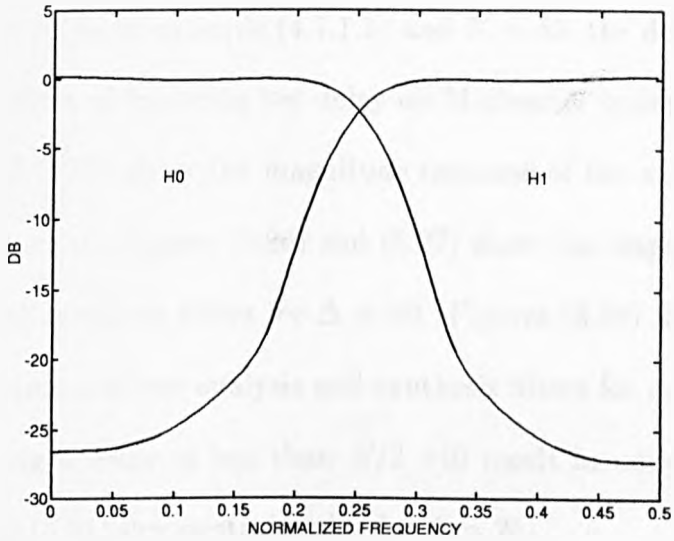

Figure 5.22: Analysis filters for $\Delta = 10$ in Example 5.4.1.2

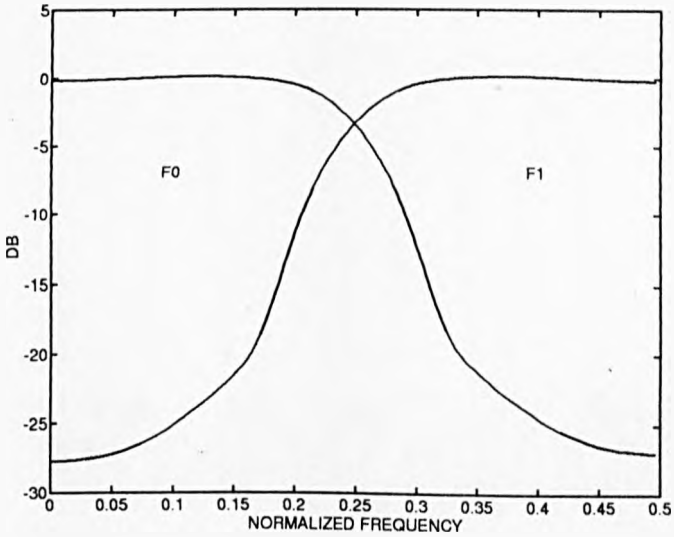

Figure 5.23: Synthesis filters for $\Delta = 10$ in Example 5.4.1.2

Example 5.4.1.3 A five channel maximally decimated filter bank is designed, with prototype filters as in example (4.7.1.1) and $N = 55$, the delay is varied to demonstrate the effect of imposing low delay on M-channel systems.

Figures (5.24) and (5.25) show the magnitude response of the analysis and synthesis filters for $\Delta = 54$. Figures (5.26) and (5.27) show the magnitude response of the analysis and synthesis filters for $\Delta = 40$. Figures (5.28) and (5.29) show the magnitude response of the analysis and synthesis filters for $\Delta = 33$.

In general imposing a delay of less than $N/2$ will result in undesirable effects, Figures (5.30) and (5.31) demonstrates this for $\Delta = 25$.

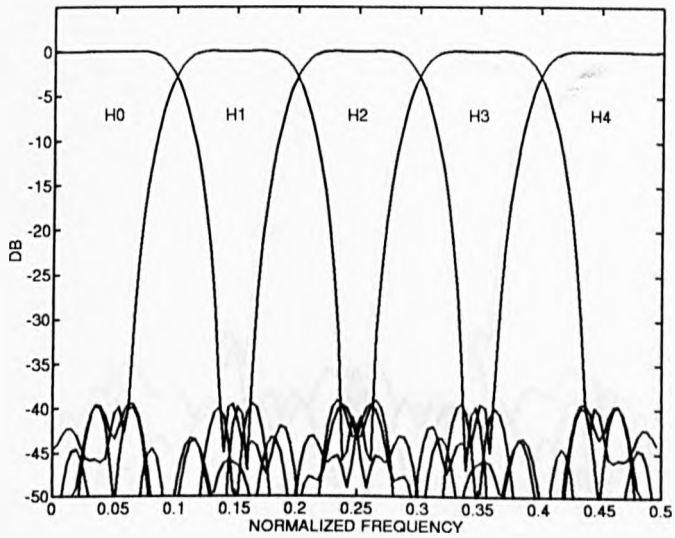

Figure 5.24: Analysis filters for $\Delta = 54$ in Example 5.4.1.3

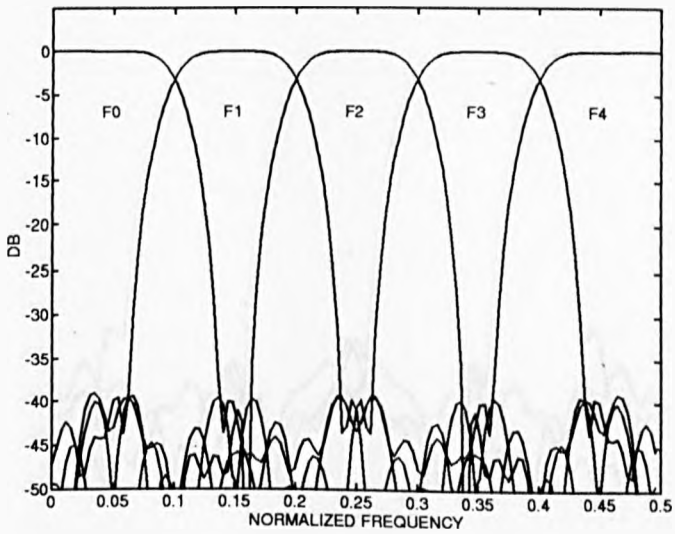

Figure 5.25: Synthesis filters for $\Delta = 54$ in Example 5.4.1.3

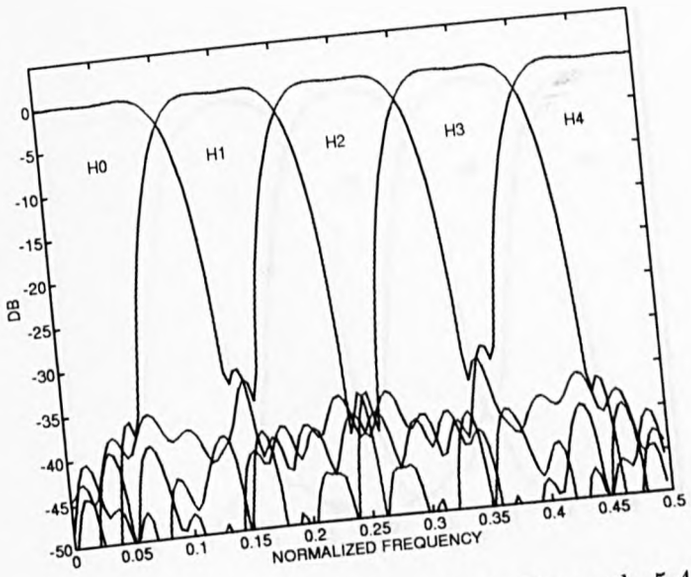

Figure 5.26: Analysis filters for $\Delta = 40$ in Example 5.4.1.3

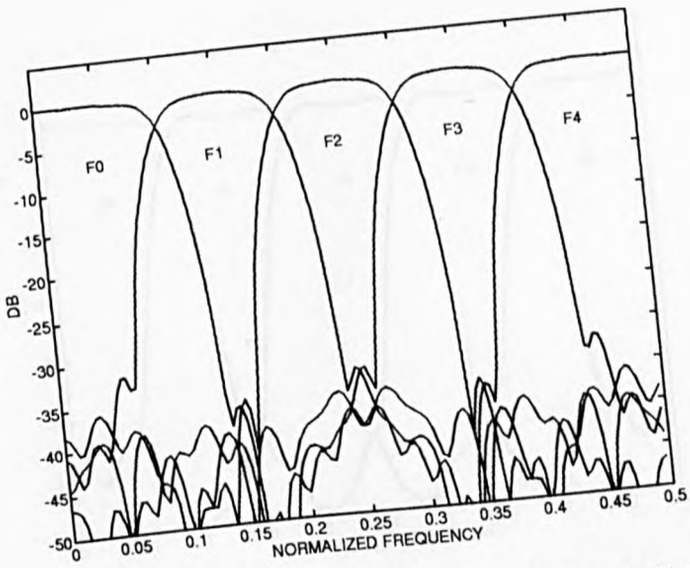

Figure 5.27: Synthesis filters for $\Delta = 40$ in Example 5.4.1.3

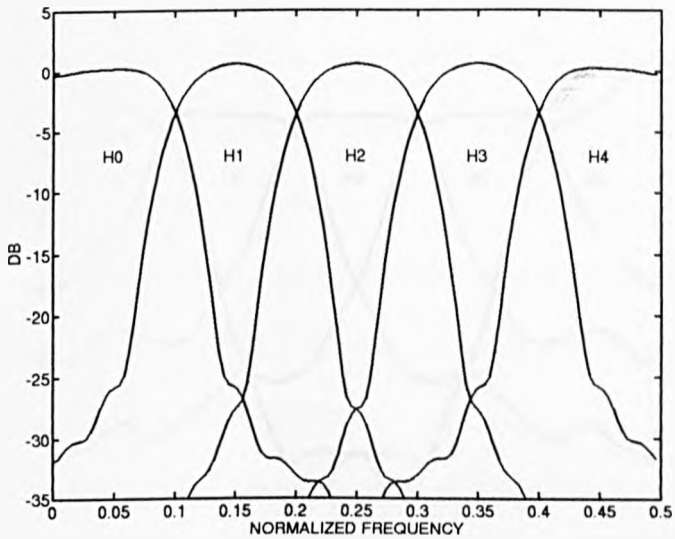

Figure 5.28: Analysis filters for $\Delta = 33$ in Example 5.4.1.3

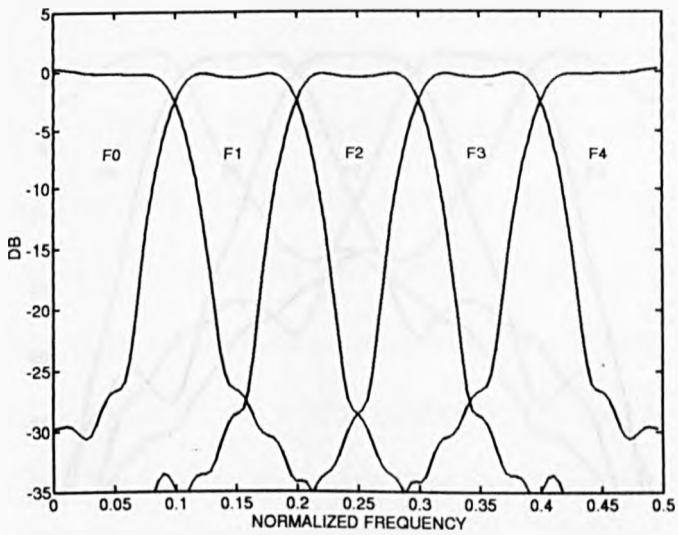

Figure 5.29: Synthesis filters for $\Delta = 33$ in Example 5.4.1.3

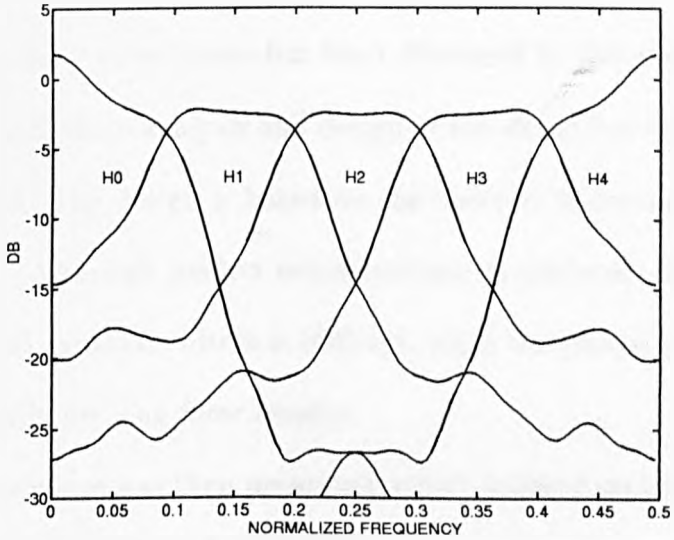

Figure 5.30: Analysis filters for $\Delta = 25$ in Example 5.4.1.3

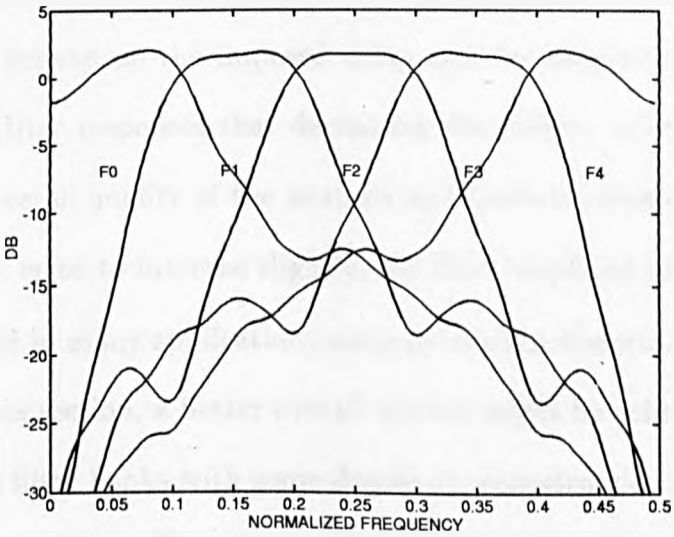

Figure 5.31: Synthesis filters for $\Delta = 25$ in Example 5.4.1.3

5.5 Conclusions

The design of low delay filter banks has been discussed in this chapter. For the first time a direct z-domain analysis and design of low delay two-channel systems has been presented. The design is based on the spectral factorization of a non-linear phase filter. Although perfect reconstruction is achieved, obtaining good quality analysis and synthesis filters is difficult, since the choice of zeros can be very tedious specially for long filter lengths.

A time-domain procedure was then presented, which is based on the time-domain algorithm developed in Chapter 4. The algorithm is modified to utilize low delay designs. This procedure is ideal for designing FIR filter banks with adjustable system delays.

Results indicate that the trade-off between the system filter characteristics and the system delay depend on the imposed delay and the length of the filters. It is clear from the filter responses that decreasing the system delay result in the reduction of the overall quality of the analysis and synthesis filters. By allowing the reconstruction error to increase slightly, the filter stopband attenuation can be improved. Since in many applications some processing distortion is generated before the synthesis section, a better overall system might be achieved, by using analysis/synthesis filter banks with some degree of reconstruction error [74].

It is believed that low delay filter banks should find applications in communication systems, audio, and other time critical applications.

Chapter 6

Wavelets and Filter Banks

6.1 Introduction

Wavelets are families of functions obtained from a single prototype function (mother wavelet) by dilation and translation, and provide expansions of functions belonging to the space of square integrable functions $L^2(R)$.

Wavelets are seen as a better solution to the problem of analysing non-stationary signals. The wavelet functions are used to decompose signals into building blocks, well localized in frequency and time.

One advantage of using wavelets is that it has the ability to "zoom" in on singularities. For example a rough approximation of a signal might look stationary, while at a more detailed level, a different behavior is observed.

This chapter is concerned with the discrete version related to FIR filter banks termed compactly supported wavelets [25]. Orthonormal and bi-orthogonal wavelets are designed using the time domain approach presented in chapter 4.

A new family of wavelets are introduced termed low-delay wavelets which addresses the problem of the growing system delay in the iterated filter banks [7]. The filter bank approach to wavelets is adopted in this chapter, which has been has been presented by Vetterli [120], and by Vaidyanathan [105].

BRITISH LIBRARY

IMAGING SERVICES NORTH
Boston Spa, Wetherby
West Yorkshire, LS23 7BQ
www.bl.uk

PAGE MISSING IN ORIGINAL

regularity (smoothness) in the iterated filters, since nonregular filter could cause discontinuities in the wavelet coefficients that are not due to the signal itself [89]. In [25] Daubechies gives a sufficient condition, which guarantees that the iterated filters converge to a continuous function.

The condition is that the low pass filter h_l should have a sufficient number of zeros at $z = -1$, or half the sampling frequency, so as to attenuate the repeated spectra. If $H_l(z)$ has length N, their can be at most $N/2$ zeros of $H_l(z)$ at $z = -1$, then the filter is known as maximally regular. The above condition can be interpreted as a flatness condition of the spectrum of $H_l(e^{j\omega})$ at half the sampling frequency $\omega = \pi$. It has been shown that the well known Daubechies orthonormal filters are deduced from "maximally flat" low pass filters [40][47]. It has also been shown that the Lagrange half band filters, and the binomial filters [10][4] are special cases of maximally flat filters that have been used to design orthonormal wavelets. It is possible to obtain smooth wavelets if $H(e^{j\omega})$ is sufficiently small at $\omega = \pi$. It has been shown that the two-channel ELT can be used to generate wavelet transforms with a sufficient degree of regularity [61]. In this section the design of orthonormal wavelets is considered using the time-domain algorithm developed in chapter 4.

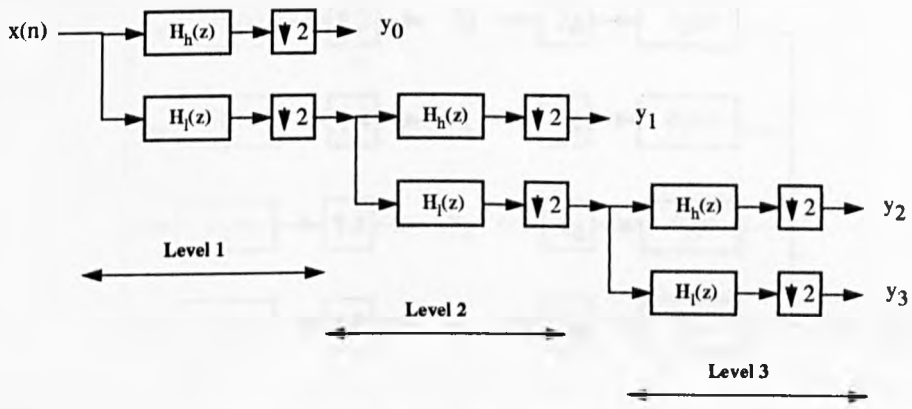

Figure 6.1: Analysis bank implementation of the 3 level DWT

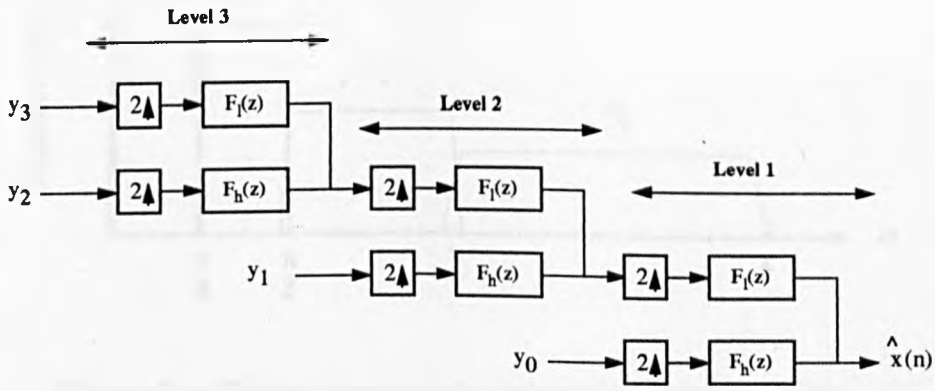

Figure 6.2: Synthesis bank implementation of the 3 level IDWT

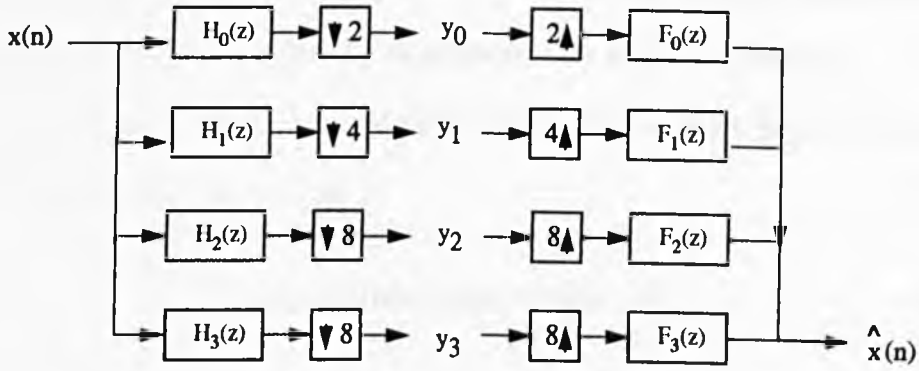

Figure 6.3: Equivalent filter bank implementation of the wavelets

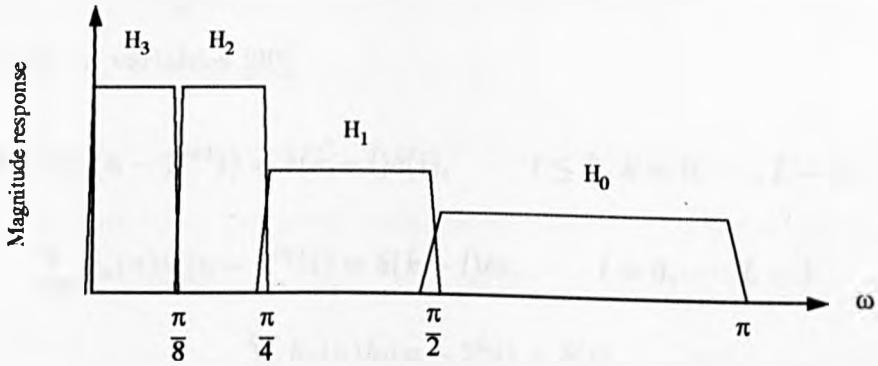

Figure 6.4: Typical magnitude responses of the wavelets

6.3 Orthonormal Wavelets

Orthonormality of the wavelet basis is a desirable property in many applications [25][59][68]. A classical example is the Haar basis [37]. However the Haar function is discontinuous and is not generally appropriate for signal processing.

For an L-level binary tree structured filter bank. The wavelet basis are said to be orthonormal if they satisfy [25]

$$\sum_n \eta_{km}(n)\eta_{li}^*(n) = \delta(k-l)\delta(m-i) \tag{6.4}$$

In terms of the analysis filter coefficients (6.4) can be expressed as (assuming real coefficients)

$$\sum_n h_k(n-2^{k+1}m)h_l(n-2^{l+1}i) = \delta(k-l)\delta(m-i), \qquad k,l = 0,\cdots,L-1 \tag{6.5}$$

$$\sum_n h_L(n-2^L m)h_l(n-2^{l+1}i) = 0, \qquad l = 0,\cdots,L-1 \tag{6.6}$$

$$\sum_n h_L(n-2^L m)h_l(n-2^L i) = \delta(m-i) \tag{6.7}$$

with a change of variables [99]

$$\sum_n h_k(n)h_l(n-2^{l+1}i) = \delta(k-l)\delta(i), \qquad l \le k,\ k = 0,\cdots,L-1 \tag{6.8}$$

$$\sum_n h_k(n)h_l(n-2^{l+1}i) = \delta(k-l)\delta i, \qquad l = 0,\cdots,L-1 \tag{6.9}$$

$$\sum_n h_k(n)h_l(n-2^L i) = \delta(i) \tag{6.10}$$

In other words for a one-level "tree" (L=1) the discrete filter with impulse response $h_l(n)$ is orthogonal to its even translates, and with $h_h(n) = (-1)^n h_l(N-1-n)$, perfect reconstruction FIR filter bank is obtained.

In matrix form the orthonormal conditions can be expressed as [121]

$$\mathbf{A}^{\mathrm{T}}\mathbf{A} = \mathbf{I}$$

where

$$\mathbf{A} = \begin{bmatrix} h_0(0) & h_1(0) & 0 & 0 & \cdots \\ h_0(1) & h_1(1) & 0 & 0 & \ddots \\ \vdots & \vdots & \ddots & \ddots & \ddots \\ h_0(N-1) & h_1(N-1) & \ddots & \ddots & \ddots \\ 0 & 0 & \ddots & \ddots & \ddots \\ \vdots & \ddots & \ddots & \ddots & \ddots \end{bmatrix} \tag{6.11}$$

This condition is equivalent to the time-domain paraunitary conditions obtained in chapter 4.

It has been shown [25][105] that binary tree structured filter banks with the same paraunitary filters on all levels generates an orthonormal basis.

Example 6.2.1 Orthonormal wavelets are generated for $L = 5$ using a two channel paraunitary filter bank with $N = 16$.

The starting filter is designed using the Parks-McClellan algorithm [66]. The pass-band and stop-band frequencies are chosen carefully such that the frequency response is sufficiently smooth with $\omega_p = 0.096\pi$ and $\omega_p = 0.9618\pi$. The minimum phase filter counter part is used as a starting filter in the algorithm. The normalisation requirement is incorporated in the algorithm simply by normalising the starting filter to unit norm (i.e $\| h_0(n) \|^2 = 1$).

The algorithm is stopped at a reconstruction error of 1×10^{-10}, Figure (6.5) shows the magnitude responses of the wavelets, and Figure (6.6) shows the magnitude

response in dB normalized to unity for convenience. Figure (6.7) shows the corresponding impulse responses of the wavelets, clearly they converge to a smooth function. Figure (6.8) shows a comparison between the designed wavelet and the maximally regular Daubechies wavelet of the same size.

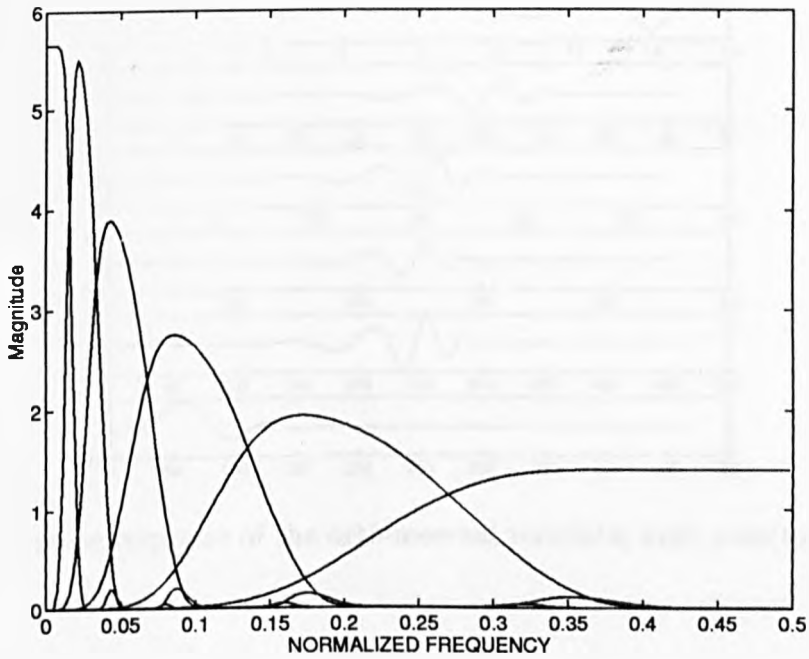

Figure 6.5: Magnitude response of the orthonormal wavelets

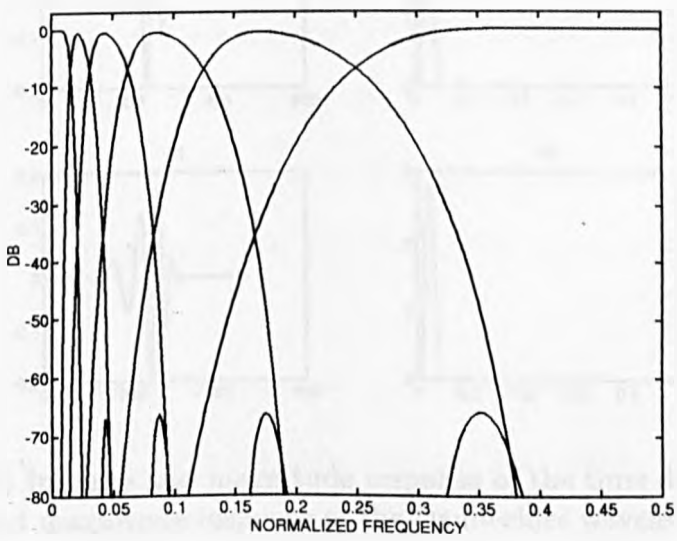

Figure 6.6: Magnitude response in dB of the orthonormal wavelets

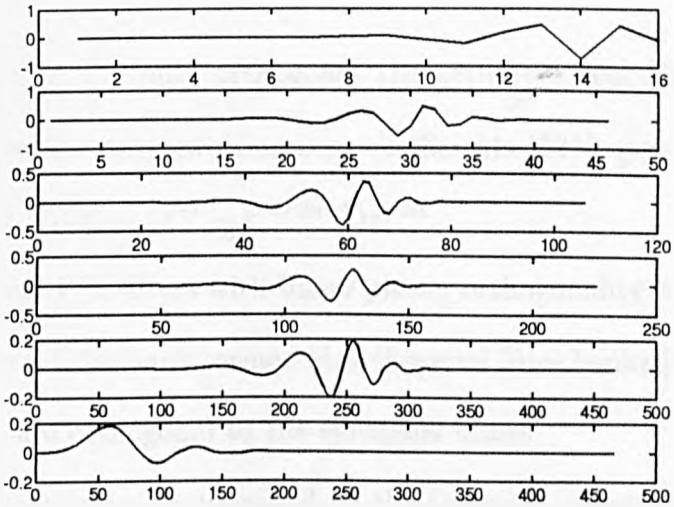

Figure 6.7: Impulse response of the orthonormal wavelets; high-pass(top) to low-pass(bottom)

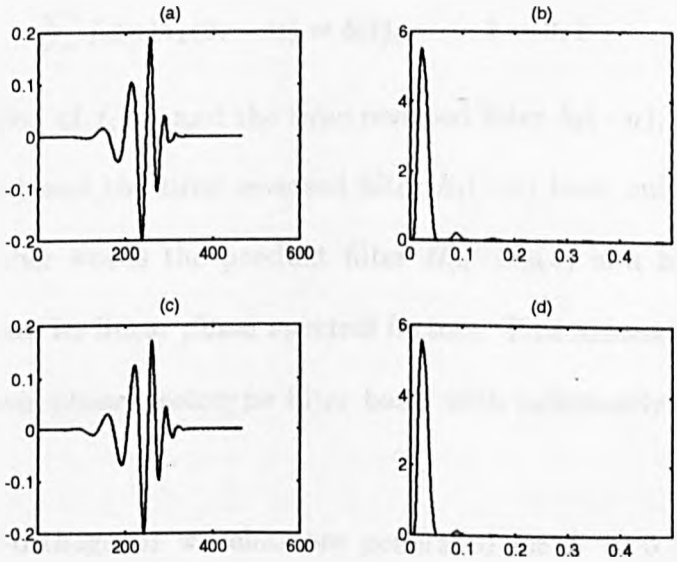

Figure 6.8: (a)(b) Impulse and magnitude response of the time domain wavelet; (c)(d) Impulse and magnitude response of the Daubechies wavelet for N=16 and L=5

6.4 Bi-orthogonal Wavelets

It is well known that the only orthogonal (paraunitary) real FIR filter bank having linear phase has only two non-zero coefficients [121], given by $H_0(z) = z^{-l} + z^{-l-2n-1}$ and $H_1(z) = (z^{-l} - z^{-l-2n-1})z^{-2n}$.

To obtain longer real FIR filters with linear phase, orthogonality has to be given up for a more general filter bank termed bi-orthogonal filter banks [121][90] where the analysis filters are orthogonal to the synthesis filters.

A bi-orthogonal system can be described by the following equations

$$\sum_n f_0(n)h_1(2i-n) = 0 \tag{6.12}$$

$$\sum_n f_1(n)h_0(2i-n) = 0 \tag{6.13}$$

$$\sum_n f_k(n)h_k(2i-n) = \delta(i), \qquad k = 0,1 \tag{6.14}$$

The cross-correlation of $f_1(n)$ and the time reversed filter $h_0(-n)$, and the cross-correlation of $f_0(n)$ and the time reversed filter $h_1(-n)$ have only odd indexed coefficients. In other words the product filter $H_0(z)F_0(z)$ is a half-band filter and $H_0(z)$, $F_0(z)$ are its linear phase spectral factors. This amounts to designing a two-channel linear phase prototype filter bank with sufficiently smooth filters [121].

Example 6.4.1 Bi-orthogonal wavelets are generated for $L = 5$ and $N = 16$, the low-pass and high-pass filters are symmetric and anti-symmetric respectively. Figure (6.9) shows the magnitude response of the bi-orthogonal wavelets, and Figure (6.10) shows the impulse response of the wavelets.

Clearly the wavelets are anti-symmetric with linear phase and sufficiently smooth.

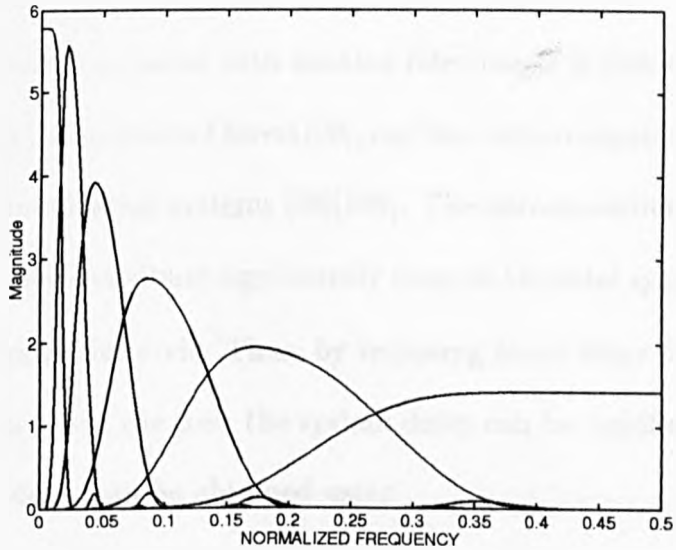

Figure 6.9: Magnitude response of the bi-orthogonal wavelets

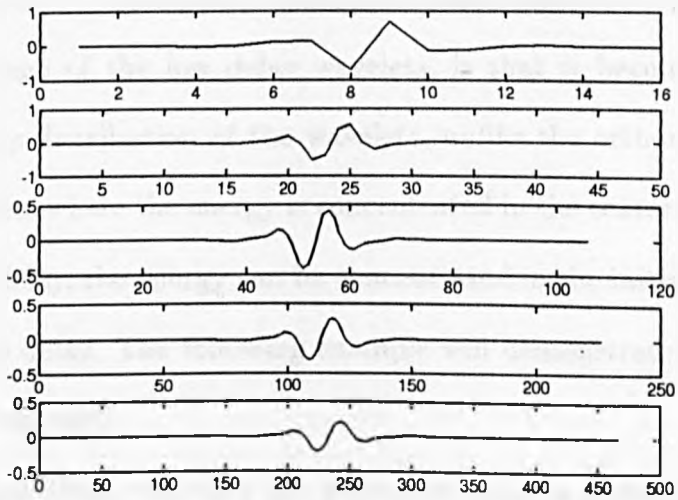

Figure 6.10: Impulse response of the bi-orthogonal wavelets; high-pass(top) to low-pass(bottom)

6.5 Low Delay Wavelets

One of the drawbacks associated with iterated filter banks is that the delay grows exponentially with the number of levels [90], and has been recognized as a problem in audio and communication systems [28][108]. The decomposition levels located further inside the tree contribute significantly more to the total system delay than the earlier decomposition levels. Thus, by imposing lower delay on the splitting levels located deep inside the tree, the system delay can be significantly reduced. The total system delay can be obtained using

$$\Delta^{(L)} = (2^L - 1)\Delta \tag{6.15}$$

where Δ is the delay for $L = 1$. It is clear that the slight reduction of the delay at the fist level, will be significant in the total system delay as L grows larger.

A unique advantage of the low delay wavelets, is that it becomes possible to control the energy distribution of the wavelets, unlike the orthonormal and bi-orthogonal wavelets where the energy is concentrated in the center of the wavelet. By reducing the delay, the energy can be concentrated in the initial samples, and thus reducing the delay. The following example will demonstrate the properties of the low delay wavelets.

Example 6.5.1 Low delay wavelets are generated using a prototype filter bank with $N = 32$ and a prototype delay of $\Delta = 15$ is imposed. Figure (6.11) shows the magnitude response of the low delay wavelets, and Figure (6.12) shows the impulse response of the wavelets. The total delay is 456 samples. Compared with 961 samples of delay for the normal systems this is a significant reduction.

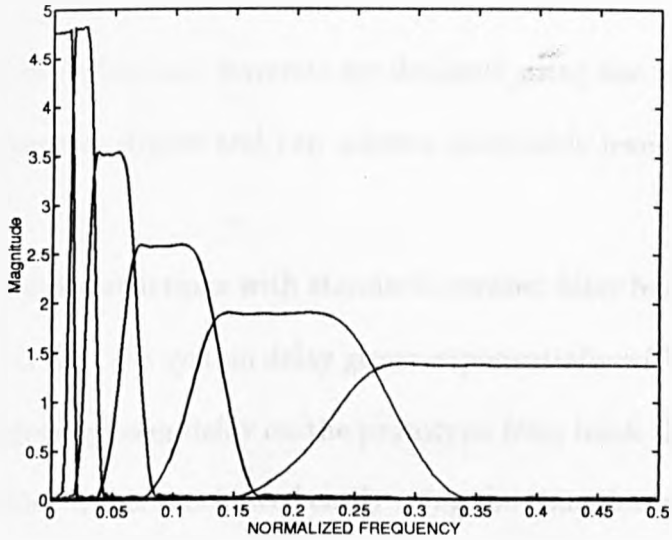

Figure 6.11: Magnitude response of the low delay wavelets

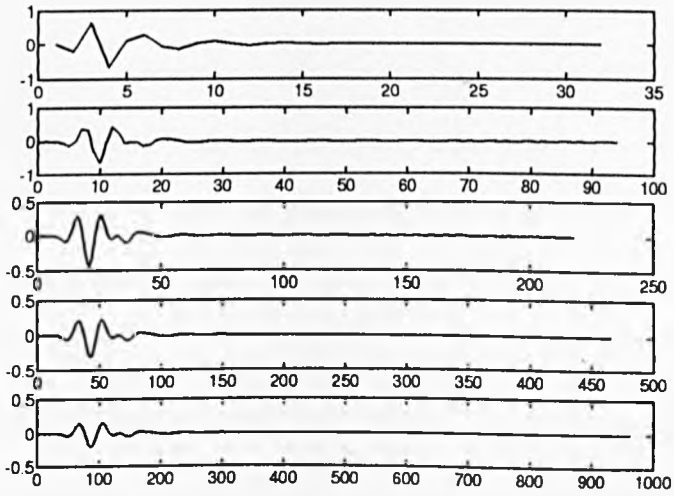

Figure 6.12: Impulse response of the low delay wavelets; high-pass(top) to low-pass(bottom)

6.6 Conclusions

Orthonormal and bi-orthogonal wavelets are designed using the time-domain approach, this approach is simple and can achieve acceptable levels of smoothness in the wavelets.

One of the recognised restrictions with standard iterated filter bank implementations of the DWT is that the system delay grows exponentially with the number of levels [90]. By imposing lower delay on the prototype filter bank the system delay is significantly reduced, this is achieved easily using the time-domain formulation.

Chapter 7

Conclusions and Future Work

7.1 Conclusions

The Analysis and design of FIR multirate filter banks have been explored in this thesis. A spectral factorization method has been used to design three channel based systems, which is simple and only requires the design of one prototype third-band filter. Magnitude and phase errors are eliminated. However this method is not very robust to the aliasing errors.

A time-domain transformation of the z-domain perfect reconstruction conditions has been demonstrated, and its relation to the polyphase and paraunitary structures has been established. The time-domain formulation has a rich algebraic structure that allows the design of various classes of filter banks with desired properties such as, arbitrary phase, filter lengths, system delay, and perfect reconstruction. An efficient design algorithm is presented which allows great flexibility

in the frequency domain.

Low delay filter banks are also considered both in the z-domain and the time-domain. Two-channel low delay systems can be designed in the z-domain which requires spectral factorization of non-linear phase filters. A general design method based on the time domain formulation is introduced to design low delay filter banks with arbitrary number of channels.

Wavelets give rise to an inherently logarithmic decomposition of the frequency domain, which can be achieved using an octave band filter bank tree structure. Because of the relationship between filter banks and wavelets, the time-domain formulation of the filter bank can be used to construct corresponding classes of wavelet bases like orthonormal, bi-orthogonal, and low delay wavelets.

7.2 Future Work

The research on multirate systems has reached a mature stage, however there remains a number of interesting problems. Most of the filter banks considered in the research are stationary that is the filters are stationary for all time. A number of researchers have proposed time varying filter banks[76][98], these filter banks have the property of switching to other filter banks with differing number of channels, or filters.

The design of filter banks based on the statistical properties of signals has gained

a lot of attention recently [91][114][102], where the filters are optimized to maximize certain statistical properties of signals in a finite number of channels.

Most of the applications of multirate filter banks have focused on deterministic signals, a few applications considered the second order statistics of random signals. An interesting problem that is still open is the effect of multirate systems on the higher-order statistics of signals [80][79]. Existing methods only consider second order statistics in the analysis and design of filter banks [18][67][85]. Also in the areas where higher order statistics are established it is interesting to consider the higher order statistics of subband signals, this can be useful in applications such as estimation, noise reduction, etc.

Also filter banks and wavelets have proved to be ideal for analysing fractal signals [29][16][48][125][126], due to their nonstationary nature, using higher-order statistics remains an open problem. Most of these problems are still open in multidimensions where it is computationally expensive [30][62][123].

Appendix A

Eigenfilters

Eigenfilters are linear phase FIR filters that are optimal in the least square sense [113]. The lowpass filter $H(z)$ is obtained by minimizing an error measure of the form

$$E = v^T \mathbf{R} v \tag{A.1}$$

where $\mathbf{R}$ is a real, symmetric, positive definite matrix, and v is a real vector related to the impulse response of the symmetric filter

$$h(n) = h(N-1-n) \tag{A.2}$$

under the constraint $v^T v = 1$.

The solution for the filter length N odd is presented here. The frequency response of the filter has the form

$$H(e^{j\omega}) = e^{-j(N-1)\omega/2} H_0(e^{j\omega}) \tag{A.3}$$

$$H(e^{j\omega}) = \sum_{n=0}^{M} b(n) cos(n\omega) \tag{A.4}$$

where N is odd, and $M = N - 1/2$. Define

$$b = [b(0), b(1), \cdots, b(M)]^T \tag{A.5}$$

and

$$c(\omega) = [1, cos(\omega), cos(2\omega), \cdots, cos(M\omega)]^T \tag{A.6}$$

$$H_0(e^{j\omega}) = b^T c(\omega) \tag{A.7}$$

The stopband error can be defined as

$$E_s = \frac{1}{\pi}\int_{\omega_s}^{\pi}[D(\omega) - H_0(e^{j\omega})]^2 d\omega \tag{A.8}$$

$$= \frac{1}{\pi}\int_{\omega_s}^{\pi} b^T c c^T b d\omega \tag{A.9}$$

$$= b^T \mathbf{R}_s b \tag{A.10}$$

where $D(\omega)$ is the desired response, and $\mathbf{R}_s$ is given by

$$\mathbf{R}_s = \frac{1}{\pi}\int_{\omega_s}^{\pi} c c^T d\omega \tag{A.11}$$

$\mathbf{R}_s$ is a real, symmetric, positive definite matrix.

The stopband error is defined as

$$E_p = \frac{1}{\pi}\int_0^{\omega_p} e_p^2(\omega) d\omega = \frac{1}{\pi}\int_0^{\omega_p} b^T(1-c)(1-c)^T b d\omega = b^T \mathbf{R}_p b \tag{A.12}$$

where $\mathbf{R}_p$ is given by

$$\mathbf{R}_p = \frac{1}{\pi}\int_0^{\omega_p}(1-c)(1-c)^T d\omega \tag{A.13}$$

The total error to be minimized is

$$E = b^T \mathbf{R} b \tag{A.14}$$

where

$$\mathbf{R} = (1 - \alpha)\mathbf{R}_p + \alpha\mathbf{R}_s \tag{A.15}$$

where $0 \leq \alpha \leq 1$ controls the passband and stopband errors.

The solution vector v is simply the eigenvector of $\mathbf{R}$ corresponding to its minimum eigenvalue according to Rayleigh's principle [81]. For $alpha = 1$ the solution reduces to the prolate spheroidal sequences [92].

Appendix B

Publications

[1] A. AL-Adnani, R. Chapman, and T.S. Durrani,"Time-domain design of FIR multirate filter banks", Elec. Lett., vol.29, No.9,pp. 752-753, April 1993.

[2] A. AL-Adnani, R. Chapman and T.S. Durrani, "Time-domain design of low delay wavelet transforms", Elec. Lett., vol.20, No.25, pp.2177-2178, Dec. 1993.

[3] A. Al-adnani,and R. Chapman, "A spectral factorization approach to 3-channel analysis/synthesis systems", vol.2, EUSIPCO-94, pp.1034-1037, Sep.1994.

[4] A. Al-Adnani, R. Chapman, and T.S.Durrani, "Time domain design of multirate filter banks and wavelets", vol.2, EUSIPCO-94, pp.1026-1027, Sep. 1994.

Bibliography

[1] A.N. Akansu. Multiplierless suboptimal PR-QMF design. pages 723–726. Proc. SPIE Vis. Comm. Image Proc., 1992.

[2] A.N. Akansu and R.A. Haddad. *Multiresolution Signal Decomposition.* academic Press, 1992.

[3] A.N. Akansu, R.A. Haddad, and H. Calgar. Perfect reconstruction QMF-wavelet transform. pages 609–612. Proc. SPIE Vis. Comm. Image Proc., 1990.

[4] A.N. Akansu, R.A. Haddad, and H. Calgar. The binomial QMF-wavelet transform for multiresolution signal decomposition. *IEEE Trans. Signal Processing*, 41(1):13–19, Jan. 1993.

[5] A. Al-adnani and R. Chapman. A spectral factorization approach to 3-channel analysis/synthesis systems. pages 1034–1037. EUSIPCO '94, Vol.2, Sep. 1994.

[6] A. AL-Adnani, R. Chapman, and T.S. Durrani. Time-domain design of FIR multirate filter banks. *Elec. Lett.*, 29(9):752–753, April 1993.

[7] A. AL-Adnani, R. Chapman, and T.S. Durrani. Time-domain design of low delay wavelet transforms. *Elec. Lett.*, 29(25):2177–2178, Dec. 1993.

[8] A. Al-Adnani, R. Chapman, and T.S.Durrani. Time domain design of multirate filter banks and wavelets. pages 1026–1027. EUSIPCO '94, Vol.2, Sep. 1994.

[9] J.B. Allen and L.R. Rabiner. A unified approach to short-time Fourier analysis and synthesis. *Proc. IEEE*, 65(11):1558–1564, Nov. 1977.

[10] R. Ansari, C. Guillemot, and J.F. Kaiser. Wavelet construction using Lagrange halfband filters. *IEEE Trans. Circuits and Systems*, 38(9):1116–1118, Sep. 1991.

[11] M. Antonini, M. Barlaud, P. Mathieu, and I. Daubechies. Image coding using wavelet transform. *IEEE Trans. Image Processing*, 1(2):205–223, April 1992.

[12] F. Argenti, G. Benelli, and A. Sciorpes. IIR implementation of wavelet decomposition for digital signal analysis. *Elec. Lett.*, 28(5):513–514, Feb. 1992.

[13] M.G. Bellanger, G. Bonnerot, and M. Coudreuse. Digital filtering by polyphase network: application to sample-rate alteration and filter banks. *IEEE Trans. Acoust. Speech, and Signal Processing*, 24:109–114, April 1976.

[14] H. Calgar and A.N. Akansu. PR-QMF design with Bernstein polynomials. page 999. Proc. IEEE Symp. Circuits Sys., 1992.

[15] P. Cassereau. *A new class of orthogonal transforms for image processing.* S.M thesis, Dept. EECS, Mass. Inst. Technol., Cambridge., May 1985.

[16] B. Chen and C. Lin. Multiscale Wiener filter for the restoration of fractal signals: Wavelet filter bank approach. *IEEE Trans. Signal Processing*, 42(11):2972–2982, Nov. 1994.

[17] C.K. Chen and J.H. Lee. Design of quadrature mirror filters with linear phase in the frequency domain. *IEEE Trans. Circuits and Systems II - Analogue and Digital Signal Processing*, 39(9):593–611, Sep. 1992.

[18] L. Cheng-Youn. Second-order statistics of the wavelet transform of multiplicative white stochastic process. pages 21–23. Int. Conf. Acoust., Speech, Signal Processing, Adelaide, 1994.

[19] Ed. C.K. Chui. *An introduction to wavelets.* Academic Press, 1992.

[20] Ed. C.K. Chui. *Wavelets: a tutorial in theory and applications.* Academic Press, 1992.

[21] R. Coifman, Y. Meyer, S. Quake, and V. Wickerhauser. Signal processing with wavelet packets. *Numerical Algorithms Research Group, Yale University*, 1990.

[22] R.V. Cox, D.E. Bock, K.B. BauerJ.D., Johnston, and J.H. Snyder. The analog voice privacy system. pages 341–344. IEEE Inter. Conf. Acoust., Speech, and Signal Processing, Paris, April 1986.

[23] R. Crochiere and L. Rabiner. *Multirate Digital Signal Processing.* Englewood Cliffs, NJ: Prentice-Hall, 1983.

[24] A. Croisier, D. Esteban, and C. Galand. Perfect channel splitting by use of interpolation/decimation/tree decomposition techniques. International Conf. on Information Science and Systems, Patras, Greece, 1976.

[25] I. Daubechies. Orthonormal basis of compactly supported wavelets. *Communications on Pure and Applied Mathematics*, XLI:909–996, 1988.

[26] Z. Doganata, P.P. Vaiyanathan, and T.Q. Nguyen. General synthesis procedure for FIR lossless transfer matrices, for perfect-reconstruction multirate filter bank applications. *IEEE Trans. Acoust., Speech, Signal Processing*, 36:1561–1574, Oct. 1988.

[27] D. Esteban and C. Galand. Application of quadrature mirror filters to split-band voice coding schemes. pages 191–195. Proc. IEEE Int. Conf. Acoust, Speech, Signal Processing, Hartford Conecticut, May 1977.

[28] G. Evangelista. Pitch-synchronous wavelet representation of speech and music signals. *IEEE Trans. Signal Processing*, 41(12):3313–3330, Dec. 1993.

[29] P. Flandrin. Wavelet analysis and synthesis of fractional brownian motion. *IEEE Trans. Inft. Theory*, 38:910–917, Mar. 1992.

[30] N.J. Fliege. *Multirate Digital Signal Processing.* John Wiley and Sons.

[31] S.W. Foo and L.F. Turner. Design of nonrecursive quadrature mirror filters. *Proc. IEE, Pt. G*, 129:61–68, June 1982.

[32] D. Gabor. Theory of communications. *J. of the IEE*, 93:429–457, 1946.

[33] C.R. Galand and H. Nussbaumer. New quadrature mirror filter structures. *IEEE Trans. Signal Processing*, 32(3):522–528, June 1984.

[34] A. Gilloire and M. Vitterli. Adaptive filtering in subbands. pages 1572–1575. Proc. Int. Conf. Acoust., Speech, Signal Processing, New York, 1988.

[35] G.H. Golub and C.F.V. Loan. *Matrix computations.* John Hopkins, Baltimore, MD, 1989.

[36] F. Grenez. Chebychev design of filters for subband coders. *IEEE Trans. Acoust. Speech Signal Processing*, 36(2):182–185, Feb. 1988.

[37] A. Grossmann and J. Morlet. Decomposition of Hardy functions into square integrable wavelets of constant shape. *SIAM, J.Math.Anal.*, 15(4):723–736, 1984.

[38] C. Herley and M. Vetterli. Linear phase wavelets: Theory and design. pages 2017–2021. Proc. IEEE Int. Conf., Acoust., Speech, Signal Processing, 1991.

[39] C. Herley and M. Vetterli. Wavelets generated by IIR filter banks. pages 601–604. Proc. Int. Conf., Acoust, Speech, Signal Processing, 1992.

[40] O. Herrman. On the approximation problem in nonrecursive digital filter design. *IEEE Trans. Circuit Theory*, 18:411–413, May 1971.

[41] B.R. Horng and A.N. Willson. The design of multiplierless two-channel linear phase FIR filter banks with applications to image subband coding. pages 650–654. Proc. IEEE Symp. Circuits Sys., 1990.

[42] B.R. Horng and A.N. Willson. Lagrange multiplier approaches to the design of two-channel perfect reconstruction linear phase filter banks. pages 1731–1734. Proc. IEEE Int. Conf. Acoust, Speech, Signal Processing, 1990.

[43] A.K. Jain. *Fundamentals of Digital Image Processing.* Prentice Hall, 1989.

[44] V.K. Jain and R.E. Crochiere. Quadrature mirror filter design in the time domain. *IEEE Trans. Acoust., Speech, Signal Processing*, 32(2):353–361, April 1984.

[45] J.H. Jeon and J.K. Kim. New linear phase QMF filter design for subband coding. *Elec. Lett.*, 27(4):319–320, Feb. 91.

[46] J.D. Johnston. A filter family designed for use in quadrature mirror filter banks. pages 291–294. IEEE Int. Conf. Acoust, Speech, Signal Processing, 1980.

[47] J.F. Kaiser. *Design subroutine(MXFLAT) for symmetric FIR low pass digital filters with maximally-flat pass and stop bands*, pages 5.3–1–5.3–6. Section 5.3, Programs for Digital Signal Processing. New York: IEEE Press, 1979.

[48] L.M. Kaplan and C.C. Kuo. Fractal estimation from noisy data via discrete fractional Gaussian noise(dfgn) and the Haar basis. *IEEE Trans. Signal Processing*, 41(12):3554–3562, Dec. 1993.

[49] G. Karlsson and M. Vetterli. Three-dimensional subband coding of video. pages 1100–1103. Proc. Int. Conf. Acoust., Speech, and Signal Processing, New York, NY, April 1988.

[50] W. Kellerman. Analysis and design of multirate systems for cancellation of acoustic echoes. pages 2570–2573. Proc. Int. Conf. Acoust., Speech, Signal Processing, New York, 1988.

[51] R. Koilpillai and P.P. Vaidyanathan. Cosine-modulated FIR filter banks satisfying perfect reconstruction. *IEEE Trans. Signal Processing*, 40(4):770–788, April 1992.

[52] R. Koilpillai and P.P. Vaidyanathan. A spectral factorization approach to Pseudo-QMF design. *IEEE Trans. Signal Processing*, 41(1):82–92, Jan 1993.

[53] J. Kovacevic and M. Vetterli. Nonseparable multidimensional perfect reconstruction filter banks and wavelet bases for r^n. *IEEE Trans. on Info. Theory*, 38(2):533–555, March 1992.

[54] T. Kronander. A new approach to recursive mirror filters with special application in subband coding of images. *IEEE. Trans. Acoust. Speech Signal Processing*, 36(9):1496–1509, Sep. 1988.

[55] R. Kronland-Martinet. The wavelet transform for analysis, synthesis, and processing of speech and music sounds. *Comput. Music J.*, 12(4):11–20, 1988.

[56] W. Li, A. Basso, A. Popat, A. Nicoulin, and M. Kunt. Design of parallel multiresolution filter banks by simulated annealing. pages 124–135. Proc. SPIE Vis. Comm. Image Processing, 1991.

[57] Y.C. Lim, R.H. Yang, and S.N. Koh. The design of weighted minimax quadrature mirror filters. *IEEE Trans. Signal Processing*, 41(5):1780–1792, May 1993.

[58] T.D. Lookabough, M.G. Perkins, and C.L. Cadwell. Analysis/synthesis systems in the presence of quantization. Proc. Int. Conf. Acoust. Speech Signal Processing, Glasgow, Scotland, May 1989.

[59] S. Mallat. A theory for multiresolution signal decomposition: the wavelet representation. *IEEE Trans. on PAMI*, 11(7):674–693, 1989.

[60] S. Mallat. Multifrequency channel decomposition of images and wavelet models. *IEEE Trans. Acoust, Speech, Signal Processing*, 37(12):2091–2110, Dec. 1989.

[61] H.S. Malvar. Fast wavelet transforms based on the extended lapped transform. *Elec. Lett.*, 28(15):1393–1395, 1992.

[62] H.S. Malvar. *Signal Processing with Lapped Transforms.* Boston: Artech House, 1992.

[63] H.S. Malvar. Lapped transforms for efficient transform/subband coding. *IEEE Trans. Acoust., Speech, Signal Processing*, 38(6):969–976, June 1990.

[64] H.S. Malvar. Extended lapped transforms: properties, applications and fast algorithms. *IEEE Trans. Signal Processing*, 40(11):2703–2714, Nov. 1992.

[65] H.S. Malvar and D.H. Staelin. The Lot : Transform coding without blocking effects. *IEEE Trans. Acoust., Speech, Signal Processing*, 37(4):552–561, April 1989.

[66] J.H. McClellan, T.W. Parks, and L.R. Rabiner. A computer program for designing optimum linear phase digital filters. *IEEE Trans. Audio Electroacoust*, 21(12):506–510, Dec. 1973.

[67] A. Mertins. Statistical optimization of PR-QMF banks and wavelets. pages 113–116. Int. Conf. Acoust., Speech, Signal Processing, Adelaide, 1994.

[68] Y. Meyer. *Ondelettes.* Vol.1, Hermann, 1990.

[69] P.C. Millar. Mirror filters with minimum delay responses for use in subband coders. Proc. Int. Conf. Acoust. Speech, Signal, Processing", PAGES =, 1984.

[70] P.C. Millar. The delay paradox when combining the outputs of the non-quadrature filter networks and its importance to subband coding systems. 1989.

[71] P.C. Millar. Recursive quadrature mirror filters - criteria specification and design method. *IEEE Trans. ,Acoust. Speech, Signal Processing*, 33(2):413–418, April 1985.

[72] F. Mintzer. On half-band, third-band, and N-th band FIR filters and their design. *IEEE Trans. Acoust, Speech, Signal Processing*, 30:734–738, Oct 1982.

[73] M. Mintzer. Filters for distortion-free two-band multirate filter banks. *IEEE Trans. Acoust., Speech, Signal Processing*, 33(6):626–630, June 1985.

[74] K. Nayebi, T.P. Barnwell, and M.J.T. Smith. Low delay FIR filter banks: Design and evaluation. *IEEE Trans. Signal Processing*, 42(1):24–31, Jan. 1994.

[75] K. Nayebi, T.P. Barnwell, and M.J.T. Smith. Time domain filter bank analysis: A new design theory. *IEEE Trans. on Signal Processing*, 4(6):1414–1429, June 1992.

[76] K. Nayebi, I. Sodagar, and T.P. Barnwell. The wavelet transform and time-varying tiling of the time-frequency plane. IEEE-SP Int. Symp. on Time-Frequency and Time-Scale Analysis, 1992.

[77] T.Q. Nguyen and P.P. Vaidyanathan. Maximally decimated perfect-reconstruction FIR filter banks with pairwise mirror-image analysis (and synthesis) frequency responses. *IEEE trans. Acoust., Speech, Signal Processing*, 36(5):693–706, May 1988.

[78] T.Q. Nguyen and P.P. Vaidyanathan. Two-channel perfect reconstruction FIR QMF structures which yield linear phase fir analysis and synthesis filters. *IEEE Trans. Acoust., Speech, Signal Processing*, 37(5):676–690, May 1989.

[79] C.L. Nikias and J.M. Mendel. Signal processing with higher-order spectra. *Signal Processing Magazine*, 10(3):10–37, July 1993.

[80] C.L. Nikias and M.R. Raghuveer. Bispectrum estimation: A digital signal processing framework. *Proceedings IEEE*, 75(7):869–891, July 1987.

[81] B. Nobel and J.W. Daniel. *Applied Linear Algebra.* Englwood Cliffs, NJ: Prentice Hall, 1977.

[82] H.J. Nussbaumer. Pseudo QMF filter bank. *IBM Tech. disclosure Bulletin*, 24:3081–3087, Nov. 1981.

[83] S.C. Pei and S.B. Jaw. A class of efficient recursive quadrature mirror filter for subband coding. *IEEE Trans. Signal Processing*, 39(12):2721, Dec. 1991.

[84] U. Pestel and K. Gruger. Design of HDTV subband filterbanks considering VLSI implementation constraints. *IEEE Trans. Circuits and Systems for Video Tech.*, 1(1):14, Mar. 1991.

[85] U. Petersohn, N.J. Fliege, and H. Unger. Exact analysis of aliasing effects and non-stationary quantization noise in multirate systems. pages 173–176. Int. Conf. Acoust., Speech, Signal Processing, 1994.

[86] J.P. Princen and A.P. Bradley. Analysis/synthesis filter bank design based on time domain aliasing cancellation. *IEEE Trans. Acoust., Speech, Signal Processing*, 34:1153–1161, Oct. 1986.

[87] T.A. Ramstad. Cosine modulated analysis-synthesis filter bank with critical sampling and perfect reconstruction. pages 1789–1792. Proc. IEEE Int. Conf. Acoust. Speech and Signal Processing, May 1991.

[88] T.A. Ramstad. Analysis/synthesis filter banks with critical sampling. Int. Conf. on Digital Signal Processing, Florence, Sept. 1984.

[89] O. Riol. Regular wavelets: A discrete-time approach. *IEEE Trans. Signal Processing*, 41(12):3572–3579, Dec. 1993.

[90] O. Riol and M. Vetterli. Wavelets and signal processing. *IEEE Signal Processing Mag.*, 8(4):14–38, Oct. 1991.

[91] V.P. Sathe and P.P. Vaidyanathan. Effects of multirate systems on the statistical properties of random signals. *IEEE Trans. Signal Processing*, 41(1):131–146, Jan. 1992.

[92] D. Slepian. Prolate spheroidal wave functions, Fourier analysis, and uncertainty -V: the discrete case. *Bell Sys. Tech. J.*, 57:1371–1430, May-June 1978.

[93] M.J.T. Smith and T.P. Barnwell. Exact reconstruction for tree-structured subband coders. *IEEE Trans. Acoust., Speech, Signal Processing*, 34(6):434–441, June 1986.

[94] M.J.T. Smith and T.P. Barnwell. A unifying framework for analysis/synthesis systems based on maximally decimated filter banks. pages

521–524. Proc. IEEE Int. Conf. Acoust., Speech, Signal Processing, Tampa, Florida, Mar. 1985.

[95] M.J.T. Smith and T.P. Barnwell. A new filter bank theory for time-frequency representation. *IEEE Trans. Acoust. Speech Signal Processing*, 35(3):314–327, Mar. 1987.

[96] M.J.T. Smith and T.P. Barnwell. A unifying framework for analysis/synthesis systems based on maximally decimated filter banks. pages 521–524. Proc. IEEE Int. Conf. Acoust, Speech, Signal Processing, Tampa, Florida, March 1985.

[97] M.J.T. Smith and S.L. Eddins. Analysis/synthesis techniques for subband coding. *IEEE Trans Acoust. Speech Signal Proc*, 38(8):1446–1456, Aug. 1990.

[98] I. Sodagar, K. Nayebi, T.P. Barnwell, and M.J.T. Smith. A novel structure for time-varying FIR filter banks. pages 157–160. Int. Conf. Acoust., Speech, Signal Processing, Adelaide, 1994.

[99] A.K. Soman and P.P. Vaidyanathan. On orthonormal wavelets and paraunitary filter banks. *IEEE Trans. Signal Processing*, 41(3):1170–1183, Mar. 1993.

[100] A.K. Soman, P.P. Vaidyanathan, and T.Q. Nguyen. Linear phase paraunitary filter banks: Theory factorizations and designs. *IEEE Trans. Signal Processing*, 41(12):3480–3496, Dec. 1993.

[101] D.B.H Tay and N.G. Kingsbury. Flexible design of multidimensional perfect reconstruction FIR 2-band filters using transformation of variables. *IEEE Trans. on Image Processing*, 2(4):466–480, Oct. 1993.

[102] A.H. Tewfik, D. Sinha, and P. Jorgensen. On the optimization choice of a wavelet for signal processing. *IEEE Trans. Acoust., Speech, Signal Processing*, 38(2):747–765, Feb. 1992.

[103] A.H. Tewfik and H. Zou. Discrete orthogonal m-band wavelet decompositions. pages 373–376. Proc. Int. Conf. Acoust., Speech, Signal Processing, San Francisco, CA, Mar. 1992.

[104] F. Tuteur. Wavelet transformations in signal detection. Proc. Int. Conf. Acoust. Speech Signal Processing, New York, Apr. 1988.

[105] P.P. Vaidyanathan. Lossless systems in wavelet transforms. Proc. IEEE Int. Symp. Circuits Syst., Singapore, 1991.

[106] P.P Vaidyanathan. Theory and design of M-channel maximally decimated filters with arbitrary M, having perfect reconstruction property. *IEEE Trans. Acoust., Speech, Signal Processing*, 35(4):476–492, April 1987.

[107] P.P. Vaidyanathan. On power-complementary FIR filters. *IEEE Trans. on Circuits and Systems*, 32(12):1308–1310, Dec. 1985.

[108] P.P Vaidyanathan. Multirate digital filters, filter banks, polyphase networks, and applications: A tutorial. *Proc. IEEE*, 78(1):56–93, Jan 1990.

[109] P.P. Vaidyanathan. Quadrature mirror filter banks, M-band extensions and perfect-reconstruction techniques. *IEEE ASSP Mag.*, 4:4–20, July 1987.

[110] P.P. Vaidyanathan and P.Q. Hoang. Lattice structures for optimal design and robust implementation of two-band perfect reconstruction QMF banks. *IEEE Trans. Acoust.,Speech, Signal Proc.*, 36(1):81–94, Jan. 1988.

[111] P.P. Vaidyanathan and S.K. Mitra. Polyphase networks, block digital filtering, lptv systems, and alias-free QMF banks:a unified approach based on pseudocirculants. *IEEE Trans. Acoust., Speech, Signal Processing*, 36:381–391, Mar. 1988.

[112] P.P. Vaidyanathan and T.Q. Nguyen. A trick for the design of FIR half-band filters. *IEEE Trans. Circuits syst.*, 34(3):297–300, Mar. 1987.

[113] P.P. Vaiyanathan and T.Q. Nguyen. Eigenfilters:a new approach to least squares FIR filter design and applications including Nyquist filters. *IEEE Trans. Acoust, Speech, Signal Processing*, 34:11–23, Jan. 1987.

[114] L. Vandendorpe. CQF filter banks optimized for zonal sampling and distortion minimization. pages 1275–1278. EUSIPCO, 1992.

[115] L. Vandendorpe. CQF filter banks matched to signal statistics. *Signal Processing*, 29(3):237–246, Dec. 1992.

[116] M. Vetterli. Filter banks allowing perfect reconstruction. *Signal Processing*, 10(3):219–244, 1986.

[117] M. Vetterli. Multi-dimensional sub-band coding: some theory and algorithms. *Signal Processing*, 6:97–112, April 1984.

[118] M. Vetterli. A theory of multirate filter banks. *IEEE Trans. Acoust., Speech, Signal Processing*, 35:356–372, Mar. 1987.

[119] M. Vetterli and D. Le Gall. Perfect reconstruction FIR filter banks: some properties and factorizations. *IEEE Trans. Acoust., Speech, Signal Processing*, 37(7):1057–1071, July 1989.

[120] M. Vetterli and C. Herley. Wavelets and filter banks: Theory and design. *Internal Rep., Columbia University*, 1990.

[121] M. Vetterli and C. Herley. Wavelets and filter banks: theory and design. *IEEE Trans. Signal Processing*, 40(9):2207–2232, Sept. 1992.

[122] E. Viscito and J.P. Allebach. The analysis and design of multidimensional FIR perfect reconstruction filter banks for arbitrary sampling lattices. *IEEE Trans. Circuits and Systems*, 38:29–41, Jan. 1991.

[123] Ed. J.W. Woods. *Subband Image Coding.* Kluwer Academic Press, 1991.

[124] J.W. Woods and S.D. O'Neil. Subband coding of images. *IEEE Trans. Acoust., Speech, Signal Processing*, 34:1278–1299, Oct. 1986.

[125] G.W. Wornell. A Karhunen-Loeve-like expansion for 1/f processes via wavelets. *IEEE Trans. Info. Theory*, 36:859–861, July 1990.

[126] G.W. Wornell and A.V. Oppenheim. Estimation of fractal signals from noisy measurements using wavelets. *IEEE Trans. Signal Processing*, 40(3):611–623, Mar. 1992.